1
Photoremovable Protecting Groups Used for the Caging of Biomolecules

1.1
2-Nitrobenzyl and 7-Nitroindoline Derivatives

John E. T. Corrie

1.1.1
Introduction

1.1.1.1 **Preamble and Scope of the Review**

This chapter covers developments with 2-nitrobenzyl (and substituted variants) and 7-nitroindoline caging groups over the decade from 1993, when the author last reviewed the topic [1]. Other reviews covered parts of the field at a similar date [2, 3], and more recent coverage is also available [4–6]. This chapter is not an exhaustive review of every instance of the subject cages, and its principal focus is on the chemistry of synthesis and photocleavage. Applications of individual compounds are only briefly discussed, usually when needed to put the work into context. The balance between the two cage types is heavily slanted toward the 2-nitrobenzyls, since work with 7-nitroindoline cages dates essentially from 1999 (see Section 1.1.3.2), while the 2-nitrobenzyl type has been in use for 25 years, from the introduction of caged ATP **1** (Scheme 1.1.1) by Kaplan and co-workers [7] in 1978.
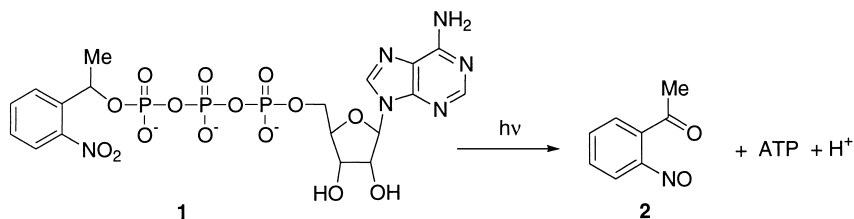
**Scheme 1.1.1** Overall photolysis reaction of NPE-caged ATP **1**.

1.1.1.2 **Historical Perspective**

The pioneering work of Kaplan et al. [7], although preceded by other examples of 2-nitrobenzyl photolysis in synthetic organic chemistry, was the first to apply this to a biological problem, the erythrocytic Na:K ion pump. As well as laying the foundation for the field, the paper contains some early pointers to difficulties and pitfalls in the design of caged compounds. Specifically, it was shown that 2-nitrobenzyl phosphate **3** and its 1-(2-nitrophenyl)ethyl analog **4** both released inorganic phosphate in near-quantitative yield upon prolonged irradiation. However, when the same two caging groups were used on ATP, namely **1** and its non-methylated analog **5**, the maximum yield of released ATP from **5** was only ~25%, whereas that from **1** was at least 80%. It was suggested that the 2-nitrosobenzaldehyde by-product released from **5**, in contrast to nitrosoketone **2** released from **1**, might react with the liberated ATP to render it inactive. This hypothesis has not been further studied, but the observations provide an indication that different substituents on the caging group may have unexpected effects. We return to this in later sections that consider rates and mechanisms of caged-compound photolysis.

3 R = H
4 R = Me

5
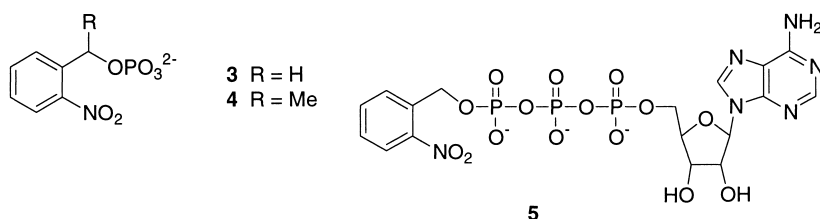
The use of nitrobenzyl-caged compounds to investigate millisecond time scale biological processes began when laser flash photolysis was used to release ATP from **1**. Initial experiments studied solution interactions between actin and myosin [8], but were soon extended to related work in skinned muscle fibers [9]. These early flash photolysis studies for release of active compounds were contemporaneous with work by the Lester group, who used *cis-trans* photoisomerization of azobenzene derivatives to manipulate pharmacological activity of receptor ligands [10, 11]. Although the latter work involves different photochemistry to that reviewed here, it has been a significant contributor to the adoption of the flash photolysis technique in biology.

In contrast to 2-nitrobenzyl photochemistry, which has its roots in 100-year old observations by Ciamician and Silber on the photochemical isomerization of 2-nitrobenzaldehyde [12], photocleavage of 1-acyl-7-nitroindolines has a much shorter history, dating from work by Patchornik and co-workers in 1976 [13]. They found that 1-acyl-5-bromo-7-nitroindolines (**6**) were photolyzed in organic solvents containing a low proportion of water, alcohols, or amines to yield the nitroindoline **7** and a carboxylic acid, ester or amide, depending on the nucleo-
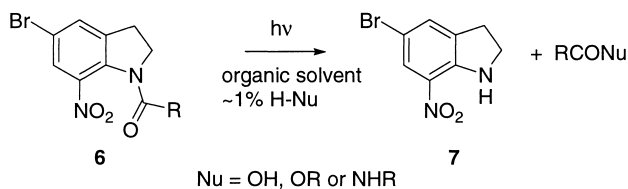
Scheme 1.1.2 Photolysis reaction of 1-acyl-nitroindolines in aprotic organic solvent containing a low proportion of water, an alcohol, or an amine.

phile present (Scheme 1.1.2). The work was briefly examined for its potential in peptide synthesis [14] but was unused for ~20 years, until our group began to use compounds of this type for the release of neuroactive amino acids (see Section 1.1.3.2). In view of the recent nature of most work on 7-nitroindolines, this review includes discussion of unpublished results to illustrate both the scope and limitations of this cage.

1.1.2
Synthetic Considerations

The development of an effective caged compound involves multiple factors, irrespective of the particular cage group employed. Not only must the chemical synthesis be achieved, but photochemical, physicochemical, and pharmacological properties must fit the intended application. Photochemical properties principally concern the efficiency and rate of photolysis upon pulse illumination by light of a suitable wavelength (normally >300 nm to minimize damage to proteins and nucleic acids). There is confusion in the literature about efficiency and rate, arising from different applications of this photochemistry. For use in time-resolved studies of bioprocesses, the relevant rate is of product release following a light flash of a few ns duration, and governs the time resolution with which the bioprocess can be observed. Other workers, using continuous illumination in synthetic photodeprotection applications, apply the term rate as a measure of conversion per unit time. While both uses are legitimate, only the former is generally relevant to studies of rapid bioprocesses. Efficiency of photoconversion, namely the percentage of caged compound converted to the effector species by the light pulse, is influenced by a combination of extinction coefficient at the irradiation wavelength (the proportion of incident light absorbed) and quantum yield (the proportion of molecules that undergo photolysis to form the desired photoproduct after absorbing a photon). Quantum yield is a property governed by the molecule itself and is not readily manipulated, so the investigator only has flexibility to vary the extinction coefficient. This can be achieved, at least for aromatic nitro compounds, by adding electron-donating groups to the aromatic ring. However, data from at least one such substituent study indicate that this can be an unpredictable exercise, sometimes with conflicting effects on extinction coefficient and quantum yield [15].

Important physicochemical properties are water solubility and resistance to hydrolysis. The significance of the latter is to avoid background hydrolytic release prior to the light flash, although stability during storage of aqueous solutions is also an issue. Finally, pharmacological properties need to be considered. In some cases attachment of a caging group can block an effector's actions but not necessarily eliminate its binding to a target protein. For example, caged ATP **1** retains affinity for actomyosin and, although not hydrolyzed by the enzyme, inhibits the shortening velocity of muscle fibers [16]. Similarly, nitroindoline-caged GABA and glycine (but not glutamate) bind to their respective receptors, in each case blunting the response to photoreleased amino acid [17].

The newly emerging field of 2-photon photolysis, first demonstrated by Webb and colleagues [18], offers the potential for highly localized photorelease (within a volume of a few μm^3) but places additional demands on optical properties of the cage. Existing 2-nitrobenzyl cages have very small 2-photon cross-sections and require light doses that cause significant photodamage to live tissue [19]. The Bhc (6-bromo-7-hydroxycoumarin-4-ylmethyl) cage is one option with a more useful 2-photon cross section [20], and some progress has also been made with the 4-methoxy-7-nitroindoline cage [21–23]. A recent paper described 1-(2-nitrophenyl)ethyl ethers of 7-hydroxycoumarins that had surprisingly high 2-photon cross-sections [25]. The underlying mechanism and generality of this approach remains to be determined.

Synthetic routes are specific to particular compounds, but some general points and matters of interest can be brought out. Often, synthesis of caged compounds is achieved by derivatizing the native effector species rather than by *de novo* synthesis. This has advantages in that the chirality present in most biological molecules is preserved, avoiding a need for asymmetric synthesis. The usual preparative method for caged ATP **1** involves treatment of ATP with 1-(2-nitrophenyl)diazoethane (**8**) in a 2-phase system, with the aqueous phase at pH ∼4 [24]. This method is applicable to phosphates in general and esterifies only the weakly acidic hydroxyl group. However, it has been found that either of the strongly acidic hydroxyls of the pyrophosphate in cyclic ADP-ribose (**9**) can be esterified when the aqueous phase is at a lower pH [26], and similar pyrophosphate esterification in nicotinamide adenine dinucleotide (NAD) has been achieved by treating its anhydrous tributylammonium salt with 1-(4,5-dimethoxy-2-nitrophenyl)diazoethane in DMF [27]. An interesting method developed by several groups in recent years has been to phosphorylate alcohols using phosphoramidite reagents that already incorporate the nitrobenzyl cage, so introducing a caged phosphate group in one synthetic step [28–31]. Examples are given in Section 1.1.3.

8

9

10

11

12

13

14
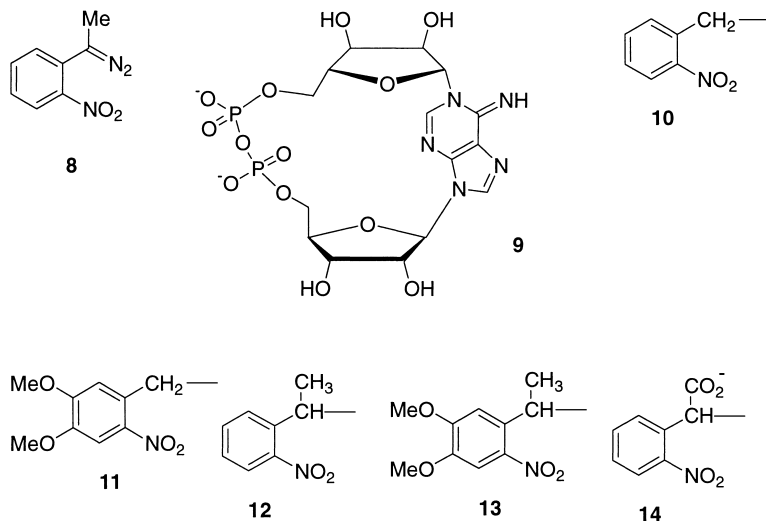
In most 2-nitrobenzyl-type caged compounds, the nitro group is introduced together with the rest of the cage moiety. In contrast, for many of the nitroindoline-caged amino acids, it has been necessary to couple an indoline with a protected amino acid and later introduce the nitro group. This is because the unreactive amino group of 7-nitroindolines can be acylated only under harsh conditions, incompatible with protecting groups on some amino acids, particularly glutamate, which has been a primary interest (see Section 1.1.3.2.2). Introducing the nitro group at a late stage is facilitated by the reactivity of the 1-acylindoline system but does require some care in the selection of reaction conditions and choice of protecting groups in the acyl side chain.

Finally, a desirable goal in this area would be to be able to cause sequential release of different effectors using different types of caging chemistry and light of two different wavelengths. Some progress has been made in recent papers, principally for selective differentiation of protecting groups in organic synthesis [32, 33], including an ingenious recent use of a kinetic isotope effect on abstraction of the benzylic proton to enhance differentiation between differently substituted 2-nitrobenzyl groups, of which one was dideuterated at the benzylic position [34]. Despite the gradual improvements being made in this area, application to caging chemistry remains as yet an unfulfilled aspiration.

1.1.3
Survey of Individual Caged Compounds and Caging Groups
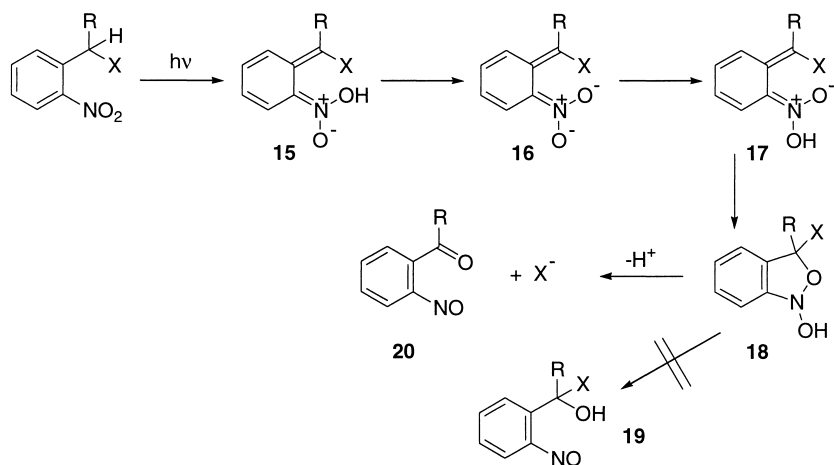
1.1.3.1   **2-Nitrobenzyl Cages**
The main structural types considered here are the parent 2-nitrobenzyl (NB) (**10**), its 4,5-dimethoxy analog (DMNB) (**11**), 1-(2-nitrophenyl)ethyl (NPE) (**12**)

and its 4,5-dimethoxy analog (DMNPE) (**13**), and the *α*-carboxy-2-nitrobenzyl (CNB) (**14**) groups. Minor variants of these are discussed in context below. Substantial work has also been done with 2-(2-nitrophenyl)ethyl derivatives, which release products by a *β*-elimination mechanism, but information on the product release rate following flash photolysis is lacking [35]. These compounds have been used as photolabile precursors in chemical synthesis, largely for the generation of oligonucleotide microarrays [36–38].

1.1.3.1.1 Mechanistic Aspects of Photocleavage and By-Product Reactions of 2-Nitrobenzyl Cages

There has been much past work on aspects of 2-nitrobenzyl photolysis (reviewed in [1]). Yip and colleagues have shown evidence for the involvement of both singlet and triplet states in the photochemistry of various compounds [39, 40]. However, most mechanistic work has focused on the dark chemistry subsequent to the photo-induced process. An interesting recent study describes observation of mechanistic steps at the single-molecule level using a DMNB derivative tethered inside the pore of a modified hemolysin. Changes in single-channel currents monitored progress of different reaction stages [41]. The study of the photolysis of caged ATP **1** by Walker et al. [24] has largely been taken as a paradigm for caged compounds. An important aspect of the mechanism was that decay of the intermediate *aci*-nitro anion **16** (Scheme 1.1.3) was the rate-determining step for ATP release, and direct measurement by time-resolved infrared spectroscopy has confirmed this [42]. It was noted that the *aci*-nitro decay rate was proportional to proton concentration below pH 9: the lower pH limit of this proportionality was not determined [24]. The pH dependence was attributed, without specific evidence, to protonation of a non-bridging oxygen in the triphosphate chain. However, recent computational and experimental studies [43, 44] suggest an alternative explanation that the *aci*-nitro anion must reprotonate to allow closure to the benzisoxazoline **18** and subsequent reaction. Thus a complete reaction scheme is more reasonably formulated as in Scheme 1.1.3, shown for a general case where R is any substituent and X is the caged species.

The photolytic process itself consists in transfer of the benzylic proton to an oxygen of the nitro group to give the *Z*-nitronic acid **15**. Ionization of this species (from 2-nitrotoluene) was observable in pure water ($k \approx 2 \times 10^7 \text{ s}^{-1}$) but in the presence of buffer salts the ionization was within the 25-ns laser flash [44]. Subsequent reprotonation to give the isomeric *E*-nitronic acid **17** allows cyclization to the *N*-hydroxybenzisoxazoline **18**. Calculations indicate that direct cyclization of anion **16** to the conjugate base of **18** is prohibitively endothermic [43]. Concurrently, this reprotonation of **16** more rationally explains dependence of the decay rate on proton concentration. So far, no direct evidence for **18** has been found, and this intermediate is assumed to decay immediately to end products, these being the nitrosocarbonyl compound **20** and the released effector species (X⁻ in Scheme 1.1.3). The study by Walker et al. [24] specifically excluded an alternative collapse of **18** to hemiacetal **19**, at least to the extent that the latter did not accumulate as a stable intermediate. However, recently it has

**Scheme 1.1.3** Detailed reaction scheme for photolysis of generalized nitrobenzyl-caged compounds. The scheme incorporates results of recent studies by Wirz and colleagues [43, 44].

unequivocally been shown for NPE-caged alcohols such as **21** that **19** is a rate-limiting intermediate, where the hemiacetal decay rate (pH 7, 2 °C) is 0.11 s^{-1} for the compound where R=CH$_2$OPO$_2$OMe$^-$, while the *aci*-nitro decay rate is ∼5000 s^{-1} [45]. Some evidence has been presented for a corresponding long-lived aminol in the photolysis of caged amides (see Section 1.1.3.1.2.1). Interestingly, the data for compounds like **21** strongly suggest that, in addition to the normal photolytic pathway via an *aci*-nitro intermediate as shown in Scheme 1.1.3, the major part of the reaction flux involves a direct, very rapid path from the initial nitronic acid (analogous to **15**) to hemiacetal **19** [45]. This anomalous, major pathway appears to operate for NPE-caged alcohols but not for analogous NB-caged alcohols. See Section 1.1.3.1.2.5 for additional comment on these compounds.
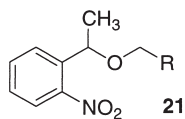

One difficulty of the caged compound field is that little available information exists to allow prediction of reaction rates or efficiencies. For example, measured *aci*-nitro decay rates of phosphates **3** and **4** (25 mM MOPS, 150 mM KCl, pH 7.0, 20 °C) were 660 and 34 300 s^{-1} respectively. Upon monomethylation of the phosphate in these compounds, the rate for the compound derived from **4** (NPE-caged methyl phosphate **23**) fell to 160 s^{-1}, while that for NB-caged methyl phosphate **22** became biphasic, with rate constants of ∼1000 and 3 s^{-1} (relative amplitudes ∼1:4) (J. E. T. Corrie and D. R. Trentham, unpublished data). The

occurrence of biphasic rate constants for the decay of *aci*-nitro transients is not uncommon (see, for example, Refs. [46–48]) and has sometimes been attributed to possible *E/Z*-isomerism of the intermediates, as in structures **24** and **25**. Recent computational studies suggest that this is unlikely, at least in intermediates from the NB series, where the *E*-isomer **24** is calculated to be of very much lower energy [45, 49], so the presence of a significant proportion of *Z*-isomer is improbable.
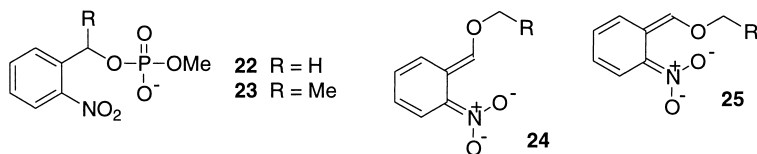
A further complication of 2-nitrobenzyl photochemistry arises from the formation of radical species, initially observed by chance during photolysis of NPE-caged ATP **1** solutions in an EPR spectrometer. The radical species was first assigned as a radical anion of caged ATP and was estimated to constitute approximately 10% of the reaction flux under the experimental conditions (10 mM caged ATP, 10 mM DTT, 200 mM buffer in the pH range 6–9, 1.5 °C) [50]. The species had non-exponential decay kinetics that were relatively insensitive to pH (times for decay to half the maximum intensity were 0.3, 0.4 and 1.2 s at pH 6, 7 and 9 respectively). The structure was later corrected to the cyclic nitroxyl **26**, and a mechanism for its formation was proposed [51]. NPE-caged methyl phosphate **23** gave a comparable EPR spectrum, indicating that only the cage group was involved in the formation of the radical [51]. No further reports of "long-lived" radical species from other caged compounds have appeared, but probably all such 2-nitrobenzyl systems generate a proportion of a radical species upon photolysis. Evidently the formation of low amounts of such radicals does not usually have deleterious effects.
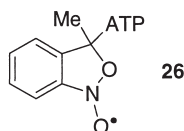

The nitrosoarylcarbonyl by-product **20** is mentioned in many papers as being of high reactivity and potentially damaging to biological systems. In fact there is scant reported evidence of such problems, apart from the archetypal case of caged ATP where an added thiol was found necessary to block enzyme inhibition [7] and a recent example in which 2-nitrosoacetophenone was postulated to bind to alkaline phosphatase, although definitive proof of this was lacking [52]. Later follow-up work suggests that the original interpretation was incorrect (L. Zhang and R. Buchet, personal communication) so the evidence for by-product interference remains minimal. Nevertheless, a protective thiol is frequently incorporated during
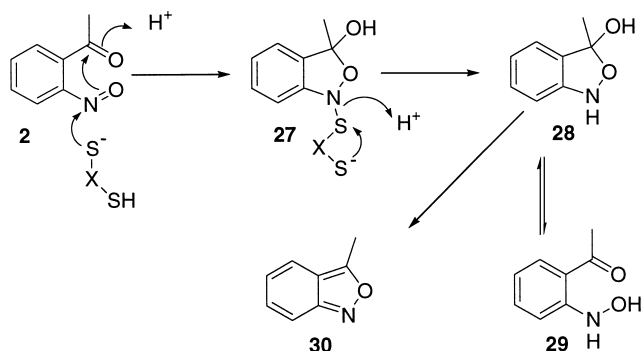
Scheme 1.1.4 Reactions of 2-nitrosoacetophenone **2** with a dithiol such as dithiothreitol. Note discussion in the text that the scheme does not apply to reactions with a monothiol such as glutathione, where the hydroxylamine product is not obtained.

photolysis, or the presence of reduced glutathione within cells ensures the same protection. The chemistry of the reaction of thiols with 2-nitrosoacetophenone (**2**) (the by-product from photolysis of NPE-caged compounds) has been clarified (Scheme 1.1.4) [42].

With DTT as the thiol, rapid-scan FTIR spectroscopy was just able to observe the intermediate **27** (no carbonyl absorption), which was rapidly reduced to a tautomeric mixture of **28** and **29**. These would be the predominant species present in a typical caged compound experiment. Dehydration to 3-methylanthranil (**30**) took place on a much slower time scale ($t_{1/2}$ 9 min at pH 7, 35 °C) [42]. However, this study of the thiol reaction of 2-nitrosoacetophenone cannot necessarily be applied to by-products from other types of cage or with other thiols. For example, Chen and Burka [53] reported that 2-nitrosobenzaldehyde, the by-product of the NB cage, reacts with a monothiol such as *N*-acetylcysteine to give 2-aminobenzaldehyde and not the hydroxylamine analogous to **28/29**. We re-examined this work and found that the product from the aldehyde and the ketone depends upon the thiol. With a monothiol (*N*-acetylcysteine in our work), both compounds give the corresponding amine, while, with a dithiol (DTT), both give the corresponding hydroxylamine (J. E. T. Corrie and V. R. N. Munasinghe, unpublished data). The different products presumably reflect operation of distinct pathways, controlled by kinetic competition after initial addition of thiol to the nitroso group. For a discussion of these reaction pathways, see Ref. [54]. An ingenious alternative method to remove the reactive nitroso by-product was described by Pirrung and colleagues [55], who prepared compounds incorporating
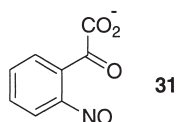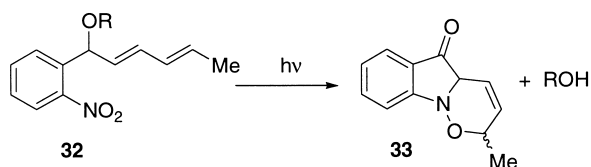
Scheme 1.1.5 Overall photolysis reaction of **32**, in which the diene side chain traps the nitrosoketone by-product of photolysis as a Diels-Alder adduct.

a pentadienyl system (such as **32**) that was able to trap the nitroso group as an intramolecular Diels-Alder adduct (**33**) (Scheme 1.1.5). Applications of this method have not yet been reported.

Many papers on the CNB cage **14** show the by-product as the nitrosopyruvate **31**, but there is little evidence for the existence of this compound, nor has its reaction with thiols been characterized. Indeed, FTIR data from a range of CNB caged compounds show that there is significant decarboxylation upon photolysis (J. E. T. Corrie and A. Barth, unpublished data), as might be expected from published data on simple nitrophenylacetates [56] and a related 2-nitrophenylglycine derivative [57]. The strong absorption band at 2343 cm^{-1}, characteristic for CO_2 in water, occurs in a region missing from the only published IR study of flash photolysis of a CNB-caged compound [58]. Current work (J. E. T. Corrie and A. Barth) aims to quantify the extent of CO_2 loss from CNB-caged compounds and to provide more definite evidence on the formation of **31**.

To summarize, investigators should be cautious in extrapolating from the relatively well-understood photocleavage of NPE-caged ATP **1** to other systems. A striking example is given by a caged diazenium diolate, that was assumed to undergo normal photocleavage of its NB group and ultimately to generate nitric oxide [59]. Subsequent studies showed that photolysis proceeded by an entirely different mechanism. The nitro group had essentially no effect on the reaction course, and formation of nitrous oxide was a minor pathway [60]. This case may be the most divergent from usual expectations but underscores the danger of unverified extrapolations. In cases where the product release rate is critical, simple measurements of *aci*-nitro decay rates may not be adequate to define the rate of product release (see the above discussion of NPE-caged alcohols **21** for a striking example). The identity of intermediates and by-products may be of less concern to most investigators, although, for example, in cases where fluorescence recordings are made after triggering a bioprocess by flash photolysis of a caged compound, awareness of light absorption of intermediates or by-products may be necessary to avoid optical artifacts (see Ref. [61] for an example of correcting a fluorescence signal for the transient inner filter effect of an *aci*-nitro intermediate).

1.1.3.1.2 **Representative Survey of Nitrobenzyl-Caged Compounds**
The following section is not a comprehensive coverage of the literature, but aims to pick out points of particular interest as a guide to general principles and opportunities for future work. The different types of 2-nitrobenzyl cage are covered in this section, which is mostly subdivided into different types of functional groups that have been caged. The first two sections deal with particular classes of caged species, as this seems a more rational classification.

Nucleotides As mentioned above, photolysis of NPE-caged ATP has been studied by FTIR difference spectroscopy, confirming directly that the *aci*-nitro decay rate is rate determining for release of ATP [42, 62]. The IR spectral assignments are discussed elsewhere in this volume. Work on caged cyclic nucleotides since 1993 has described NPE- and DMNB-caged versions of 8-bromo-cAMP and -cGMP and reinforces previous conclusions that the axial isomers of these caged compounds are significantly more resistant to hydrolysis than the equatorial isomers, as well as that electron-donating groups in the cage group increase the hydrolysis rate [63–64]. Caged cyclic nucleotides where the NB group bears a charged substituent that has electron-withdrawing properties (for example cGMP derivative **34**) have high stability and solubility in water [65]. Responses to photorelease of cGMP from either NPE-caged cGMP or **34** have been compared [66].
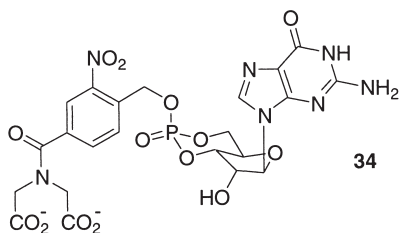

Extensive studies have led to nicotinamide coenzymes caged in various ways. NAD was caged on its pyrophosphate group (as for cyclic ADP-ribose, discussed in Section 1.1.2) and NADP on the 2′-phosphate of its adenosine moiety, in both cases with the DMNPE cage [27]. The amide nitrogen of the nicotinamide in both nucleotides was CNB-caged by a mix of enzymatic and chemical steps [27]. The caged NADP **35** had an *aci*-nitro decay rate of only 30 s^{-1}, very much slower than reported for most other CNB-caged compounds. These caged NADP compounds were used in time-resolved crystallographic studies of isocitrate dehydrogenase [67]. In related work, several NADP compounds caged on the nicotinamide were synthesized with NB, DMNB, CNB, NPE and a novel 4-carboxy-NPE group. These papers [68, 69] include useful synthetic detail on 2-nitrobenzyl chemistry and show evidence for long-lived intermediates in the photolysis of some of the caged NADP derivatives, postulated to be aminols analogous to the hemiacetal described in Section 1.1.3.1.1. The available data suggest that these putative aminols have lifetimes of hundreds of seconds (pH 7.3) [69], so the

compounds are unlikely to be useful in applications requiring high time-resolution. It is noteworthy that there appears to be some discrepancy between the data for similar CNB-caged NAD/NADP compounds [27, 67, 69], and further investigation may be appropriate. These studies again underline the importance of reliably establishing product release rates for new caged compounds.


35
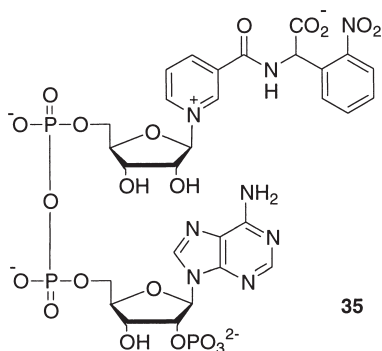
In addition to studies with simple mono- and dinucleotides, oligonucleotide sequences can be photomanipulated either by simple uncaging or by generating strand breaks. Thus, caged RNA sequences have been accessed from an NB-caged precursor such as **36**, that can be used in automated oligonucleotide synthesis [70, 71]. Photolysis releases intact RNA. These site-specific caged sequences contrast with non-specific modification of the backbone phosphates in DNA or RNA by a 4-coumarinylmethyl cage [72]. In complementary work, single- and double-strand breaks at specific sites in DNA sequences can be photogenerated by caged linkers introduced into the sequence during chemical synthesis [73, 74]. Structure **36** is an example that generates both 3′- and 5′-phosphate-terminated strand breaks directly by photolysis of each cage group. In an alternative approach, DNA oligomers with a 2-nitrobenzyl group at C-5′ can directly generate breaks terminated in a 5′-phosphate but need base treatment to liberate the 3′-end [75]. Creation of strand breaks in specific locations is expected to aid studies of nucleic acid repair processes.


36
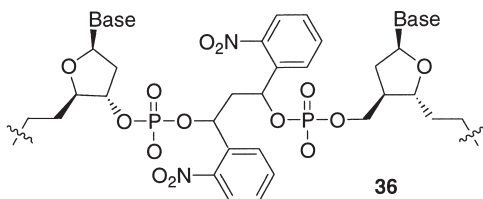
Peptides and proteins   Current reviews [76, 77] detail much past work in this field, so only recent studies with features of particular interest are covered here. A further very recent review covers synthesis of caged proteins by biosynthetic

incorporation of unnatural amino acids, which allows caging at specific sites with a flexibility impossible to achieve by chemical modification of whole proteins [78]. Thus, caging of peptides and proteins is moving from early (often non-specific) modifications to more highly designed blocking. In one such study, self-assembly of an amyloidogenic peptide was blocked by attachment of a pentacationic modified peptide joined to the amyloidogenic peptide by a photocleavable nitrobenzyl-type linker. Irradiation cleaved the inhibitory unit and initiated fibril formation [79]. Photocleavage kinetics were not determined, but, based on related data [80], are probably $\sim 2000 \text{ s}^{-1}$ (pH 7.5, 20 °C). A new promising strategy is peptide caging by a 2-nitrobenzyl group on a backbone amide, so the caging position is not limited by the presence of particular side chains [81, 82]. The *aci*-nitro decay rate is rapid ($\sim 27\,000 \text{ s}^{-1}$ at pH 7, ambient temperature), although the observation of long-lived aminols from other caged amides [69] raises caution about the actual rate of product release. A novel methionine-caged protein (horse heart cytochrome *c*) was prepared by alkylation at pH 1.5, where only the methionine side chains were reactive [83]. This strategy could only be applicable to proteins that refold after exposure to such low pH but may be useful for methionine-containing peptides. In a different strategy, the Michael acceptor **37** has been used for specific alkylation of thiol groups, for example, to prepare a caged papain [84]. Lastly, serine, threonine, and tyrosine phosphopeptides have been prepared in NPE-caged form, using an NPE-phosphoramidite reagent for direct introduction of the caged phosphate group during solid-phase peptide synthesis [30].
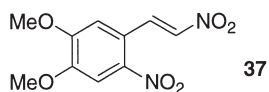

Caged carboxylates NB- and NPE-caged carboxylate groups generally have slow *aci*-nitro decay rates, limiting their value in studies of rapid processes (see Ref. [85] for the recent example of NPE-caged isocitrate, $k \approx 60 \text{ s}^{-1}$ at pH 7, 25 °C). One means to overcome this slow rate has been with the CNB group, extensively studied as CNB esters of neuroactive amino acids including L-glutamate [86], GABA [87], NMDA [88], and glycine [89]. Recently, a modified CNB group with an additional *para*-carboxylate (DCNB) has been used as a more hydrophilic cage on D-aspartate (compound **38**) [90]. *Aci*-nitro decay rates for these CNB esters are typically biphasic (although the relative amplitude of the phases varies between compounds), with the major component having rates (pH ~ 7, ambient temperature) in the range 20 000–150 000 s^{-1}. The fast component for DCNB ester **38** was slightly slower, at $16\,500 \text{ s}^{-1}$. Time-resolved infrared measurements indicate that the release rate of L-glutamate from its CNB γ-ester parallels the *aci*-nitro decay rate [58]. This compound had the least biphasic *aci*-nitro decay of all those described (90% of the amplitude at $33\,000 \text{ s}^{-1}$), so the IR measurements do not help interpret the release rates from compounds with a higher

proportion of a slow phase in the decays. Reported spontaneous hydrolysis rates for CNB esters close to neutral pH and at ambient temperature are $\sim 1\%$ in 24 h, which in general requires some care to minimize contamination by free amino acid, but all these compounds have been used in experiments with appropriate isolated neuronal cells. It was reported that CNB-caged GABA had no significant pharmacological effects [87], but a recent study has found significant and novel pharmacology for this compound [91].


38
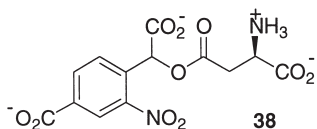
Apart from the nitroindoline cage discussed in Section 1.1.3.2, two other cages for carboxylates have been described. One is the 2,2′-dinitrobenzhydryl group, used as the β-ester of NMDA [92], where the *aci*-nitro decay rate was $165\,000$ s^{-1} and cleanly monophasic (pH 7, 22 °C), as well as being ~ 5-fold faster than for the CNB ester of the same carboxylate. The compound was reported to be stable to hydrolysis under these conditions, but the analogous caged glycine was rapidly hydrolyzed at pH 7 [93], as would be expected for the ester of an α-amino acid, so this cage group must be applied with caution. The second cage is a hydroxylated NPE structure, as in caged arachidonic acid **39**. This paper noted that CNB-caged fatty acids were chemically unstable and that the hydroxy-NPE compounds had *aci*-nitro decay kinetics significantly faster than for NPE-caged carboxylates [94].

39
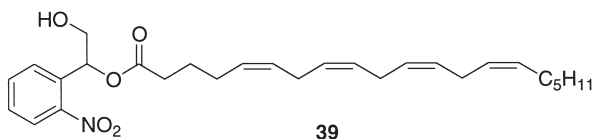
In applications outside the neuroscience area, a range of caged strong acids, such as trichloroacetic acid, has been described for photorelease in anhydrous solvents in conjunction with photodirected oligonucleotide synthesis [95]. Modified lipids have been described that have additional carboxylate groups at the terminus of the normal fatty acid chains. When these carboxylates were caged (with NB, DMNB, NPE, or DMNPE groups) the lipids could be assembled into liposomes. Irradiation to release these carboxylates destabilized the liposomes and allowed leakage of their contents [96]. Similar results were obtained for liposomes with a DMNB-carbamate-caged amino group of a phosphatidylethanolamine [97].

Caged amines and amides   Amines can be caged in two principal forms, either by direct attachment of a caging group, in which case the charge state of the amine is maintained, or indirect attachment via a carbonyl group to form a carbamate, in which case the amine, normally cationic at physiological pH, becomes a neutral

species. Recent examples of each strategy applied to sphingolipids have been reviewed [98] and are of particular interest for examples of chemoenzymatic synthesis of caged compounds. Otherwise, little new work on direct amine cages has appeared in the last decade (apart from caged Ca^{2+} reagents, see below). Note that unpublished data (J. E. T. Corrie and A. Barth) indicate that compounds such as *N*-2-nitrobenzylglycine (**40**) undergo substantial decarboxylation upon photolysis. Work is in hand to quantify the extent of this side reaction, which is also observed with the isomeric 4-nitro compound, indicating that it operates by a different photochemical process than the normal cleavage reaction.
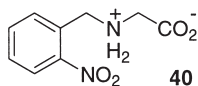
Carbamate derivatives of amines involve two stages for amine release: photocleavage of the caging group to leave a carbamate salt, which then undergoes nonphotochemical decarboxylation (Scheme 1.1.6). Either step can be rate-limiting for overall release of the amine. This has been explored for two cages which illustrate rate limitation by different processes. Thus the NPE-caged glutamate **41** and related carbamate-caged amino acids are rate limited by decay of the *aci*-nitro intermediate, the process which generates the carbamate salt [99]. In contrast, the dimethoxybenzoin derivative **43** generates the carbamate salt on a sub-µs time scale, and release of the amine is controlled by the thermal decarboxylation ($150 \, s^{-1}$ at pH 7, 21 °C) [100]. The decarboxylation rate will vary with the pK of the particular amino group but will always be an upper limit on the amine release rate from any carbamate derivative. Strategies that focus on rapid photocleavage of the cage group from carbamates, as from the CNB-derivative **42** [101], cannot avoid this limitation.
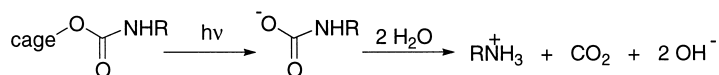
Scheme 1.1.6 Generalized scheme for photolysis of a carbamate-caged amine, showing the separate stages of photocleavage of the cage and thermal decarboxylation of the resulting carbamate salt.

41 R = CH_3
42 R = CO_2^-

43
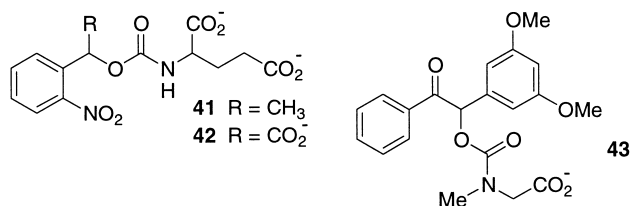
Most new work on caged amides has been described above in relation to caged NAD and NADP and has a particular caveat discussed in that Section about long-lived intermediates in the photocleavage process that limit the product release rate. In other applications, a series of NB, NPE and CNB-caged derivatives of asparagine, glutamine, GABA amide, and glycinamide were investigated [102]. Photolysis rates of the NB-, NPE- and CNB-caged glutamines were 385, 1925 and 900 s^{-1} respectively (pH 7.5, ambient temperature), where relevant being for the faster phase of biphasic traces. The suggested mechanism shows an aminol intermediate, but no evidence was presented for this or for its possible effect on the product release rate. Finally, the caged biotins **44** (R = H or CH$_3$) have been used as a means to control assembly of arrays of biological molecules on surfaces [103, 104]. By uniformly coating a surface with a caged biotin and irradiating defined areas through a mask, patterns of tethered biotin can be created which subsequently bind avidin or streptavidin and allow immobilization of species via conventional biotin/avidin layers.
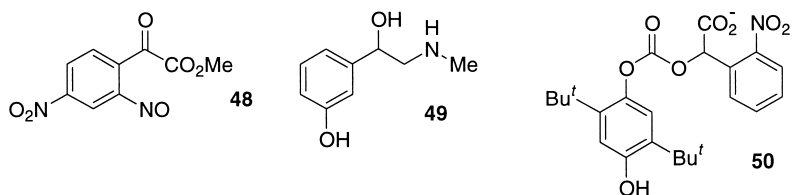

44
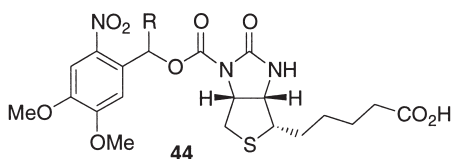
Caged alcohols and phenols   A major finding for NPE-caged alcohols has been discussed in Section 1.1.3.1.1 in relation to a long-lived hemiacetal intermediate that causes much slower product release than inferred from the *aci*-nitro decay rate [45]. This rate limitation appears to be general for NPE-caged alcohols, so applies to the NPE-caged choline reported by Peng and Goeldner [47], invalidating the μs time scale claimed for choline release. The NPE-caged 2-deoxyglucose **45 b** has been described [105] but without data on release kinetics. Other caged sugars include the NB-glucoside and ether derivatives **45 a** [105] and **46 a, b** [46, 106]. As noted in Section 1.1.3.1.1, these and other NB-caged alcohols studied to date appear not to involve a long-lived hemiacetal intermediate in their photocleavage step, so product release is at the *aci*-nitro decay rate. However, a very recent detailed study of 2-nitrobenzyl methyl ether by Wirz and co-workers [107] did find evidence for a rate-limiting hemiacetal ($t_{1/2} \approx 2$ s at pH 7, 23 °C), and subsequent studies of 2-nitrobenzyloxyacetic acid gave similar results (J. Wirz, personal communication). In contrast, biological responses to release of glucose from the NB-caged glucose **46 a** were faster [106], suggesting either a significantly faster decay rate or non-involvement of a hemiacetal. On balance, it seems probable that the process of product release from NB- and NPE-caged alcohols always proceeds via a hemiacetal. However, particularly in the NB case, the extent to which this intermediate accumulates and so limits the rate of product release is apparently very sensitive both to the precise compound and to the solution conditions. Further work to clarify aspects of this reaction is in progress (J. Wirz and J. E. T. Corrie, unpublished data).

45a R = H
45b R = Me

46a R = H
46b R = Me

47
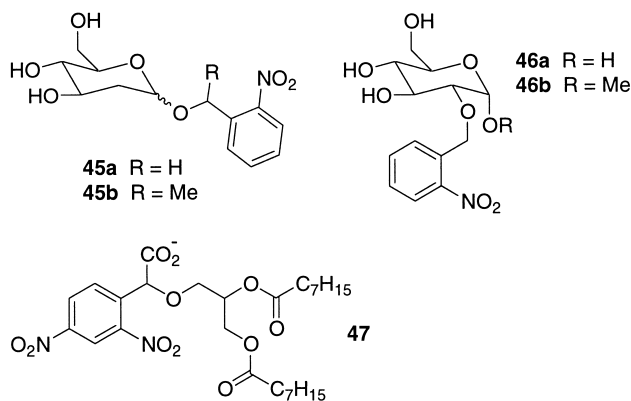
A novel 4-nitro-CNB cage is present in the caged diacyl glycerol **47** [108], which
has been used in a number of physiological studies. The additional nitro group
was not commented upon but probably facilitates the synthetic route. As well as
the free acid **47**, the corresponding methyl ester was prepared, from which the
photolysis by-product **48** was isolated and characterized. Notably, in view of the
discussion of decarboxylation during photolysis of other CNB compounds (Sec-
tion 1.1.3.1.1), it was reported that the free acid corresponding to **48** could not
be isolated, although this was attributed to instability [108]. A related caged dia-
cyl glycerol using the Bhc cage [20] has been prepared to enable 2-photon re-
lease at different sites within a tissue preparation [109].

Caged phenols are largely represented by derivatives of phenylephrine **49**, an
α-adrenergic agonist. Walker et al. described NB-, NPE-, DMNB- and CNB-deri-
vatives caged on the phenolic oxygen, with *aci*-nitro rates (pH 7, 22 °C) between
$\sim 2 \, s^{-1}$ (NB) and $\sim 2000 \, s^{-1}$ (CNB) [110]. Other workers prepared NB-, DMNB-
and CNB-derivatives caged on the amino group [111, 112] and concluded that
the *N*-linked NB-caged compound best blocked pharmacological activity [112].
The *N*-linked compounds tended to have faster *aci*-nitro decay rates than the
corresponding *O*-linked compounds.

The CNB-caged phenolic carbonate **50** was prepared to study effects of 2,5-di-
t-butylhydroquinone, a reversible inhibitor of the sarcoplasmic Ca^{2+} ATPase
[113]. As for the carbamates discussed above (Scheme 1.1.6), release of the end
product involves both photochemical and thermal cleavage steps. Here the *aci*-
nitro decay rate was biphasic with its major component at $\sim 3800 \, s^{-1}$, while the
thermal loss of CO_2 was estimated at $\sim 130 \, s^{-1}$ so was rate limiting for release
of the phenol. It is noteworthy that the rate of CO_2 loss from an aliphatic
monoalkyl carbonate, as formed on photolysis of a caged alcohol such as the
Bhc-caged diacyl glycerol mentioned above [109], is predicted to be very much
slower on the basis of previous studies of this decarboxylation [114], with an es-
timated half-time of $\sim 30 \, s$ (pH 7) for release of the final product. This may not
be important for diacyl glycerols, which probably diffuse slowly from the photo-

lysis site, but would seriously limit a carbonate cage for more diffusible caged alcohols. Further experimental verification of this expectation is desirable.

Caged phosphates Most work related to caged phosphates has been described in earlier sections relating to general synthetic methods or to nucleotides. A substantial advance mentioned in Section 1.1.2 is the use of phosphoramidite reagents to introduce a caged phosphate group as a complete entity, as opposed to modification of an existing phosphate [28–31]. Applications include synthesis of a caged sphingosine phosphate [29] and caged phosphopeptides [30]. An interesting use has been to prepare inositol phosphates caged on specific phosphate groups [28, 115], in contrast to the method originally used for IP$_3$, where caging was distributed among the three phosphate groups and relied on separation to obtain the biologically inert P^4- or P^5-caged isomers [116]. Note that regiospecific caging has also been achieved for a thiophosphate analog, 1-D-*myo*-inositol 1,4-bisphosphate 5-phosphorothioate, where the *S*-caged derivative **51** was formed by alkylating the free thiophosphate with 1-bromo-1-(2-nitrophenyl)-ethane [117]. In the context of inositol phosphates, an alternative approach to a caged IP$_3$ analog is **52**, caged on a free hydroxyl group and derivatized on the phosphates to make the compound cell-permeant. It can be loaded into cells where it is hydrolyzed by non-specific esterases to generate the caged IP$_3$ analog within the cell [118]. Previous uses of intracellular caged IP$_3$ have generally involved patch-clamped single cells, where the reagent was introduced via the patch pipette (for example, see Ref. [119]). Finally, in this Section, caging of phosphates has been extended to caged phosphoramides to prepare potential prodrugs of phosphoramide mustards [120].
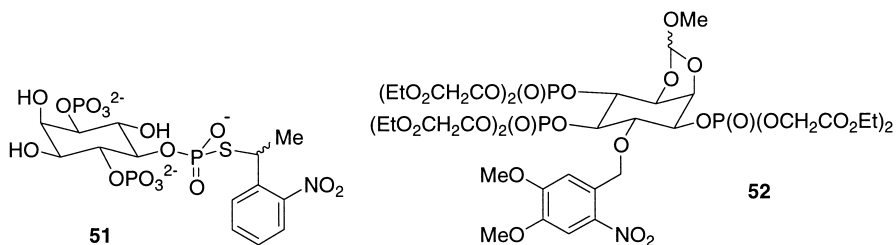
Caged protons   Several classes of caged compound, including nitrobenzyl-type cages, release a proton during the photolytic process (Scheme 1.1.1), but the focus of interest is usually directed to the other released species, as in all the compounds described above. Depending on the pK of the released effector compound, the proton may remain free or be taken up again as the effector is released. In most cases where the proton remains free, it is rapidly buffered by cellular or external medium buffers, but in experimental situations with minimal buffering, the released proton induces rapid acidification. To allow study of rapid proton-mediated events alone, it is desirable to use a reagent from which the other released component is not bioactive. One such is 2-nitrobenzaldehyde, which photoisomerizes to 2-nitrosobenzoic acid [12, 121, 122]. Other compounds more directly related to the general 2-nitrobenzyl type are the NPE-caged hydroxyphenyl phosphate **53** [123] and NPE-caged sulfate **54** [124]. The pH jumps that can be achieved by these compounds are restricted by the pK of the other released species, which will buffer the released proton. Thus **53** can achieve acidification to about pH 5, while **54** can reach pH ~ 2 (if sufficient photolysis can be achieved to generate ~ 10 mM proton concentration). For each of these compounds, liberation of the proton upon photolysis should occur within a ~ 25-ns laser flash [44].
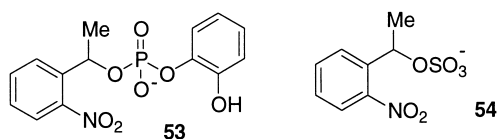
Caged calcium   Caged calcium reagents are unique among caged compounds, since release of Ca^{2+} depends on a change in the affinity of a photolabile chelating agent rather than direct rupture of a covalent bond between the calcium ion and the cage. The process is illustrated for DM-nitrophen (**55**) in Scheme 1.1.7, which shows rupture of the intact high-affinity chelator to fragments of much lower affinity. A very recent comprehensive review discusses interplay of the calcium affinity before and after photolysis, the desired free Ca^{2+} level before and after photolysis, and how photochemical parameters of different available cages influence the choice of reagent. It also covers progress with 2-photon photolysis of caged calcium reagents [125]. The main point of interest not in the review concerns details of the photochemical cleavage, which appears not solely to be as depicted in Scheme 1.1.7. In unpublished work (J. E. T. Corrie and A. Barth), we have observed substantial CO_2 formation on photolysis of DM-nitrophen, with or without Ca^{2+} present. Work now in hand aims to quantify the extent of this decarboxylation process and to determine to what extent it may affect modeling of the Ca^{2+} transients [126] induced by flash photolysis.
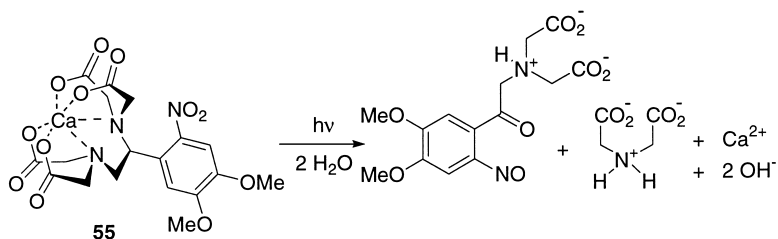
Scheme 1.1.7 Release of Ca^{2+} upon cleavage of a photolabile Ca^{2+} chelating agent (DM-nitrophen).

Caged fluorophores General strategy in caging fluorophores is to perturb the electronic structure by attachment of the caging group to make the molecule either non-fluorescent or very weakly so. Photolysis allows the delocalized electronic structure of the free fluorophore to re-establish, thereby regenerating fluorescence. An early example of the approach is caged fluorescein (**56**), in which alkylation of both phenolic groups locks the compound into the non-fluorescent lactone form [127]. The field is dominated by applications of the reagents rather than by particular chemical innovation. Most chemical and cell biological work with caged fluorophores has been by the Mitchison group in a series of elegant studies and has been recently reviewed [128]. A variant of a caged Q-rhodamine linked to dextran for cell lineage measurements has been described [129]. None of the work focuses on release rates of the fluorophores, as the cell biology applications have been more concerned with spatial definition of the released fluorescence than with high time resolution. Outside cell biology, the caged hydroxypyrenetrisulfonate **57** has been used to define the amplitude and/or temporal stability of concentration jumps of biologically active compounds [17, 130]. This is a useful technique for photolysis in small volumes, such as on a microscope stage, where the photolysis light is focused only on part of the field, and direct measurement of the released concentration is difficult. The surprising 1- and 2-photon photochemistry of NPE-caged 7-hydroxycoumarins is another recent approach but needs further work to establish its generality [25].
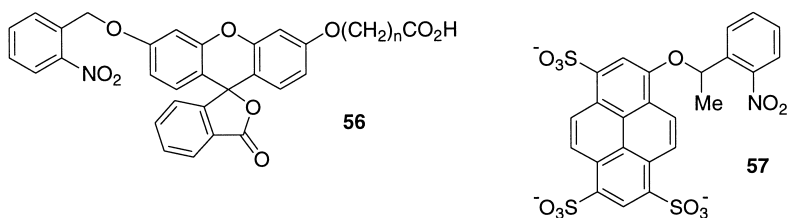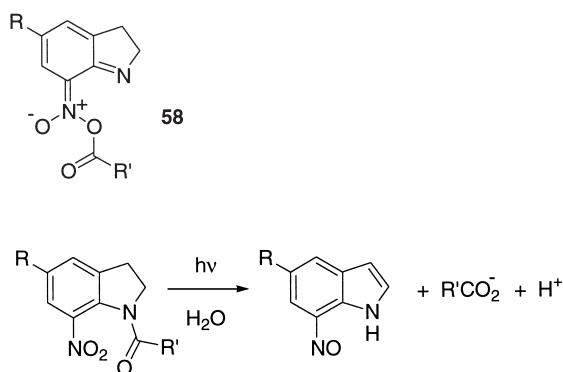
1.1.3.2 **7-Nitroindoline Cages**

As mentioned in Section 1.1.2, interest in this caging group was revived only in 1999, so this Section contains much less material than that on 2-nitrobenzyl cages. Applications to date are restricted to photorelease of neuroactive amino acids, but photochemical synthesis of amides in organic solutions has also been described, where an acyl group on the indoline nitrogen is transferred to a different primary or secondary amine [131–134].

1.1.3.2.1 **Mechanistic and Structural Aspects of Photochemical Cleavage of 1-Acyl-7-nitroindolines**

Unlike 2-nitrobenzyl compounds, photocleavage of nitroindoline cages gives different by-products in organic and aqueous media. The original work by Amit and colleagues [13] in aprotic solvent plus 1% water gave products shown in Scheme 1.1.2, where the water present in the solvent was incorporated into the released carboxylic acid. The same process enables the photochemical amide syntheses mentioned above. However, in 100% aqueous solution, the reaction gives not a nitroindoline but a nitrosoindole (Scheme 1.1.8), as well as the carboxylic acid: solvent water is not incorporated into the products [135]. There is a smooth transition from the nitroindoline to the nitrosoindole by-product as the proportion of water in the reaction solvent increases from 1 to 100% [136]. The carboxylate release rate in fully aqueous medium is $\sim 5 \times 10^6 \, s^{-1}$, and photocleavage involves a triplet state of the nitroindoline [136]. It was inferred that a common intermediate, the carboxylic nitronic anhydride **58**, was formed in either organic or aqueous solution, with partition into the different reaction products being determined by the ionizing power of the solvent and to some extent by the pK of the departing carboxylate group.

Scheme 1.1.8 Photolysis reaction of 1-acyl-nitroindolines in aqueous solution, showing formation of the nitrosoindole by-product.

In the recrudescence of the nitroindoline cage, we first replaced the 5-bromo substituent used by Amit [13] by a substituted alkyl group, as in **59** [135]. This led to improved solubility and an ~2-fold gain in photoefficiency. A substituent at C5 is useful to prevent nitration there, which otherwise takes place in competition with C7 nitration. In later work, different substituents were used, aiming to improve photosensitivity by enhanced near-UV absorption. Of three substituted species investigated, the 4-methoxy compound **60** had the best gain in sensitivity over **59**, although during synthesis a varying proportion of the 5-nitro isomer was always obtained [137, 138]. Blocking the 5-position in **61** to avoid 5-nitration led to decreased photosensitivity, probably because steric effects reduce overlap of the 4-substituent with the aromatic ring. Compound **62**, substituted with the strongly electron-releasing 4-dimethylamino group, was inert upon irradiation, probably because a competing process involving electron transfer from the tertiary amino substituent quenches an excited state [137].

60 R = H, R' = OMe
61 R = Me, R' = OMe
62 R = H, R' = NMe$_2$
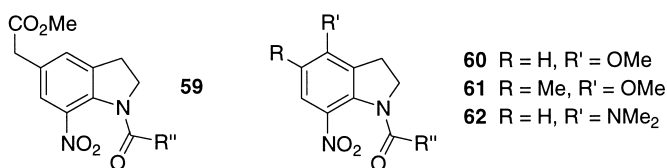
1.1.3.2.2 Survey of 7-Nitroindoline Caged Compounds

The discussion focuses on successful applications of the nitroindoline cage, but also, to illustrate its limitations, describes unpublished cases where the methodology has failed. Our work has been directed principally to synthesis of caged neuroactive amino acids, largely L-glutamate, GABA, and glycine. Initial work produced nitroindoline-caged versions of these compounds, namely **63–65**. Note that for synthetic reasons the side chain ester at C5 of the indoline in the caged glycine was hydrolyzed to the free acid, but this did not affect photochemical release [17, 135]. Significant points about these compounds were their very high resistance to hydrolysis, so no leakage from the caged species occurs upon incubation near neutral pH [135], and the fact that their photochemical release rates [136] are more than adequate to mimic physiological release. The glutamate conjugate **63** had no detectable pharmacological activity before photolysis at concentrations up to at least 1 mM, but this was not so for the GABA **64** and glycine **65** conjugates, which showed evidence of binding to the relevant receptors [17]. At least in the case of GABA, this result, together with reported pharmacological activity of CNB-caged GABA [91], shows that an optimal caged GABA remains a challenge.

63 R = Me, R' = $(CH_2)_2CH(NH_3^+)CO_2^-$

64 R = Me, R' = $(CH_2)_3NH_3^+$

65 R = H, R' = $CH_2NH_3^+$
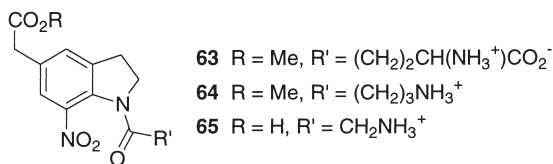
As mentioned above, later studies showed that a 4-methoxy substituent is beneficial to photolysis efficiency and the L-glutamate analog of **60** has been used in several physiological applications [17, 139–142], including work where localized release was achieved by 2-photon photolysis [21–23]. These results, together with the synthetic applications of nitroindoline photolysis described above [131–134] indicate that the strategy has broad applicability to caging carboxylic acids. However, in the course of attempts to extend applicability of the method, we have encountered examples where this cage was not useful (J. E. T. Corrie and G. Papageorgiou, unpublished data). Studies of the nitroindoline-caged Ca^{2+} chelating agent **66** were ultimately frustrated as the compound did not photolyze either in the presence or absence of Ca^{2+}. This is similar but not identical to data of Adams and colleagues, who reported that the dinitroindoline derivative **67** photolyzed only when excess Ca^{2+} was present [143]. We also prepared the EDTA derivative **68** and found that it photolyzed cleanly in the presence of a large excess of Ca^{2+}, but without the metal ion it decomposed to a complex, uncharacterized mixture, accompanied by CO_2 formation. We speculatively attribute the failure of **66** to photolyze to a quenching of the excited state by the electron-rich aryl rings of the BAPTA moiety, although this does not fully explain the disparate reactivity of **66** and **67**. Some additional evidence for possible quenching came from the nitroindolinyl carbamate derivative **69**, which was synthesized as a potential alternative to the caged fluorophore **57**. Compound **69** was also resistant to photolysis. The behavior of the EDTA derivative **68** is broadly consistent with electron transfer from the aliphatic tertiary amino group(s) to an excited state of the nitroindoline. Such single-electron transfer in this compound would be expected to cause decarboxylation, well precedented for cation radicals of α-amino acids [144].

66 R = Me
67 R = NO_2

68
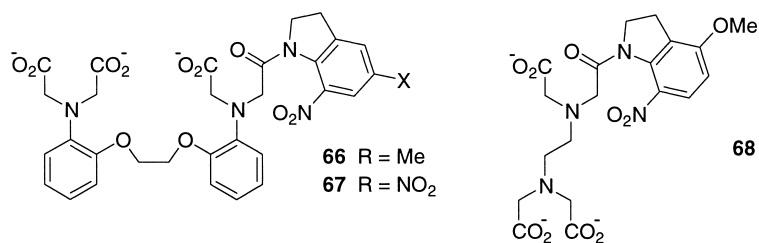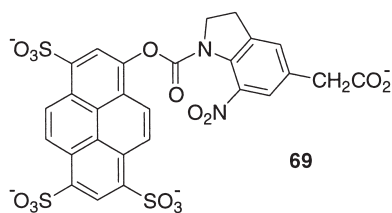
Despite these isolated failures, we continue to develop the strategy, notably in pursuit of higher photolytic efficiency and elimination of residual pharmacological activity in derivatives such as the caged GABA **64**. Very recently, we have shown that intramolecular triplet sensitization by an attached benzophenone can significantly enhance photosensitivity [145], and other results of these studies will be reported in the future.

1.1.4
Conclusion

Although caged compounds of the 2-nitrobenzyl type have been in use for 25 years, opportunities for modification of existing cages and extension to individual new caged effectors continue to arise. Hand in hand with this effort are mechanistic studies of particular compounds that clarify release rates of effectors and underline that the *aci*-nitro decay rate does not always correspond to the rate of product release. Development of the 7-nitroindoline cage has provided new opportunities that have begun to impact on neurophysiological research. Nevertheless, our understanding of many nuances of these photocleavage processes remains incomplete, for example, the failure adequately to explain the frequently observed biphasic rates of *aci*-nitro decay processes, the implications of the decarboxylation reactions observed for CNB cages, and the still somewhat unpredictable reactivity of the nitroindoline system. Several examples described in this chapter indicate that more attention should be paid to direct determination of product release rates, especially in cases where this is a critical parameter in physiological experiments. Progress with localized release by multi-photon uncaging makes this particularly important. If an end product is only released after a delayed series of dark reactions, the advantages of localized photolysis will be lost by diffusion of the photolytically generated intermediate. To conclude, cooperation between groups with separate expertise in chemistry, physiology, and optics is likely to deliver further improvements in reagents for the future.

References

1 J.E.T. Corrie, D.R. Trentham, In *Bioorganic Photochemistry*, H. Morrison, Ed., Wiley, New York, Vol. 2, pp 243–305, **1993**.

2 S.R. Adams, R.Y. Tsien, *Annu. Rev. Physiol.*, **1993**, *55*, 755–784.

3 J.H. Kaplan, *Annu. Rev. Physiol.*, **1990**, *52*, 897–914.

4 G. Marriott, Ed. *Methods in Enzymology*, Vol. 291, Academic Press, San Diego, **1998**.

5 A.P. Pelliccioli, J. Wirz, *Photochem. Photobiol. Sci.*, **2002**, *1*, 441–458.

6 R.S. Givens, P.G. Conrad, A.L. Yousef, J.I. Lee, In *CRC Handbook of Organic Photochemistry and Photobiology*, W. Horspool, F. Lenci, Eds., 2nd Edition, CRC Press, Boca Raton, pp 69.1–69.46, **2003**.

7 J.H. Kaplan, B. Forbush, J.F. Hoffman, *Biochemistry*, **1978**, *17*, 1929–1935.

8 J.A. McCray, L. Herbette, T. Kihara, D.R. Trentham, *Proc. Natl. Acad. Sci. USA.*, **1980**, *77*, 7237–7241.

9 Y.E. Goldman, M.G. Hibberd, J.A. McCray, D.R. Trentham, *Nature*, **1982**, *300*, 701–705.

10 H.A. Lester, J.M. Nerbonne, *Ann. Rev. Biophys. Bioeng.*, **1982**, *11*, 151–175.

11 A.M. Gurney, H.A. Lester, *Physiol. Rev.*, **1987**, *67*, 583–617.

12 G. Ciamician, P. Silber, *Chem. Ber.*, **1901**, *34*, 2040–2046.

13 B. Amit, D.A. Ben-Efraim, A. Patchornik, *J. Am. Chem. Soc.*, **1976**, *98*, 843–844.

14 S. Pass, B. Amit, A. Patchornik, *J. Am. Chem. Soc.*, **1981**, *103*, 7674–7675.

15 C.P. Holmes, *J. Org. Chem.*, **1997**, *62*, 2370–2380.

16 H. Thirlwell, J. Sleep, M.A. Ferenczi, *J. Muscle Res. Cell Motil.*, **1995**, *16*, 131–137.

17 M. Canepari, L. Nelson, G. Papageorgiou, J.E.T. Corrie, D. Ogden, *J. Neurosci. Methods*, **2001**, *112*, 29–42.

18 W. Denk, J.H. Strickler, W.W. Webb, *Science*, **1990**, *248*, 73–76.

19 N.I. Kiskin, R. Chillingworth, J.A. McCray, D. Piston, D. Ogden, *Eur. Biophys. J.*, **2002**, *30*, 588–604.

20 T. Furuta, S.S.H. Wang, J.L. Dantzker, T.M. Dore, W.J. Bybee, E.M. Callaway, W. Denk, R.Y. Tsien, *Proc. Natl. Acad. Sci. USA.*, **1999**, *96*, 1193–1200.

21 M. Matsuzaki, G.C.R. Ellis-Davies, T. Nemoto, Y. Miyashita, M. Iino, H. Kasai, *Nat. Neurosci.*, **2001**, *4*, 1086–1092.

22 M.A. Smith, G.C.R. Ellis-Davies, J.C. Magee, *J. Physiol.*, **2003**, *548*, 245–258.

23 M. Matsuzaki, N. Honkura, G.C.R. Ellis-Davies, H. Kasai, *Nature*, **2004**, *429*, 761–766.

24 J.W. Walker, G.P. Reid, J.A. McCray, D.R. Trentham, *J. Am. Chem. Soc.*, **1988**, *110*, 7170–7177.

25 Y. Zhao, Q. Zheng, K. Dakin, K. Xu, M.L. Martinez, W.H. Li, *J. Am. Chem. Soc.*, **2004**, *126*, 4653–4663.

26 R. Aarhus, K. Gee, H.C. Lee, *J. Biol. Chem.*, **1995**, *270*, 7745–7749.

27 B.E. Cohen, B.L. Stoddard, D.E. Koshland, *Biochemistry*, **1997**, *36*, 9035–9044.

28 J. Chen, G.D. Prestwich, *Tetrahedron Lett.*, **1997**, *38*, 969–972.

29 L. Qiao, A.P. Kozikowski, A. Olivera, S. Spiegel, *Bioorg. Med. Chem. Lett.*, **1998**, *8*, 711–714.

30 D.M. Rothman, M.E. Vázquez, E.M. Vogel, B. Imperiali, *Org. Lett.*, **2002**, *4*, 2865–2868.

31 C. Dinkel, O. Wichmann, C. Schultz, *Tetrahedron Lett.*, **2003**, *44*, 1153–1155.

32 C.G. Bochet, *Tetrahedron Lett.*, **2000**, *41*, 6341–6346.

33 A. Blanc, C.G. Bochet, *J. Org. Chem.*, **2002**, *67*, 5567–5577.

34 A. Blanc, C.G. Bochet, *J. Am. Chem. Soc.*, **2004**, *126*, 7174–7175.

35 S. Walbert, W. Pfleiderer, U.E. Steiner, *Helv. Chim. Acta*, **2001**, *84*, 1601–1611.

36 A. Hasan, K.P. Stengele, H. Giegrich, P. Cornwell, K.R. Isham, R.A. Sachleben, W. Pfleiderer, R.S. Foote, *Tetrahedron*, **1997**, *53*, 4247–4264.

37 M. Beier, A. Stephan, J.D. Hoheisel, *Helv. Chim. Acta*, **2001**, *84*, 2089–2095.

38 M.C. Pirrung, L. Wang, M.P. Montague-Smith, *Org. Lett.*, **2001**, *3*, 1105–1108.

39 R.W. Yip, D.K. Sharma, R. Giasson, D. Gravel, *J. Phys. Chem.*, **1985**, *89*, 5328–5330.

40 R.W. Yip, Y.X. Wen, D. Gravel, R. Giasson, D.K. Sharma, *J. Phys. Chem.*, **1991**, *95*, 6078–6081.

41 T. Luchian, S.H. Shun, H. Bayley, *Angew. Chem. Int. Ed.*, **2003**, *42*, 1926–1929.

42 A. Barth, J.E.T. Corrie, M.J. Gradwell, Y. Maeda, W. Mäntele, T. Meier, D.R. Trentham, *J. Am. Chem. Soc.*, **1997**, *119*, 4149–4159.

43 Y.V. Il'ichev, J. Wirz, *J. Phys. Chem. A*, **2000**, *104*, 7856–7870.

44 M. Schwörer, J. Wirz, *Helv. Chim. Acta*, **2001**, *84*, 1441–1457.

45 J.E.T. Corrie, A. Barth, V.R.N. Munasinghe, D.R. Trentham, M.C. Hutter, *J. Am. Chem. Soc.* **2003**, *125*, 8546–8554.

46 J.E.T. Corrie, *J. Chem. Soc., Perkin Trans. 1*, **1993**, 2161–2166.

47 L. Peng, M. Goeldner, *J. Org. Chem.*, **1996**, *61*, 185–191.

48 G.C.R. Ellis-Davies, J.H. Kaplan, R.J. Barsotti, *Biophys. J.*, **1996**, *70*, 1006–1016.

49 I.R. Dunkin, J. Gebicki, M. Kiszka, D. Sanin-Leira, *J. Chem. Soc., Perkin Trans. 2*, **2001**, 1414–1425.

50 J.E.T. Corrie, J. Baker, E.M. Ostap, D.D. Thomas, D.R. Trentham, *J. Photochem. Photobiol. A*, **1998**, *115*, 49–55.

51 J.E.T. Corrie, B.C. Gilbert, V.R.N. Munasinghe, A.C. Whitwood, *J. Chem. Soc., Perkin Trans. 2*, **2000**, 2483–2491.

52 L. Zhang, R. Buchet, G. Azzar, *Biophys. J.*, **2004**, *86*, 3873–3881.

53 L.J. Chen, L.T. Burka, *Tetrahedron Lett.*, **1998**, *39*, 5351–5354.

54 C. Diepold, P. Eyer, H. Kampffmeyer, K. Reinhardt, *Adv. Exp. Biol. Med.*, **1982**, *136B*, 1173–1181.

55 M.C. Pirrung, Y.R. Lee, K. Park, J.B. Springer, *J. Org. Chem.*, **1999**, *64*, 5042–5047.

56 J.D. Margerum, C.T. Petrusis, *J. Am. Chem. Soc.*, **1969**, *91*, 2467–2472.

57 C.D. Woodrell, P.D. Kehayova, A. Jain, *Org. Lett.*, **1999**, *1*, 619–621.

58 V. Jayaraman, S. Thiran, D.R. Madden, *FEBS Lett.*, **2000**, *475*, 278–282; Q. Cheng, M.G. Steinmetz, V. Jayaraman, *J. Am. Chem. Soc.*, **2002**, *124*, 7676–7677.

59 L.R. Makings, R.Y. Tsien, *J. Biol. Chem.*, **1994**, *269*, 6282–6285.

60 A. Srinivasan, N. Kebede, J.E. Saavedra, A.V. Nikolaitchik, D.A. Brady, E. Yourd, K.M. Davies, L.K. Keefer, J.P. Toscano, *J. Am. Chem. Soc.*, **2001**, *123*, 5465–5472.

61 Z.H. He, R.K. Chillingworth, M. Brune, J.E.T. Corrie, M.R. Webb, M.A. Ferenczi, *J. Physiol.*, **1999**, *517*, 839–854.

62 A. Barth, K. Hauser, W. Mäntele, J.E.T. Corrie, D.R. Trentham, *J. Am. Chem. Soc.*, **1995**, *117*, 10311–10316.

63 V. Hagen, C. Djeza, S. Frings, J. Bendig, E. Krause, U.B. Kaupp, *Biochemistry*, **1996**, *35*, 7762–7771.

64 V. Hagen, C. Djeza, J. Bendig, I. Baeger, U.B. Kaupp, *J. Photochem. Photobiol. B*, **1998**, *42*, 71–78.

65 L. Wang, J.E.T. Corrie, J.F. Wootton, *J. Org. Chem.*, **2002**, *67*, 3474–3478.

66 J. Pollock, J.H. Crawford, J.F. Wootton, J.E.T. Corrie, R.H. Scott, *Neurosci. Lett.*, **2003**, *338*, 143–146.

67 B.L. Stoddard, B.E. Cohen, M. Brubaker, A.D. Mesecar, D.L. Koshland, *Nat. Struct. Biol.*, **1998**, *5*, 891–897.

68 C.P. Salerno, M. Resat, D. Magde, J. Kraut, *J. Am. Chem. Soc.*, **1997**, *119*, 3403–3404.

69 C.P. Salerno, D. Magde, A.P. Patron, *J. Org. Chem.*, **2000**, *65*, 3971–3981.

70 S.G. Chaulk, A.M. MacMillan, *Nucl. Acids Res.*, **1998**, *26*, 3173–3178.

71 S.G. Chaulk, A.M. MacMillan, *Angew. Chem. Int. Ed.*, **2001**, *40*, 2149–2152.

72 H. Ando, T. Furuta, R.Y. Tsien, H. Okamoto, *Nat. Genet.*, **2001**, *28*, 317–325.

73 P. Ordoukhanian, J.S. Taylor, *Bioconjug. Chem.*, **2000**, *11*, 94–103.

74 K. Zhang, J.S. Taylor, *Biochemistry,* **2001**, *40*, 153–159.

75 A. Dussy, C. Meyer, E. Quennet, T.A. Bickle, B. Giese, A. Marx, *Chembiochem,* **2002**, *3*, 54–60.

76 Y. Shigeri, Y. Tatsu, N. Yumoto, *Pharmacol. Ther.,* **2001**, *91*, 85–92.

77 G. Marriott, P. Roy, K. Jacobson, *Methods Enzymol.,* **2003**, *360*, 274–288.

78 E.J. Petersson, G.S. Brandt, N.M. Zacharias, D.A. Dougherty, H.A. Lester, *Methods Enzymol.,* **2003**, *360*, 258–273.

79 C.J. Bosques, B. Imperiali, *J. Am. Chem. Soc.,* **2003**, *125*, 7530–7531.

80 D. Ramesh, R. Wieboldt, A.P. Billington, B.K. Carpenter, G.P. Hess, *J. Org. Chem.,* **1993**, *58*, 4599–4605.

81 Y. Tatsu, T. Nishigaki, A. Darszon, N. Yumoto, *FEBS Lett.,* **2002**, *525*, 20–24.

82 M.C. Pirrung, S.J. Drabik, J. Ahamed, H. Ali, *Bioconjug. Chem.,* **2000**, *11*, 679–681.

83 T. Okuno, S. Hirota, O. Yamamuchi, *Biochemistry,* **2000**, *39*, 7538–7545.

84 R. Golan, U. Zehavi, M. Naim, A. Patchornik, P. Smirnoff, M. Herchmann, *J. Protein Chem.,* **2000**, *19*, 117–122.

85 M.J. Brubaker, D.H. Dyer, B. Stoddard, D.E. Koshland, *Biochemistry,* **1996**, *35*, 2854–2864.

86 R. Wieboldt, K.R. Gee, L. Niu, D. Ramesh, B.K. Carpenter, G.P. Hess, *Proc. Natl. Acad. Sci. USA,* **1994**, *91*, 8752–8756.

87 K.R. Gee, R. Wieboldt, G.P. Hess, *J. Am. Chem. Soc.,* **1994**, *116*, 8366–8367.

88 K.R. Gee, L. Niu, K. Schaper, G.P. Hess, *J. Org. Chem.,* **1995**, *60*, 4260–4263.

89 C. Grewer, J. Jäger, B.K. Carpenter, G.P. Hess, *Biochemistry,* **2000**, *39*, 2063–2070.

90 K. Schaper, S.A.M. Mobarekeh, C. Grewer, *Eur. J. Org. Chem.,* **2002**, 1037–1046.

91 P. Molnár, J.V. Nadler, *Eur. J. Pharmacol.,* **2000**, *391*, 255–262.

92 K.R. Gee, L. Niu, V. Jayaraman, G.P. Hess, *Biochemistry,* **1999**, *38*, 3140–3147.

93 S. Ueno, J. Nabekura, H. Ishibashi, N. Akaike, T. Mori, M. Shiga, *J. Neurosci. Methods,* **1995**, *58*, 163–166.

94 J. Xia, X. Huang, R. Sreekumar, J.W. Walker, *Bioorg. Med. Chem. Lett.,* **1997**, *7*, 1243–1248.

95 P.J. Seranowski, P.B. Garland, *J. Am. Chem. Soc.,* **2003**, *125*, 962–965.

96 K. Yamaguchi, Y. Tsuda, T. Shimakage, A. Kusumi, *Bull. Chem. Soc. Jpn.,* **1998**, *71*, 1923–1929.

97 Z.Y. Zhang, B.D. Smith, *Bioconjug. Chem.,* **1999**, *10*, 1150–1152.

98 R.H. Scott, J. Pollock, A. Ayer, N.M. Thatcher, U. Zehavi, *Methods Enzymol.,* **2000**, *312*, 387–400.

99 J.E.T. Corrie, A. De Santis, Y. Katayama, K. Khodakhah, J.B. Messenger, D.C. Ogden, D.R. Trentham, *J. Physiol.,* **1993**, *465*, 1–8.

100 G. Papageorgiou, J.E.T. Corrie, *Tetrahedron,* **1997**, *53*, 3917–3932.

101 F.M. Rossi, M. Margulis, C.M. Tang, J.P.Y. Kao, *J. Biol. Chem.,* **1997**, *272*, 32933–32939.

102 D. Ramesh, R. Wieboldt, A.P. Billington, B.K. Carpenter, G.P. Hess, *J. Org. Chem.,* **1993**, *58*, 4599–4605.

103 S.A. Sundberg, R.W. Barrett, M. Pirrung, A.L. Lu, B. Kiangsoontra, C.P. Holmes, *J. Am. Chem. Soc.,* **1995**, *117*, 12050–12057.

104 M.C. Pirrung, C.Y. Huang, *Bioconjug. Chem.,* **1996**, *7*, 317–321.

105 S. Watanabe, R. Hirokawa, M. Iwamura, *Bioorg. Med. Chem. Lett.,* **1998**, *8*, 3375–3378.

106 R. Lux, V.R.N. Munasinghe, F. Castellano, J.W. Lengeler, J.E.T. Corrie, S. Khan, *Mol. Biol. Cell,* **1999**, *10*, 1133–1146.

107 Y.V. Il'ichev, M.A. Schwörer, J. Wirz, *J. Am. Chem. Soc.,* **2004**, *126*, 4581–4595.

108 R. Sreekumar, Y.Q. Pi, X.P. Huang, J.W. Walker, *Bioorg. Med. Chem. Lett.,* **1997**, *7*, 341–346.

109 V.G. Robu, E.S. Pfeiffer, S.L. Robia, R.C. Balijepalli, Y.Q. Pi, T.J. Kamp, J.W. Walker, *J. Biol. Chem.,* **2003**, *278*, 48154–48161.

110 J. W. WALKER, H. MARTIN, F. R. SCHMITT, R. J. BARSOTTI, *Biochemistry*, **1993**, *32*, 1338–1345.

111 S. MURALIDHARAN, J. M. NERBONNE, *J. Photochem. Photobiol. B*, **1995**, *27*, 123–137.

112 W. A. BOYLE, S. MURALIDHARAN, G. M. MAHER, J. M. NERBONNE, *J. Photochem. Photobiol. B*, **1997**, *41*, 233–244.

113 F. M. ROSSI, J. P. Y. KAO, *J. Biol. Chem.*, **1997**, *272*, 3266–3271.

114 Y. POCKER, B. L. DAVIDSON, T. L. DEITS, *J. Am. Chem. Soc.*, **1978**, *100*, 3564–3567.

115 C. DINKEL, C. SCHULTZ, *Tetrahedron Lett.*, **2003**, *44*, 1157–1159.

116 J. W. WALKER, J. FEENEY, D. R. TRENTHAM, *Biochemistry*, **1989**, *28*, 3272–3280.

117 J. F. WOOTTON, J. E. T. CORRIE, T. CAPIOD, J. FEENEY, D. R. TRENTHAM, D. C. OGDEN, *Biophys. J.*, **1995**, *68*, 2601–2607.

118 W. H. LI, J. LLOPIS, M. WHITNEY, G. ZLOKARNIK, R. Y. TSIEN, *Nature*, **1998**, *392*, 936–941.

119 D. OGDEN, T. CAPIOD, *J. Gen. Physiol.*, **1997**, *109*, 741–756.

120 R. REINHARD, B. F. SCHMIDT, *J. Org. Chem.*, **1998**, *63*, 2434–2441.

121 G. BONETTI, A. VECLI, C. VIAPPIANI, *Chem. Phys. Lett.*, **1997**, *269*, 268–273.

122 S. ABBRUZZETTI, C. VIAPPIANI, J. R. SMALL, L. J. LIBERTINI, E. W. SMALL, *Biophys. J.*, **2000**, *79*, 2714–2721.

123 S. KHAN, F. CASTELLANO, J. L. SPUDICH, J. A. MCCRAY, R. S. GOODY, G. P. REID, D. R. TRENTHAM, *Biophys. J.*, **1993**, *65*, 2368–2382.

124 A. BARTH, J. E. T. CORRIE, *Biophys. J.*, **2002**, *83*, 2864–2871.

125 G. C. R. ELLIS-DAVIES, *Methods Enzymol.*, **2003**, *360*, 226–238.

126 G. C. R. ELLIS-DAVIES, J. H. KAPLAN, R. J. BARSOTTI, *Biophys. J.*, **1996**, *70*, 1006–1016.

127 G. A. KRAFFT, W. R. SUTTON, R. T. CUMMINGS, *J. Am. Chem. Soc.*, **1988**, *110*, 301–303.

128 T. J. MITCHISON, K. E. SAWIN, J. A. THERIOT, K. GEE, A. MALLAVARAPU, Chapter 4 of Ref. [4].

129 K. R. GEE, E. S. WEINBERG, D. J. KOZLOWSKI, *Bioorg. Med. Chem. Lett.*, **2001**, *11*, 2181–2183.

130 R. JASUJA, J. KEYOUNG, G. P. REID, D. R. TRENTHAM, S. KHAN, *Biophys. J.*, **1999**, *76*, 1706–1719.

131 K. C. NICOLAOU, B. S. SAFINA, N. WINSSINGER, *Synlett*, **2001**, *SI*, 900–903.

132 C. HELGEN, C. G. BOCHET, *Synlett*, **2001**, 1968–1970.

133 K. VIZVARDI, C. KREUTZ, A. S. DAVIS, V. P. LEE, B. J. PHILMUS, O. SIMO, K. MICHAEL, *Chem. Lett.*, **2003**, *32*, 348–349.

134 C. HELGEN, C. G. BOCHET, *J. Org. Chem.*, **2003**, *68*, 2483–2486.

135 G. PAPAGEORGIOU, D. C. OGDEN, A. BARTH, J. E. T. CORRIE, *J. Am. Chem. Soc.*, **1999**, *121*, 6503–6504.

136 J. MORRISON, P. WAN, J. E. T. CORRIE, G. PAPAGEORGIOU, *Photochem. Photobiol. Sci.*, **2002**, *1*, 960–969.

137 G. PAPAGEORGIOU, J. E. T. CORRIE, *Tetrahedron*, **2000**, *56*, 8197–8205.

138 G. PAPAGEORGIOU, J. E. T. CORRIE, *Synth. Commun.*, **2002**, *32*, 1571–1577.

139 M. CANEPARI, G. PAPAGEORGIOU, J. E. T. CORRIE, C. WATKINS, D. OGDEN, *J. Physiol.*, **2001**, *533*, 765–772.

140 M. CANEPARI, D. OGDEN, *J. Neurosci.*, **2003**, *23*, 4066–4071.

141 G. LOWE, *J. Neurophysiol.*, **2003**, *90*, 1737–1746.

142 M. CANEPARI, C. AUGER, D. OGDEN, *J. Neurosci.*, **2004**, *24*, 3563–3573.

143 S. R. ADAMS, J. P. Y. KAO, R. Y. TSIEN, *J. Am. Chem. Soc.*, **1989**, *111*, 7957–7968.

144 K. O. HILLER, B. MASLOCH, M. GÖBL, K. D. ASMUS, *J. Am. Chem. Soc.*, **1981**, *103*, 2734–2743.

145 G. PAPAGEORGIOU, M. LUKEMAN, P. WAN, J. E. T. CORRIE, *Photochem. Photobiol. Sci.*, **2004**, *3*, 366–373.

1.2
**Coumarin-4-ylmethyl Phototriggers**

Toshiaki Furuta

1.2.1
Introduction

Coumarin-4-ylmethyl groups are newly developed phototriggers that have been used to make caged compounds of phosphates, carboxylates, amines, alcohols, phenols, and carbonyl compounds. Coumarin, the parent compound of the chromophore, is the common name of benzo-*a*-pyrone, highlighted in bold with numbering in Scheme 1.2.1. The photochemistry typifying coumarin-4-yl-methyls can be realized as that of a member of arylalkyl-type photo-removable protecting groups [1]. Upon photolysis, the C-heteroatom bond (mostly oxygen) between C-4 methylene and X (leaving groups) is cleaved to produce an anion of the leaving group and a solvent-trapped coumarin as a photo by-product.

This chapter presents an overview of spectroscopic and photochemical properties, and synthetic methods of the reported coumarin-type phototrigger structural variants. The application of coumarin phototriggers remains limited in number, but the importance of coumarins as potential replacements for conventional 2-nitrobenzyls has been accepted widely. References that have appeared through January 2004 will be addressed.

Studies of coumarins have mainly addressed the utilization of their fluorescent properties [2]: fluorescent labeling agents, fluorogenic enzyme substrates, and laser dyes. About 20 years ago, Givens and Matuszewski first noticed that a phosphate ester of (coumarin-4-yl)methanol is photosensitive [3]. A benzene solution of (7-methoxycoumarin-4-yl)methyl ester of diethylphosphate (MCM-DEP) was photolyzed with a quantum yield of 0.038. They also demonstrated its use as a fluorescent labeling agent for nucleophilic molecules (Nu) including proteins, suggesting generation of an electrophilic coumarin-4-ylmethyl cation upon photolysis (Scheme 1.2.2).
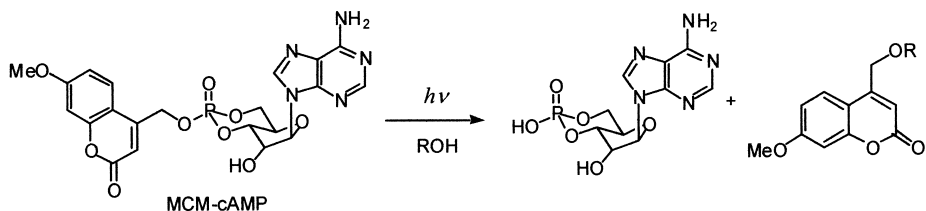
About 10 years later, the reaction was reinvestigated as a replacement for the 2-nitrobenzyl-type cages [4]. Photochemical properties of MCM-cAMP were compared to those of the 1-(2-nitrophenyl)ethyl and desyl ester of cAMP under a simulated physiological environment. MCM-cAMP was photolyzed to produce
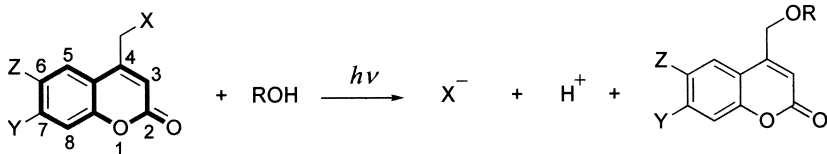
Scheme 1.2.1
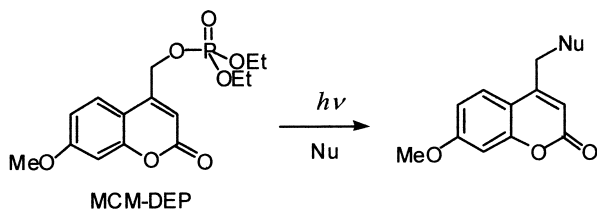
Scheme 1.2.2

Scheme 1.2.3

the parent cAMP with nearly quantitative yield upon 340-nm irradiation (Scheme 1.2.3). It also offers advantages over those reported previously, including improved stability in the dark and high photolytic efficiency [5]. From that time, MCM group and their structural variants, with their improved properties, have been synthesized and employed to produce several caged compounds, such as second messengers, neurotransmitters and DNA/RNA. Some of those caged compounds have been applied successfully to the investigation of cell chemistry.

1.2.2
Spectroscopic and Photochemical Properties

1.2.2.1 Overview
Fig. 1.2.1 shows structures of coumarin phototriggers reported thus far. They can be grouped into (1) 7-alkoxy group [3–18], (2) 6,7-dialkoxy group [14, 15, 18–21], (3) 6-bromo-7-alkoxy group [18, 22–29], and (4) 7-dialkylamino group

7-alkoxy group
MCM (R = CH$_3$)
HCM (R = H)
ACM (R = CH$_3$CO)
PCM (R = CH$_3$CH$_2$CO)
CMCM (R=CH$_2$CO$_2$H)

6,7-dialkoxy group
DMCM (R=CH$_3$)
BCMCM (R=CH$_2$CO$_2$H)
BECMCM (R = CH$_2$CO$_2$Et)

6-bromo-7-alkoxy group
Bhc (R = H)
Bhc/Ac (R = CH$_3$CO)

7-dialkylamino group
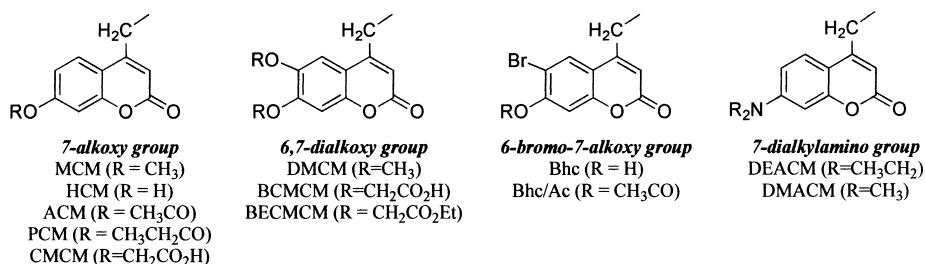DEACM (R=CH$_3$CH$_2$)
DMACM (R=CH$_3$)

Fig. 1.2.1 Structures and acronyms of coumarin-4-ylmethyl phototriggers.

[14, 15, 18, 30, 31] in view of their structural similarity. Photochemical and photophysical properties as well as physical properties of coumarin-caged compounds depend on the nature of the structure of attached molecules. Especially important are the types of functional groups to be protected. For that reason, the properties of each compound will be collected and their differences assessed one by one for each functional group. Notwithstanding, it would be useful to overview spectroscopic and photochemical properties of the four groups to emphasize their distinctions and differences.

Tab. 1.2.1 summarizes the reported photochemical and photophysical properties of the four groups. The absorption properties of the groups differ remarkably. Absorption spectra of the four coumarin-4-ylmethanols – (7-methoxycoumarin-4-yl)methanol (MCM-OH), (6,7-dimethoxycoumarin-4-yl)methanol (DMCM-OH), (6-bromo-7-hydroxycoumarin-4-yl)methanol (Bhc-OH) and (7-diethylaminocoumarin-4-yl)methanol (DEACM-OH) – which represent the four groups as well as 4,5-dimethoxy-2-nitrobenzyl alcohol (NVOC-OH) were recorded in a simulated physiological environment (Fig. 1.2.2; M. Kawamoto, T. Watanabe, unpublished results). The parent coumarin-4-ylmethanol has its absorption maximum at 310 nm [15], whereas an electron-donating substitution on the C6 or C7 of the coumarin ring shifts the absorption maximum to longer wavelengths. The dialkylamino substitution on the C7 produces a strong red
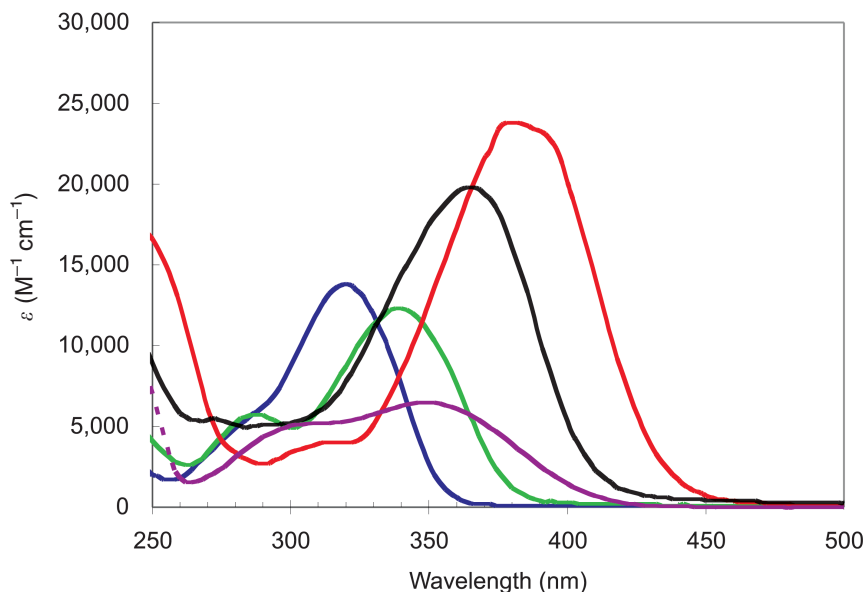

Fig. 1.2.2 UV/Vis spectra of coumarin-4-ylmethanols in KMOPS (pH 7.2). Red: DEACM-OH; Black: Bhc-OH; Green: DMCM-OH; Blue: MCM-OH; Purple: NVOC-OH, 337: N_2 laser (337 nm), 355: YAG laser (355 nm), 364: Ar laser (364 nm), 405: blue laser (405 nm). BP 330–385: transparent wavelength range of a wide band pass filter BP 330–385.

Tab. 1.2.1 Spectroscopic and photochemical properties of the coumarin phototriggers

Groups[a]	7-Alkoxy MCM, HCM, ACM, PCM and CMCM	6,7-Dialkoxy DMCM, BCMCM and BECMCM	6-Bromo-7-alkoxy Bhc and Bhc/Ac	7-Dialkylamino DEACM and DMACM
λ_{max}[b]	325	345	375[c]	395
ε_{max}[d]	4000–12000	10000–12000	13000–19000	16000–20000
Φ_{chem}[e]	ca. 0.1	ca. 0.1	ca. 0.1	ca. 0.3
k[f]	ca. 10^8			ca. 10^9
λ_{em}[g] (Φ_f[h])	394 (0.65)	438 (0.59)	465 (0.61)	484 (0.082) 491 (0.21)
Light sources[i]	Xe, Hg, 337	Xe, Hg, 355, 364	Xe, Hg, 355, 364, 405	Xe, Hg, 364, 405
Functional groups[i]	P, C, S, Al	P, Al	P, C, Am, Al, Ph	P, Al
Comments	ACM and PCM are membrane permeable. CMCM has high water solubility	BECMCM is membrane permeable. BCMCM has high water solubility	Bhc/Ac is membrane permeable. Bhc has high 2-photon absorption cross-sections	Can be activated by longer wavelength UV/vis with improved efficiency
Refs.	3–18	14, 15, 18–21	18, 22–29	14, 15, 18, 30–32

a) The acronyms and full IUPAC nomenclature are: MCM, (7-methoxycoumarin-4-yl)methyl; HCM, (7-hydroxycoumarin-4-yl)methyl; ACM, (7-acetoxycoumarin-4-yl)methyl; PCM, (7-propionyloxycoumarin-4-yl)methyl; CMCM, (7-carboxymethoxycoumarin-4-yl)methyl; BCMCM, [6,7-bis(carboxymethoxy)coumarin-4-yl]methyl; BECMCM, [6,7-bis(ethoxycarbonylmethoxy)coumarin-4-yl]methyl; DMCM, (6,7-dimethoxycoumarin-4-yl)methyl; DMACM, (7-dimethylaminocoumarin-4-yl)methyl; DEACM, (7-diethylaminocoumarin-4-yl)methyl; and Bhc, (6-bromo-7-hydroxycoumarin-4-yl)methyl.
b) Absorption maximum (nm).
c) at pH 7. The value depends on a pH.
d) Molar absorptivity ($M^{-1}cm^{-1}$).
e) Quantum yields for disappearance of starting materials upon irradiation.
f) Rate constants of photolysis (s^{-1}).
g) Emission maxima (nm) of the MCM-OH, DMCM-OH, Bhc-OH, DEACM-OH, and DMACM-OH.
h) Fluorescence quantum yield.
i) Possible light sources. Xe: Xe lamps, Hg: Hg lamps, 337: N_2 laser (337 nm), 355: YAG laser (355 nm), 364: Ar laser (364 nm), 405: blue laser (405 nm)
j) Functional groups that have been caged. P: phosphates, C: carboxylates, S: sulfates, Al: alcohols, Am: amines, Ph: phenols.

shift of more than 80 nm. Bhc group was designed to lower the pKa of the C7 hydroxyl group so that the O-H bond is deprotonated at pH 7, causing a red shift of the absorption maximum by 60 nm.

Substantial overlaps between emission profiles of light sources and absorption profiles of phototriggers are necessary to achieve maximum photolysis efficiency. Therefore, ideal wavelength regions for excitations are 300–340 nm for

the MCM, 320–360 nm for the DMCM, 330–420 nm for the Bhc, and 350–450 nm for the DEACM groups. Regarding cell biological applications, photoactivation is usually done by fluorescent microscopes equipped with an extra light source for photoactivation, including a Xe lamp with a band pass UV filter (for example, BP 330–385) and a UV laser. Light sources for epi-illumination can also be used for photoactivation. Tab. 1.2.1 shows possible light sources for each group and wavelengths.

Most coumarins have strong fluorescence, which may overlap with emission spectra of some fluorescent probes and cause difficulties in monitoring specific effects by fluorescence imaging after photoactivation. Tab. 1.2.1 summarizes emission maximum wavelengths and fluorescence quantum yields of the representative photo-byproducts 4-hydroxymethylcoumarins.

Overall, coumarin-type phototriggers offer the following advantages over other phototriggers: (1) large extinction coefficient at the wavelength greater than 350 nm; (2) high photolysis efficiency upon UV irradiation; (3) acceptable stability in the dark; (4) fast photolysis kinetics; and (5) practically useful 2-photon excitation cross-sections. Furthermore, the absorption properties, membrane permeability, and water solubility can be optimized easily by the nature of substitutions on the coumarin ring. In addition, diverse collections of phototriggers are already available.

1.2.2.2 Phototriggers

1.2.2.2.1 MCM Groups: 7-Alkoxy-Substituted Coumarins

Each group has a membrane-permeable and a water-soluble structural variant. They are designed to facilitate methods to incorporate the compounds into biological systems. The MCM family comprises the MCM, ACM, PCM, HCM, and CMCM groups. Most compounds reported to date are phosphate esters. Groups can also cage carboxylates, sulfates, and alcohols. The ACM and the PCM groups are designed to improve membrane permeability. After incorporation into live cells by simple diffusion, acetyl (or propionyl) moiety would be hydrolyzed by intrinsic esterases to produce a more polar HCM group that has almost no membrane permeability and might accumulate inside cells [6, 7]. Carboxylic acid in the CMCM group is almost fully ionized at a physiological pH. Consequently, CMCM-caged compounds should be highly water-soluble [14, 16]. All members have a single alkoxy substitution at the C7 position. They also have similar absorption and photochemical properties as summarized in Tab. 1.2.1. Typical values of the absorption maximum wavelength are around 325 nm with molar absorptivity of 4000 to 12 000 $M^{-1}cm^{-1}$; the value varies depending on molecular structures. Photolysis quantum yields were as high as 0.1, implying that the efficiency of photolysis, $\Phi\varepsilon$, the product of photolysis quantum yield and molar absorptivity, would be up to 1000. That value is more than one order of magnitude larger than those of 2-nitrobenzyls when photolysis is done at around 325 nm. Early examples using MCM-type phototriggers proved advanta-

geous over others [5, 11–13]. Nevertheless, the absorption maximum at 325 nm is not ideal for cell biological applications. For that reason, new structural variants with longer absorption maxima have been developed: longer than 350 nm is desirable.

1.2.2.2.2 DMCM Groups: 6,7-Dialkoxy-Substituted Coumarins

The family consists of BCMCM, BECMCM, and DMCM groups, and is utilized to make caged compounds of phosphates and alcohols [14, 15, 18–21]. The BCMCM group has two carboxylic acids and renders the corresponding caged compounds highly water soluble [14]. The BECMCM is the membrane-permeable version of BCMCM. The two carboxylic acids in BCMCM are converted to ethyl esters in BECMCM, and the negative charges are thereby masked. Hydrolysis of the ethyl esters by intrinsic esterases is postulated after the compound is incorporated into live cells [20]. Tab. 1.2.1 summarizes the spectroscopic and photochemical properties of the groups. Longer-wavelength absorption maxima were red shifted by 20 nm compared to those of the MCM-type. Single alkoxy substitution on C6 must be responsible for the red shift because Eckardt et al. reported that introduction of an electron-donating substitution on the C6 position, not C7, causes a large red shift of the absorption maxima [15]. For unknown reasons, photolysis quantum yields of the DMCM groups are always lower than those of the corresponding MCM analogs. These results show that overall photochemical properties closely resemble, or are even worse than, those of the MCM groups. Therefore, no compelling reason exists for using the DMCM groups instead of the MCM groups.

1.2.2.2.3 Bhc Groups: 6-Bromo-7-alkoxy-Substituted Coumarins

The Bhc group has been applied to cage carboxylates, amines, phosphates, alcohols, and carbonyl compounds [18, 22–29]. It has already been proved to be a replacement for conventional 2-nitrobenzyl-type phototriggers. The Bhc group can add a substantial amount of water solubility to corresponding caged compounds because most C7 phenolic hydroxyl moiety in the Bhc is ionized at physiological pH. On the other hand, caged compounds having Bhc/Ac, in which the C7 hydroxyl is masked by acetylation, accumulate remarkably inside live cells, as in the case of their debromo analog, ACM. Results show that the Bhc group can render a target molecule either water soluble or membrane permeable [28, 29]. These are advantages of the Bhc group over other phototriggers, including other members of coumarins, because no single phototrigger, except for Bhc, satisfies all the following criteria: (1) has a strong absorption band at more than 350 nm; (2) has a substantially high photolysis quantum yield; (3) has a practically usable stability; (4) renders a target molecule water soluble; and (5) adds membrane permeability by simple modification. Another advantage that must be noted is its two-photon chemistry. Two-photon-induced uncaging action cross-

sections of the Bhc caged glutamates were reported to be almost 1 GM upon 740-nm irradiation, which is more than two orders of magnitude larger than those of the 2-nitrobenzyls [22].

The Bhc group was designed to solve problems observed with the HCM group. The HCM group has two absorption maxima: one at around 325 nm corresponds to the protonated form of C7 hydroxyl moiety; the other, at 375 nm, corresponds to the ionized form. The protonated form is predominant at a physiological pH (pH 7) because the pKa of the C7 hydroxyl is 7.9. Consequently, its absorption maximum at 325 nm is larger than that at 375 nm. Introduction of an electron-withdrawing group into C6 should enhance acidity of the C7 phenolic oxygen through an inductive effect. In fact, the introduction of bromo substitution on C6 caused the lowering of the pKa by almost two units. Therefore, the Bhc group has a single absorption maximum at around 375 nm with a large molar absorptivity (ca. 19 000 $M^{-1}cm^{-1}$) under a simulated physiological environment (Fig. 1.2.2). Moreover, the bromine atom is known to accelerate the rate of intersystem crossing (heavy atom effect), leading to the increase in the fraction of excited triplet state. We compared photolysis quantum yields of the four types of coumarin-caged acetates with or without halogen substitutions: HCM-OAc, Bhc-OAc, Chc-OAc, and tBhc-OAc (see Fig. 1.2.5 for structures). Single bromine substitution increased the photolysis quantum yield by 150% (HCM vs Bhc), whereas a chloro substitution, which has almost no heavy atom effect, decreased it by 40% (HCM vs Chc). These results suggest that: (1) introduction of an electron-withdrawing substitution on HCM is unfavorable for the photolysis reaction, probably because it interferes with a through-bond electron transfer from the C7 oxygen to the C2 carbonyl at an electronically excited state (see a proposed mechanism of the reaction); (2) a heavy-atom effect of a bromine atom might compensate for this unfavorable electronic interaction, suggesting the existence of a triplet state as a reactive excited state. The existence of this state is further supported by the fact that 3,6,8-tribromo-7-hydroxycoumarin-4-ylmethyl (tBhc) acetate was photolyzed with a quantum yield of 0.065, which corresponds to 260% enhancement (HCM vs tBhc).

The absorption maximum of the Bhc group would be blue shifted by 40–50 nm if photolysis were performed under an environment where the protonated form is predominant. This blue shift would occur because the large absorption band at 375 nm comes from the ionized form of the C7 hydroxyl moiety, which has a pKa of 6.2. That consequent blue shift of the group might be disadvantageous if the compound is applied to an acidic compartment such as those in mitochondria.

1.2.2.2.4 DEACM Groups: 7-Dialkylamino-Substituted Coumarins

Dialkylamino substitution on C7 improved the spectroscopic and the photochemical properties remarkably. The absorption maxima are at 390–400 nm with a molar absorptivity of 20 000 M^{-1} cm^{-1}. Photolysis quantum yields are as high as 0.3, which is the highest among the reported coumarin cages. No remarkable difference is apparent between the dimethylamino (DMACM) and the

diethylamino (DEACM) variants, except that the fluorescence intensity of the DEACM-OH Φ_f=0.082) is considerably smaller than that of the DMACM-OH Φ_f=0.21) [15]. Reported applications of the group to caging chemistry were limited to phosphates [14, 15, 30–32] and alcohols [18]. However, the observed spectroscopic and photochemical properties were highly desirable. For those reasons, the group must be considered as a potential replacement for conventional 2-nitrobenzyl phototriggers. Taking account of the structural similarity to the Bhc group, the DEACM group must be used to protect carboxylates, amines, diols, and carbonyl compounds. Although no structural variants other than DEACM and DMACM are reported at present, modification to enhance water solubility or improve membrane permeability is possible.

1.2.2.3 **Target Molecules**

1.2.2.3.1 **Phosphates**

Caged phosphates are the most successful applications of coumarin phototriggers. Hagen, Bendig, and Kaupp's group has contributed generously to the knowledge of coumarin-caged phosphate chemistry. Their studies have mainly focused on caged cyclic nucleotides; related topics will be discussed in other sections. In this chapter, representative examples of each structural variant will be examined to elucidate their differences and similarities. Reported caged phosphates are cAMP [5–7, 13–15, 19–21, 28, 29], cGMP [13, 14, 20, 21, 28, 29], 8-Br-cAMP [10, 12, 32], 8-Br-cGMP [10–12, 32], cytidine-5′-diphosphate (CDP) [30], adenosine-5′-monophosphate (AMP), adenosine-5′-diphosphate (ADP), adenosine-5′-triphosphate (ATP) [31], DNA, and RNA [23] (Fig. 1.2.3). Tab. 1.2.2 summarizes selected examples of spectroscopic and photochemical properties.

For cyclic nucleotides, all variations are available. Slight but acceptable differences were observed between axial and equatorial isomers: the axial isomers have larger photolytic quantum yields and better stabilities in an aqueous solution in most cases. The CMCM-cNMPs [14] showed highest water solubility (200–1000 μM); the second carboxylate in the BCMCM contributes almost nothing to solubility. DEACM-cNMPs [14] have the largest photolysis quantum yields (Φ of ca. 0.21) among the coumarin-caged cNMPs. Moreover, they provide fast kinetics for the cNMP release ($k > 10^9$ s^{-1}). Bhc-cNMPs [28] showed good photosensitivity under one- and two-photon excitation conditions and a certain water solubility. In addition, they can be converted to membrane-permeable derivatives by acetylation. One can choose compounds having appropriate properties for a variety of situations. Suggested guidelines for the selection of suitable compounds could include the following:

(1) photo-activated by Xe or Hg lamp with wide-band U-filter (330–385 nm): desirable – Bhc and DEACM
(2) photo-activated by YAG (355 nm) laser: desirable – Bhc and DEACM
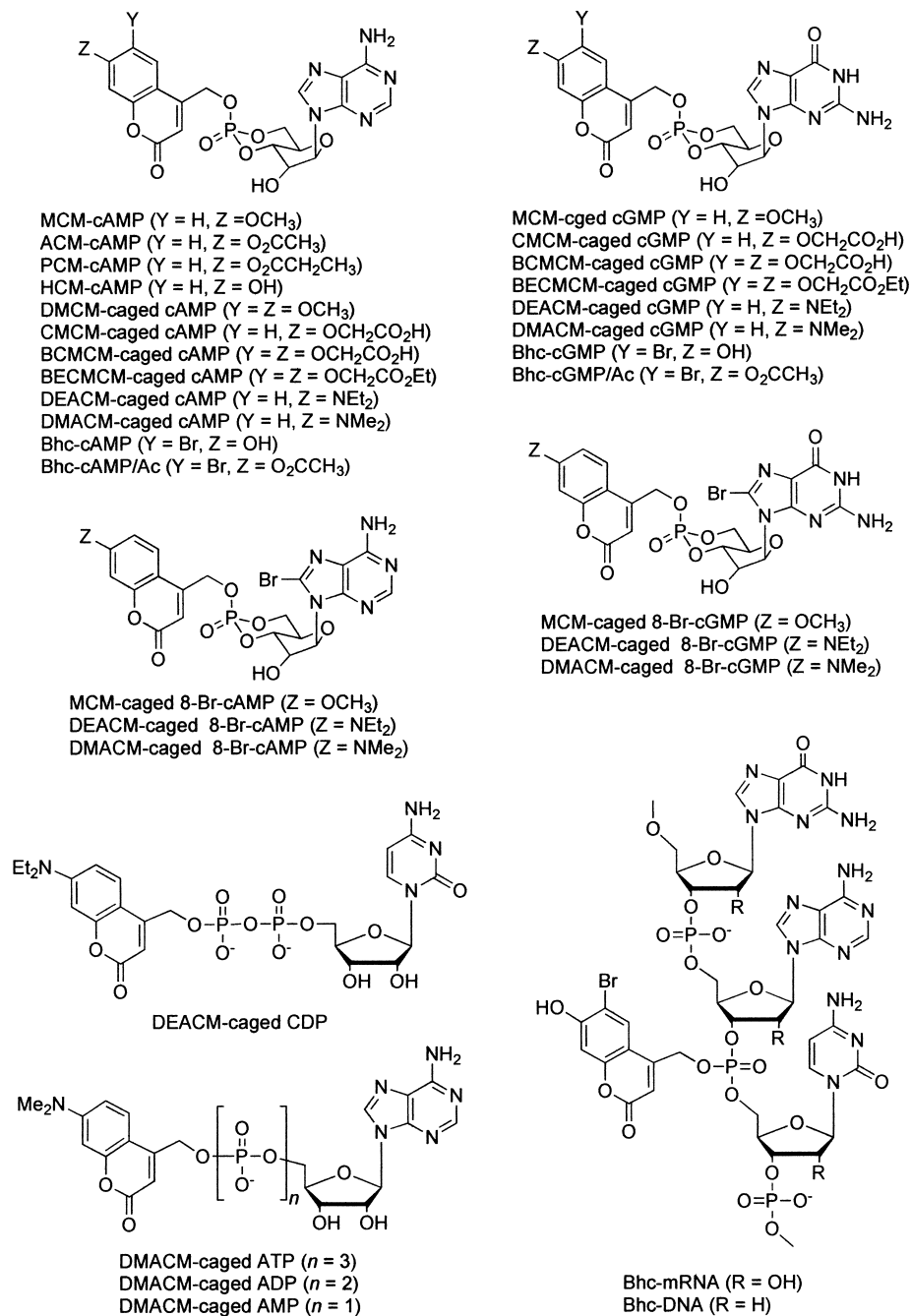(3) photo-activated by 405 nm laser: desirable – DEACM; usable – Bhc

MCM-cAMP (Y = H, Z =OCH$_3$)
ACM-cAMP (Y = H, Z = O$_2$CCH$_3$)
PCM-cAMP (Y = H, Z = O$_2$CCH$_2$CH$_3$)
HCM-cAMP (Y = H, Z = OH)
DMCM-caged cAMP (Y = Z = OCH$_3$)
CMCM-caged cAMP (Y = H, Z = OCH$_2$CO$_2$H)
BCMCM-caged cAMP (Y = Z = OCH$_2$CO$_2$H)
BECMCM-caged cAMP (Y = Z = OCH$_2$CO$_2$Et)
DEACM-caged cAMP (Y = H, Z = NEt$_2$)
DMACM-caged cAMP (Y = H, Z = NMe$_2$)
Bhc-cAMP (Y = Br, Z = OH)
Bhc-cAMP/Ac (Y = Br, Z = O$_2$CCH$_3$)

MCM-cged cGMP (Y = H, Z =OCH$_3$)
CMCM-caged cGMP (Y = H, Z = OCH$_2$CO$_2$H)
BCMCM-caged cGMP (Y = Z = OCH$_2$CO$_2$H)
BECMCM-caged cGMP (Y = Z = OCH$_2$CO$_2$Et)
DEACM-caged cGMP (Y = H, Z = NEt$_2$)
DMACM-caged cGMP (Y = H, Z = NMe$_2$)
Bhc-cGMP (Y = Br, Z = OH)
Bhc-cGMP/Ac (Y = Br, Z = O$_2$CCH$_3$)

MCM-caged 8-Br-cGMP (Z = OCH$_3$)
DEACM-caged 8-Br-cGMP (Z = NEt$_2$)
DMACM-caged 8-Br-cGMP (Z = NMe$_2$)

MCM-caged 8-Br-cAMP (Z = OCH$_3$)
DEACM-caged 8-Br-cAMP (Z = NEt$_2$)
DMACM-caged 8-Br-cAMP (Z = NMe$_2$)

DEACM-caged CDP

DMACM-caged ATP (*n* = 3)
DMACM-caged ADP (*n* = 2)
DMACM-caged AMP (*n* = 1)

Bhc-mRNA (R = OH)
Bhc-DNA (R = H)

Fig. 1.2.3 Coumarin-caged phosphates.

Tab. 1.2.2 Spectroscopic and photochemical properties of coumarin-caged phosphates

Compounds	λ_{max} (ε)	Φ_{dis}[a]	Φ_{app}[b]	k[c]	$t_{1/2}$[d]	s[e]	Comments	Refs.
MCM-cAMP (ax)	325[f] (13 300)	0.12[g]	0.10[g]	4.2	1000[g]			5, 13
MCM-cGMP (ax)[h]	327 (13 300)	0.21						13
MCM-cGMP (eq)[h]	325 (13 300)	0.092						13
MCM-8-Br-cAMP (ax)	326[h] (13 500)	0.14[h]		0.25	>400[h]	20[i]		12
ACM-cAMP	313[f] (7650)	0.056[g]					membrane permeable	7
PCM-cAMP	313[f] (6500)	0.054[g]					membrane permeable	7
HCM-cAMP	326[f] (16 800)	0.062[g]			28.8 (a) 18.9 (e)			7
CMCM-caged cAMP (ax)[j]	326 (12 500)	0.12				900	equatorial isomer is less soluble (200 μM)	14
CMCM-caged cGMP (ax)[j]	326 (11 700)	0.16				350	equatorial isomer is more soluble (>1000 μM)	14
DMCM-caged cAMP (ax)[j]	349 (11 000)	0.04						15
BCMCM-caged cAMP (ax)[j]	346 (10 700)	0.10				500	equatorial isomer is more soluble (1000 μM)	14
DEACM-caged cAMP (ax)	402[i] (18 600)	0.21[h]		>1		135[i]	equatorial isomer is less soluble (15 μM)	14
DEACM-CDP[i]	392 (16 200)	0.029		0.2				30
DMACM-ATP[i]	385 (14 300)	0.072		1.6				31
DMACM-ADP[i]	385 (15 000)	0.063						31
DMACM-AMP[i]	385 (15 300)	0.072						31
Bhc-mRNA[k]	333, 383							23

Bhc-cAMP (eq)[l]	374 (16 300)	0.11	0.10	90	axial isomer is more stable ($t_{1/2} = 260$ h)	28
Bhc-cGMP (eq)[l]	374 (15 300)	0.12	0.12	420	axial isomer is more stable ($t_{1/2} = 1240$ h)	28

a) Quantum yields for disappearance of starting materials upon irradiation.
b) Quantum yields for appearance of the starting material.
c) Rate constants of photolysis ($\times 10^9$ s^{-1}).
d) Half-life (h) in the dark.
e) Solubility (μM).
f) In CH$_3$OH.
g) In DMSO/Ringer's solution (1/99) pH 7.4.
h) In CH$_3$OH/HEPES-KCl buffer (20/80) pH 7.2.
i) CH$_3$CN/HEPES-KCl buffer (5/95) pH 7.2.
j) In HEPES-KCl buffer pH 7.2.
k) In Tris-HCl pH 7.4.
l) In DMSO/KMOPS (0.1/99.9) pH 7.2.

(4) photo-activated by Ti-Sapphire laser (720–820 nm): Bhc
(5) highly water soluble: desirable – CMCM and BCMCM; usable – Bhc
(6) membrane permeable: Bhc/Ac, PCM, ACM and BECMCM

Hagen and Bendig's group (Fig. 1.2.4) proposed a mechanism for photolytic cleavage of MCM-, DMCM-, and DEACM-caged phosphates [13–15]. The mechanism involves heterolysis of the CH_2-OP bond from the lowest excited singlet state (S_1), an escape of the resulting ion pairs from the solvent cage, and trapping of the coumarin-4-ylmethyl cation by the solvent. Several pieces of evidence collected for photolysis of MCM-caged phosphates supported the mechanism. (1) A photoproduct aside from the parent phosphate was a (7-methoxycoumarin-4-yl)methanol (MCM-OH) when the photolysis was performed in an aqueous solution. (2) Photolysis of MCM-DEP in ^{18}O-labeled water resulted in incorporation of [18]O only in the MCM-OH, confirming that the reaction proceeded via the photo S_N1 mechanism and not by the photo solvolysis reaction. (3) No phosphorescence was detected from any of the MCM-caged compounds. (4) Only traces (<0.5%) of 4-methyl-7-methoxycoumarin, which is derived from homolysis pathway, were detected.

The fluorescence quantum yield of the MCM-cAMP (ax) is 0.030, whereas that of the MCM-OH is 0.65. Therefore, a strong fluorescence enhancement was observed as photolysis proceeded. Similar behavior was observed for other coumarin phototriggers. Measurement of the increased fluorescence would allow estimation of the amount of photochemically released cAMP because the fluorescence intensity is directly proportional to the molar fraction of the liberated MCM-OH (and therefore the liberated cAMP). However, fluorescence of MCM-OH was quenched completely in HEK 293 cells. Consequently, it could not be used for estimation.

The strong fluorescent property of the liberated coumarin-4-ylmethanol allows estimation of the rate constant of photolysis reaction. Thereby, the rate constants for the photolysis of the DEACM and the DMACM caged cyclic nucleotides were determined as $k = 10^9 \, s^{-1}$, i.e., the concentration jump of the parent cyclic nucleotides occurred within a nanosecond.
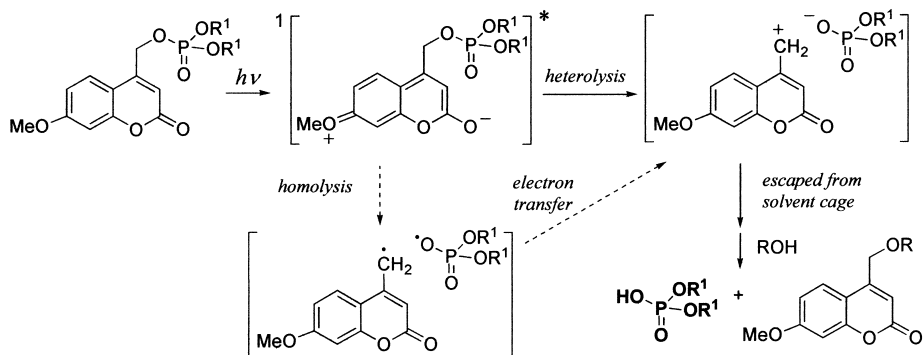

Fig. 1.2.4 Proposed mechanism of the photolysis of MCM-caged phosphates.

1.2.2.3.2 **Carboxylates and Sulfates**

Although coumarin-4-ylmethyl esters of carboxylates and sulfates should undergo analogous photochemistry to that of the phosphate esters, only a few examples have been reported so far (Fig. 1.2.5), partly because of the reported low photolysis efficiencies of the MCM esters of simple aliphatic acids. For example, the photolysis quantum yield for the MCM ester of heptanoic acid (MCM-OHep) is 0.0043 [13], which is more than one order of magnitude smaller than that of MCM-phosphates. The first successful application was the Bhc-caged glutamate [22]. The photolytic quantum yield of the Glu(γ-Bhc) was 0.019. The overall uncaging efficiency ($\Phi\varepsilon$) was more than one order of magnitude larger than that of the CNB- and the DMNPE-Glu. This difference indicates that the uncaging light intensity could be reduced 10-fold when Bhc-caged glutamates were used. The 2-photon uncaging action cross-sections of the Glu(γ-Bhc) were 0.89 GM at 740 nm and 0.42 GM at 800 nm, which are both more than two orders of magnitude larger than those of the conventional 2-nitrobenzyl caged compounds. Tab. 1.2.3 summarizes selected examples of spectroscopic and photochemical properties.

Low photosensitivity of the MCM ester can be overcome when a carboxylic acid with higher acidity is used. MCM and CMCM esters of α-amino acid derivatives were photolyzed with reasonably high quantum yields: 0.06 for MCM-TBOA and 0.04 for CMCM-TBOA [16], which is ten times as large as that of the MCM-OHep. A typical pKa value of α-carboxylate in α-amino acid is around two, which is lower than that of a simple aliphatic acid by two units: it approaches the pK_a of a phosphate. Differing acidities among simple aliphatic and α-amino acids must partially explain the variations in the quantum yields. Another matter for consideration is solvent polarity. Photolytic efficiencies of coumarin-caged phosphates [13] and carbonates [18] are less favorable when photo-
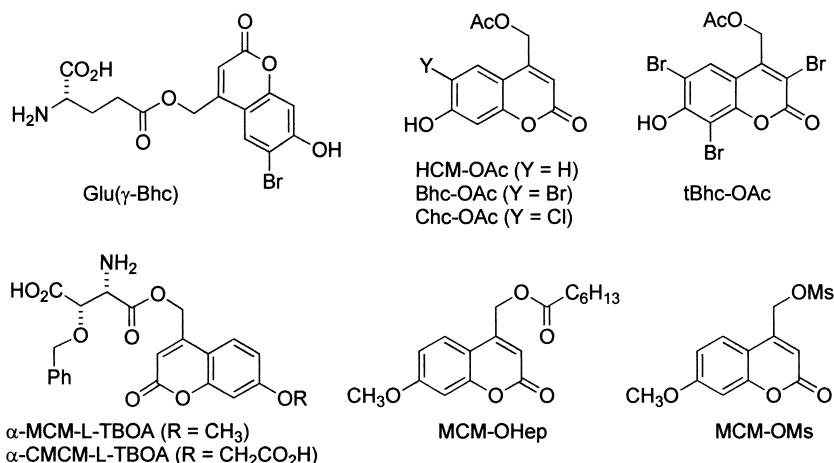

Fig. 1.2.5 Coumarin-caged carboxylates and sulfate.

Tab. 1.2.3 Spectroscopic and photochemical properties of coumarin-caged compounds

Compounds	λ_{max} (ε)	Φ_{dis} [a]	Φ_{app} [b]	k [c]	$t_{1/2}$ [d]	δ_u [e]	Refs.
Carboxylates							
MCM-OHep	324[f] (13 500)	0.0043[g]		0.0030			13
Glu(γ-Bhc)[h]	369 (19 550)	0.019			50	0.89 (740)	22
						0.42 (800)	
HCM-OAc[h]	325 (11 600)	0.025					22
Bhc-OAc[h]	370 (15 000)	0.037			183	1.99 (740)	22
						0.42 (800)	
Chc-OAc[h]	370 (16 000)	0.01					22
tBhc-OAc[h]	397 (15 900)	0.065			218	0.96 (740)	22
						3.1 (800)	
α-MCM-L-TBOA[i]	325 (4300)	0.06					16
α-CMCM-L-TBOA[i]	325 (4600)	0.04					16
Sulfates							
MCM-OMs	325[f] (13 000)	0.081[g]		0.41			13
Amines							
Bhcmoc-Glu[h]	368 (17 470)	0.019			stable after 35 h	0.95 (740)	22
						0.37 (800)	
MCM-NBu$_3$[j]	344 (11 700)	0.39					9
Alcohols and Phenols							
MCMoc-Gal[h]	322 (12 100)	0.020					18
DMCMoc-Gal[h]	344 (10 800)	0.0065					18
DEACM-Gal[h]	396 (17 300)	0.0058					18
Bhcmoc-Gal[h]	374 (15 000)	0.015					18
Bhcmoc-diC$_8$	343[h] (11 600)	0.014[h]			37[h]		18
	380[k] (15 000)	0.2[k]					27
Tyr(Bhcmoc)-OMe[h]	372 (13 900)	0.022	0.020		38		18
Bhcmoc-Adenosine[h]	373 (13 700)	0.012	0.010		467		18
Bhcmoc-Phenol[h]	372 (17 900)	0.067					18
Bhc-acetal[l]		0.028			stable after 2 weeks		24
Carbonyls							
Bhc-diol-acetophenone[h]	370 (18 000)	0.030				1.23 (740)	26
Bhc-diol-benzaldehyde[h]	370 (18 000)	0.057				0.90 (740)	26

a) Quantum yields for disappearance of starting materials upon irradiation.
b) Quantum yields for appearance of the starting material.
c) Rate constants of photolysis ($\times 10^9$ s^{-1}).
d) Half-life (h) in the dark.
e) Two-photon uncaging action cross sections ($\times 10^{-50}$ cm^4 s/photon, GM).
f) In CH$_3$CN/HEPES-KCl buffer (30/70) pH 7.2.
g) In CH$_3$OH/HEPES-KCl buffer (20/80) pH 7.2.
h) In DMSO/KMOPS (0.1/99.9) pH 7.2.
i) In PBS (+) solution.
j) In benzene.
k) In ethanol/Tris (50/50) pH 7.4.
l) In CH$_3$OH/HEPES-KCl (50/50) pH 7.4.

lysis is performed in an organic solvent. The solvent effect must be another reason for the lower quantum yield observed for MCM-OHep. The observed quantum yield of 0.0043 would improve if the reaction were performed in a 100% aqueous environment because the reaction of MCM-OHep was investigated in the presence of 20% methanol. In fact, HCM-OAc has a photolytic quantum yield of 0.025 in an aqueous buffer [22]. The reactions of the MCM- and the CMCM-TBOAs were performed in PBS. Therefore, photochemical properties of MCM esters of carboxylates must be reinvestigated under a simulated physiological environment.

1.2.2.3.3 **Amines**

Both carbamate and alkyl ammonium salts have been reported (Fig. 1.2.6). Although the examples remain limited to the Bhcmoc (6-bromo-7-hydroxycoumarin-4-ylmethoxycarbonyl) group [22, 25], coumarin-4-ylmethoxycarbonyls can serve as phototriggers of an amino group, such as aliphatic amines, amino acids, and nucleotides, and should have broader applicability than the alkyl ammonium salts. Photochemical properties of the Bhcmoc-Glu were almost identical to those of the carboxylate counterpart, Glu(γ-Bhc). A large $\Phi\varepsilon$ value of the Bhcmoc-Glu compared to that of the CNB-Glu was also seen for activation of GluR channels in rat brain slices [22]. Overall, coumarin-carbamates are highly photosensitive upon 1- and 2-photon excitation, applicable to protect primary and secondary amines, and stable under a simulated physiological environment. Tab. 1.2.3 summarizes selected examples of spectroscopic and photochemical properties.

A potential drawback is the relatively slow kinetics in comparison to those of phosphates and carboxylates. Photolysis is expected to proceed via a photo-induced cleavage followed by decarboxylation of the resultant carbamic acid. The rate constant for the decarboxylation reaction is estimated to be 2×10^2 s^{-1} at pH 7.2 [33]. Consequently, the rate constant for release of amines is no larger than 2×10^2 s^{-1}, which could pose a serious obstacle when a faster kinetic analysis, say that within a microsecond time window, is needed.

Neckers [8, 9] and Giese [17] reported the photocleavage of C-N bond in MCM amines. Homolytic cleavage of the C4-N bond in a radical anion intermediate was proposed. Such cleavage might be initiated by photo-induced electron transfer from appropriate electron donors (borates, amines, or thiols) to the C2 carbonyl in the coumarin ring (Fig. 1.2.8).
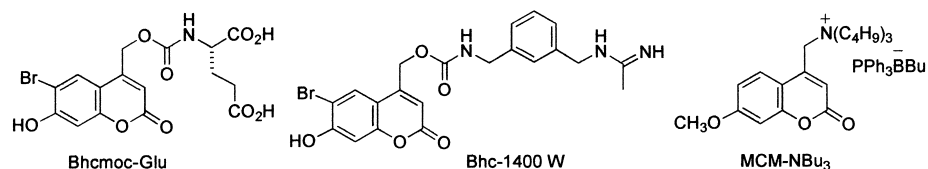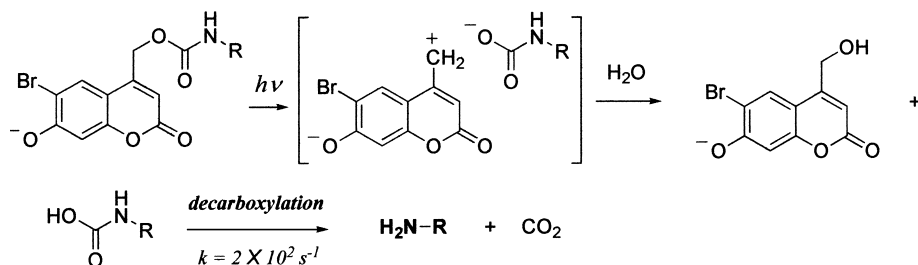

Fig. 1.2.6 Coumarin-caged amines.
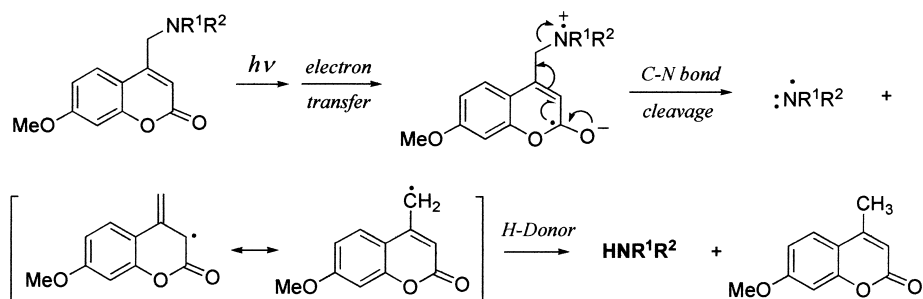
Fig. 1.2.7 Photolysis of Bhcmoc-caged amines.

Fig. 1.2.8 Proposed mechanism of photolysis of coumarinyl amines.

1.2.2.3.4 **Alcohols and Phenols**

Coumarin-4-ylmethyl carbonates are photolabile. They release parent alcohols or phenols upon irradiation. All four types of coumarin-caged carbonates having the same leaving group were synthesized [18]. Their photochemical properties were investigated. Overall uncaging efficiencies, $\Phi\varepsilon$, of all coumarin derivatives were more than ten times better than that of the NVOC phototrigger at 350 nm. Surprisingly, a remarkable difference in photolytic quantum yield was observed between the MCMoc-Gal ($\Phi = 0.020$) and the DMCMoc-Gal ($\Phi = 0.0065$). Photolytic quantum yields decreased markedly when photolysis was performed in the presence of organic solvents: the quantum yield of MCMoc-Gal in 50% THF-H_2O was only 0.0029. The DEACMoc and the Bhcmoc groups showed similar reactivity. Both compounds must be favorable for making caged compounds of alcohols by converting them to the corresponding carbonates. The Bhcmoc-phenol has a higher photolytic quantum yield than those of the aliphatic alcohols, probably because the carbonic acid anion derived from phenol has a better leaving-group ability. Therefore, the Bhcmoc group was applied to produce caged compounds of dioctanoyl glycerol (Bhcmoc-diC$_8$), tyrosine methyl ester (Tyr(Bhcmoc)-OMe) and adenosine (5′-Bhcmoc-adenosine). Like coumarin carbamates, coumarin carbonates suffer from relatively slow kinetics of decarboxylation reactions from an intermediate carbonic acid.
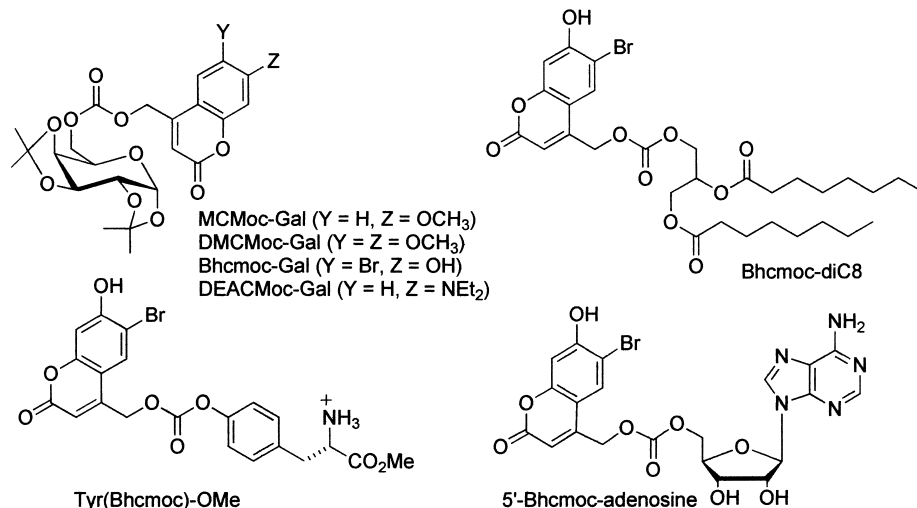
Fig. 1.2.9 Coumarin-caged alcohols and phenols.

Although no kinetic study is available, the rate constant of an alcohol release must not exceed 2×10^2 s^{-1} (Fig. 1.2.10).

Aliphatic ethers do not deprotect upon photolysis. Lin and Lawrence [24] proposed an interesting strategy for construction of caged 1,2-diols. They found that 1,3-dioxolanes of the 4-formylated Bhc were photolyzed to release parent 1,2-diols with quantum yields of 0.0278–0.0041. Fig. 1.2.11 shows a proposed mechanism of photocleavage. The adjacent oxygen in Bhc-acetal assists with the departure of the alkoxide anion, thereby stabilizing the resultant coumarin-4-yl-methyl cation. Interestingly, the six-membered counterparts, 1,3-dioxanes, were not photosensitive. The presence of a tertiary amine caused a seven-fold increase of the photolytic quantum yield, probably because the tertiary amine serves as a proton donor during acetal hydrolysis, which eventually accelerates the overall photorelease reaction.
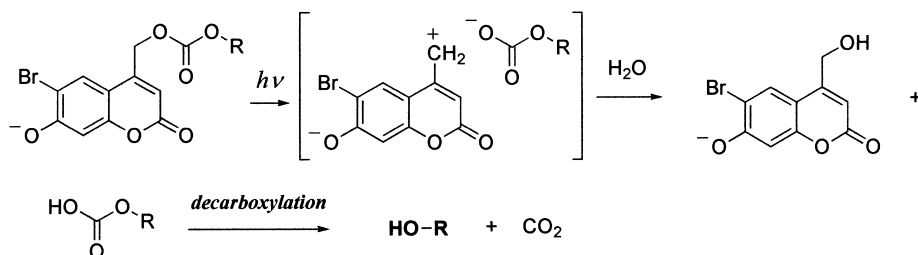

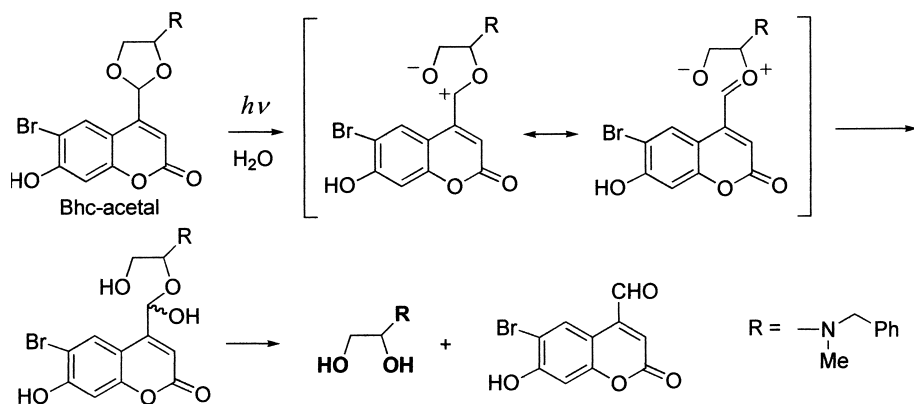**Fig. 1.2.10** Photolysis of Bhcmoc-caged alcohols and phenols.

Fig. 1.2.11 Photolysis of Bhc-acetal.

1.2.2.3.5 Carbonyl Compounds

Dore and colleagues [26] found that aldehydes and ketones can be caged by 6-bromo-4-(1,2-dihydroxyethyl)-7-hydroxycoumarin (Bhc-diol) as corresponding acetals. The possible reaction mechanism shown in Fig. 1.2.12 involves the zwitterionic intermediate in which C4 methylene cation must be stabilized by the adjacent alkoxymethyl substitution. Photolytic quantum yields ($\Phi = 0.030$–0.057) were comparable to those of the other Bhc-caged compounds. Two photon uncaging cross-sections, δ_u, were measured to be 0.51–1.23 GM. These results are the only example of a phototrigger capable of releasing aldehydes and ketones by a two-photon excitation condition. They must have great potential for cell biological applications.

1.2.3
Synthesis

1.2.3.1 Synthesis of Precursor Molecules (Caging Agents)

Introduction of coumarin-type "phototriggers" into molecules of interest has been achieved using five types of precursor molecules having reactive functional
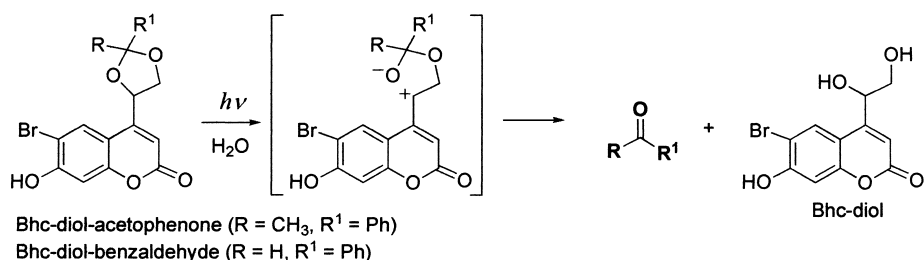

Bhc-diol-acetophenone (R = CH$_3$, R^1 = Ph)
Bhc-diol-benzaldehyde (R = H, R^1 = Ph)

Fig. 1.2.12 Photolysis of Bhc-diol-protected aldehydes and ketones.
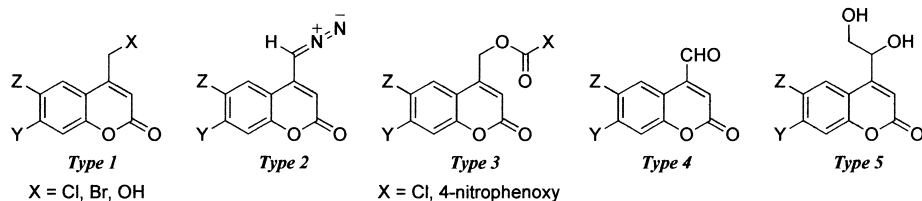
Fig. 1.2.13 Precursor molecules for synthesis of coumarin-caged compounds.

groups on the C-4 position (Fig. 1.2.13). The halo- or hydroxymethyl (type 1) and the diazomethyl (type 2) precursors can be used to prepare corresponding coumarin-4-ylmethyl esters of phosphates, carboxylates, and sulfates. Amino- and hydroxyl-containing molecules can be converted into corresponding carbamates and carbonates using chloroformate or 4-nitrophenylcarbonate precursors (type 3). The type 4 precursor is used for caged 1,2-diols and type 5 for caged aldehydes and ketones.

Extensive studies of the synthesis of substituted coumarins have been made [34]; some substituted coumarins are commercially available. Fig. 1.2.14 shows the structures of commercially available coumarins that have been used to prepare caged compounds. Br-Mmc [35] and Br-Mac [36], which were originally developed as fluorescent labeling agents of carboxylates and alcohols, can be used for the synthesis of MCM- and ACM-caged phosphates and carboxylates. The remaining compounds also have the desired substitution pattern in which electron-donating substituents such as alkoxy and amino groups are located on the C7 position and a methyl group on the C4 position. Donor substitutions at C7 help the chromophore to be ionized via through-bond electron movement when the coumarins are excited electronically, facilitating cleavage of the CH_2-X bond [13]. Alkyl substitutions at the C4 position can undergo allylic oxidation. In addition, further modification to introduce appropriate functional groups is possible. These compounds have been utilized to produce caged compounds having MCM, DMCM, and DEACM phototriggers.
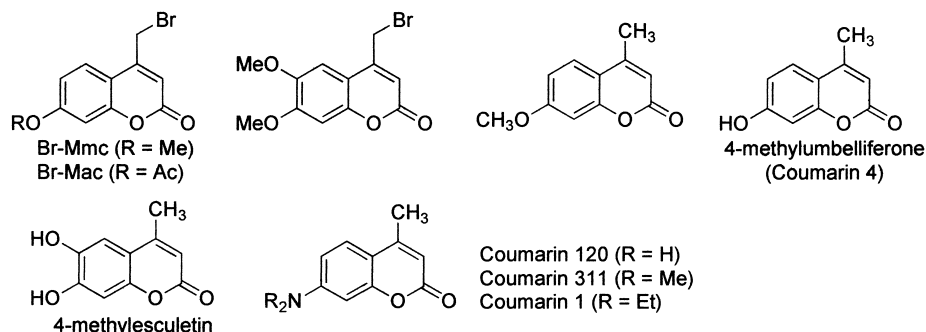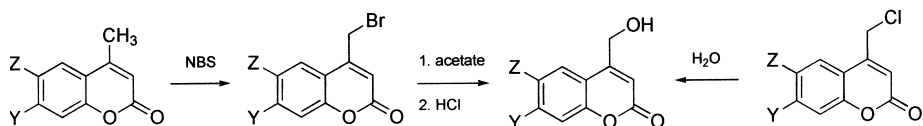

Fig. 1.2.14 Structures of commercially available coumarins with common names.

Type 1 precursors having the 4-bromomethyl group were prepared by radical bromination (NBS) of 4-methylcoumarins [15]; 4-hydroxymethyl group were prepared by hydrolysis of corresponding acetates [15] or chlorides [22].
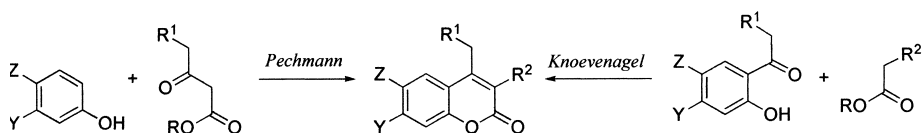

Scheme 1.2.4

Type 2 and 4 precursors were synthesized from 4-methylcoumarins according to the procedure of Ito [37]: the C4-methyl group was oxidized by selenium dioxide (or manganese dioxide) followed by tosylhydrazone formation and base-induced diazo formation.
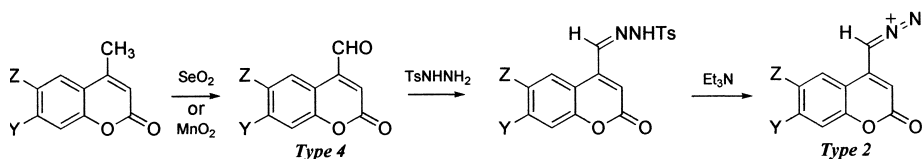

Scheme 1.2.5

For cases where an appropriate starting material is not commercially available, coumarin frameworks must be constructed starting from substituted phenols, either by the Pechmann reaction [38] or the Knoevenagel condensation [39] (Scheme 1.2.6).

Scheme 1.2.6

Synthesis of the Bhc group has been performed using the Pechmann reaction. Scheme 1.2.7 illustrates synthetic routes toward the type 1 [22], 3 [18] and 5 [26] precursors of the Bhc group. The Bhc frameworks were constructed by the acid-catalyzed condensation of 4-bromoresorcinol and ethyl acetoacetate derivatives. Other type 3 precursors can be prepared in a similar manner [18].

In principle, conventional synthetic methods for esters, carbamates, carbonates, and acetals can be applied to the synthesis of coumarin-caged com-

Scheme 1.2.7
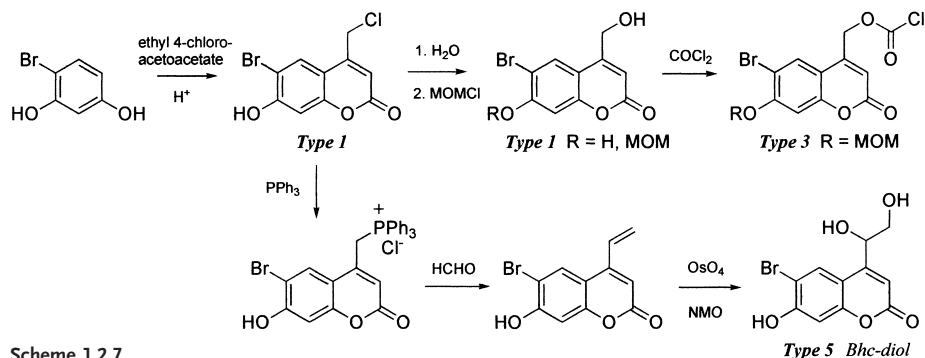
pounds. Examples in subsequent sections will be limited to biologically relevant molecules. Their synthetic strategies are discussed briefly.

1.2.3.1.1 Phosphates

The coumarin phototriggers can be introduced into acidic molecules such as phosphates, carboxylates, and sulfates using type 1 and the type 2 precursors. Multi-step synthesis using protection-deprotection chemistry is required when a target compound has more than a single functional group. An exception is synthesis of caged nucleotides. For example, a free phosphoric acid of cAMP was esterified with Br-Mmc or Br-Mac in the presence of silver (I) oxide [38] to yield MCM-cAMP in 44% yield (ax/eq=7/3) and ACM-cAMP in 14% yield (ax/eq=1/1), respectively [5–7]. The MCM-cAMP was also prepared by reaction of the tetra-*n*-butylammonium salt of cAMP with Br-Mmc (64% yield, ax/eq=8/2) [13]. Analogously, DMCM-caged cAMP was prepared either by the silver oxide method (18.7%, ax/eq=55/45) or the ammonium salt method (57.3%, ax/eq=85/15) [15]. Improved yields and better axial selectivity were observed in the ammonium salt method. In these reactions, protections of other functional groups are not necessary. Attempts to apply the methods to make HCM-cAMP and MCM-caged cGMP have failed [7, 13]. For that reason, the methods seem to be limited to the MCM, ACM and DCMCM groups, which have no free acidic hydroxy functional group on the coumarin ring. In contrast, HCM-, DEACM-, DMACM- and Bhc-cNMPs were synthesized using corresponding 4-diazomethylcoumarins, type 2 precursors, in 10–30% isolated yields [7, 14, 15, 28]. The 4-diazomethyl precursors are superior to other methods for preparation of caged cyclic nucleotides. Analogously, Bhc-caged RNAs (encode EGFP or a transcription factor en2) were prepared by the reaction of 4-diazomethyl-7-hydroxycoumarin (Bhc-diazo) and synthetic full-length mRNAs in DMSO [23].

1.2.3.1.2 Carboxylates

The synthesis of Glu(γ-Bhc) involves DBU-promoted esterification of the appropriately protected glutamate with the 4-chloromethyl-7-hydroxycoumarin [22]. The DBU method was developed for the synthesis of optically active amino acid esters [39]. No racemization was detected during the reaction. However, Shimamoto and colleagues [16] observed copious epimerization in the synthesis of caged L-TBOA. Therefore, they used the corresponding 4-diazomethylcoumarins to prepare MCM- and CMCM-L-TBOAs. Ito [37] and Goya [40] have studied the reaction of 4-diazomethylcoumarins with various carboxylic acids. Most carboxylic acids can be esterified by 4-diazomethylcoumarins without adding any catalysts or additives. However, dramatic acceleration was observed in the presence of either silica gel (known to catalyze the generation of carbene intermediates from diazoalkanes) or tetrafluoroborate (a strong Lewis acid).

1.2.3.1.3 Amines

Precursor molecules that can be used are 4-nitrophenyl carbonates and chloroformates (type 3). Introduction of the Bhcmoc group into the amino moiety of the protected glutamate was achieved via the 4-nitrophenyl carbonate intermediate with 31% isolated yield [22]. The yield is acceptable, but needs to be optimized. A potential precursor is the corresponding chloroformate. Use of (6-bromo-7-methoxymethoxycoumarin-4-yl)methyl chloroformate (MOM-Bhcmoc-Cl) [18] greatly improved yields of amino protections (T. Watanabe, unpublished results).

1.2.3.1.4 Alcohols and Phenols

Introduction of the Bhcmoc group into alcohols and phenols proceeded with almost quantitative yield when the MOM-Bhcmoc-Cl was used as a precursor [18]. Synthesis of Bhcmoc-diC8 (91% overall yield in 2 steps) and Tyr(Bhcmoc)-OMe (100% overall yield in 2 steps) were successful examples. Chloroformate precursors are so reactive that chemoselective protection of a hydroxyl moiety failed in the presence of an aromatic amino group. Therefore, the 4-nitrophenyl-carbonate precursor was used in synthesis of 5′-Bhcmoc-adenosine.

1.2.4
Applications

Applications of coumarin phototriggers to cell chemistry remain limited in number. However, the results are extremely promising. This section is intended to give an overview of reported applications of coumarin-caged compounds. Most of the reported live cell applications will be collected, including biological tests. To avoid repetition of information in related chapters, this section will specifically address the reaction conditions including cell types, methods of application to cells, types of the light sources, and monitoring methods (Tab. 1.2.4). The types of the compounds were second messengers (cAMP, cGMP, diC$_8$), a

Tab. 1.2.4 The reported biological applications of coumarin-caged compounds

Compounds	Cell types	Methods of application to cells	Light sources	Monitoring methods	Observed effects	Refs.
MCM-cAMP ACM-cAMP PCM-cAMP	Fish melanophores	Bathing	Xe lamp	Optical microscope	Pigment dispersion	5–7
MCM-8-Br-cAMP and cGMP	HEK 293 cells	Patch pipette and bathing	100 W Hg lamp and N_2 laser	Patch clamp and Ca^{2+} imaging	CNG channel opening	11, 12
MCM-8-Br-cGMP	Bovine sperm cells	Bathing	N_2 laser	Ca^{2+} imaging	CNG channel opening	10
DEACM-cAMP	HEK 293 cells	Patch pipette	405 nm laser	Patch clamp	CNG channel opening	14
BCMCM-cAMP	HEK 293 cells	Patch pipette	Xe lamp	Patch clamp	CNG channel opening	14
BECMCM-cAMP	Sea urchin and starfish sperms	Bathing	Xe flash lamp	Ca^{2+} imaging and motility	Ca^{2+} influx and movement	20, 21
BCMCM-cAMP	Rat olfactory receptor neuron	Patch pipette	Xe lamp	Patch clamp	CNG channel opening	19
DMACM-8-Br-cAMP and -cGMP DEACM-8-Br-cGMP	HEK 293 cells	Patch pipette and bathing	100W Hg lamp and Ar laser	Patch clamp and Ca^{2+} imaging	CNG channel opening	32
DMACM-caged ATP	Mouse astrocytes and brain slices	Bathing	Ar laser	Ca^{2+} imaging	transient $[Ca^{2+}]_i$ increase	31
Bhcmoc-diC8	Rat ventricular myocytes	Bathing	Ti/Sapphire laser	CLSM	twitch response	27
Bhcmoc-Glu	Rat brain slices	Bathing	N_2 and Ti/Sapphire lasers	Patch clamp	GluR opening	22

Tab. 1.2.4 (continued)

Compounds	Cell types	Methods of application to cells	Light sources	Monitoring methods	Observed effects	Refs.
Bhc-1400W	Purified proteins		366 nm and Ti/Sapphire laser		iNOS inhibition	25
α-CMCM-L-TBOA	MDCK cells	Bathing	365 nm	[^{14}C]Glu uptake	Blocks Glu transporters	16
Bhc-mRNA/DNA	Zebrafish embryos	Microinjection	355 nm	Phenotype	Ectopic expression of proteins	23
Bhc-cAMP	Newt olfactory receptor cells	Patch pipette	Xe lamp	Patch clamp	CNG channel opening	28
Bhc-cAMP/Ac	Fish melanophores	Bathing	Xe lamp	Optical microscope	Pigment dispersion	28
Bhc-cAMP/Ac	Sea urchin sperms	Bathing	Xe flash lamp	Ca^{2+} imaging	CNG channel opening	29
Bhc-cGMP/Ac						

neurotransmitter (glutamate), an isoform-specific enzyme inhibitor (1400W), a blocker for glutamate transporters (L-TBOA), a receptor ligand (ATP), DNA and mRNAs. Three compounds, Bhcmoc-Glu, Bhcmoc-diC$_8$ and Bhc-1400W, were photo-activated under two-photon excitation conditions.

1.2.5
Conclusion and Perspective

Progress in the field of caged compounds depends largely on the development of new compounds. Although *in vitro* measurement has shown that coumarin-4-yl-methyl groups have desirable properties as phototriggers for several types of biologically relevant molecules, few biological examples have been reported to date. One reason is that only limited types of compounds were synthesized compared to 2-nitrobenzyl type phototriggers; none of the coumarin-caged compounds are commercially available. The following target molecules may be useful to dissect cellular processes by taking advantage of DEACM and Bhc-type phototriggers.

Molecules that play a crucial role in signaling pathways are important targets. Intracellular signaling pathways depend largely on spatial and temporal distribution of signaling molecules. Photo-regulation of signaling molecules offers an ideal method to mimic a function of the molecule under a given physiological condition. Collections of small-molecular-weight caged compounds should be expanded by extension of the already existing chemistry of coumarin phototriggers. In addition to neurotransmitters and second messengers, the compounds that would be useful to be caged must include receptor ligands that can activate gene expressions, subtype specific inhibitors of various kinases, and small synthetic molecules that can alter specific cellular functions.

Photochemical regulation of a protein function is a goal for caging chemistry. Toward this end, caged compounds of mRNAs, DNAs, and proteins must be considered further. The Bhc-caged mRNA technology paves the way for controlling intracellular concentration of proteins in live animals in a spatially and temporally regulated manner. The method is applicable to produce caged plasmid DNAs which would provide a method to photo-control protein functions in mammalian cells. Several approaches can be considered for construction of caged proteins. Recent advances in methods to incorporate non-natural amino acids into proteins enable the construction of caged proteins in which an active site amino acid residue is modified by a coumarin phototrigger. Alternatively, multiple introductions of phototriggers can perturb the protein conformation, thereby inactivating the protein function. In this case, it is not necessary to introduce a phototrigger into an amino acid that is critical to an activity. For this reason, this method is applicable to all proteins even if the active site amino acid is unknown. However, the method is not practical when a 2-nitrobenzyl-type phototrigger is used because cleavage of multiply introduced phototriggers requires prolonged irradiation time to restore the original activity. Multiple modifications can be feasible when highly improved photosensitivity of coumarin phototriggers is utilized.

The multi-photon excitation technique is the most promising and elegant advance in the field because it offers true three-dimensional resolution, which is useful for photo-activation reaction on tissue slice samples and in whole organisms. The Bhc group has already proved itself useful for two-photon excitation. However, only a limited example is available for both *in vitro* and *in vivo* excitation conditions. Systematic investigation of two-photon absorption properties is needed, especially of various phototriggers and Bhc groups' uncaging action cross-sections and wavelength dependencies. Such obtained data would form the basis for designing new phototriggers that are favorably photo-activated under multi-photon excitation conditions.

References

1 S. A. FLEMING, J. A. PINCOCK, in *Molecular and Supramolecular Photochemistry 3 (Organic Molecular Photochemistry)*, V. RAMAMURTHY and K. S. SCHANZE, Eds. Marcel Dekker: New York, **1999**, pp 211–281.

2 For example, P. S. MUKHERJEE, H. T. KARNES, *Biomed. Chromatogr.* **1996**, *10*, 193–204.

3 R. S. GIVENS, B. MATUSZEWSKI, *J. Am. Chem. Soc.* **1984**, *106*, 6860–6861.

4 T. FURUTA, H. TORIGAI, T. OSAWA, M. IWAMURA, *Chem. Lett.* **1993**, 1179–1182.

5 T. FURUTA, H. TORIGAI, M. SUGIMOTO, M. IWAMURA, *J. Org. Chem.* **1995**, *60*, 3953–3956.

6 T. FURUTA, A. MOMOTAKE, M. SUGIMOTO, M. HATAYAMA, H. TORIGAI, M. IWAMURA, *Biochem. Biophys. Res. Commun.* **1996**, *228*, 193–198.

7 T. FURUTA, M. IWAMURA, *Methods Enzymol.* **1998**, *291*, 50–63.

8 A. M. SARKER, Y. KANEKO, A. V. NIKOLAITCHIK, D. C. NECKERS, *J. Phys. Chem. A* **1998**, *102*, 5375–5382.

9 A. M. SARKER, Y. KANEKO, D. C. NECKERS, *J. Photochem. Photobiol. A* **1998**, *117*, 67–74.

10 B. WIESNER, J. WEINER, R. MIDDENDORFF, V. HAGEN, U. B. KAUPP, I. WEYAND, *J. Cell. Biol.* **1998**, *142*, 473–484.

11 B. WIESNER, V. HAGEN, *J. Photochem. Photobiol. B.* **1999**, *49*, 112–119.

12 V. HAGEN, J. BENDIG, S. FRINGS, B. WIESNER, B. SCHADE, S. HELM, D. LORENZ, U. B. KAUPP, *J. Photochem. Photobiol. B* **1999**, *53*, 91–102.

13 B. SCHADE, V. HAGEN, R. SCHMIDT, R. HERBRICK, E. KRAUSE, T. ECKARDT, J. BENDIG, *J. Org. Chem.* **1999**, *64*, 9109–9117.

14 V. HAGEN, J. BENDIG, S. FRINGS, T. ECKARDT, S. HELM, D. REUTER, U. B. KAUPP, *Angew. Chem. Int. Ed.* **2001**, *40*, 1046–1048.

15 T. ECKARDT, V. HAGEN, B. SCHADE, R. SCHMIDT, C. SCHWEITZER, J. BENDIG, *J. Org. Chem.* **2002**, *67*, 703–710.

16 K. TAKAOKA, Y. TATSU, N. YUMOTO, T. NAKAJIMA, K. SHIMAMOTO, *Bioorg. Med. Chem. Lett.* **2003**, *13*, 965–970.

17 R. O. SCHOENLEBER, B. GIESE, *Synlett.* **2003**, 501–504.

18 A. Z. SUZUKI, T. WATANABE, M. KAWAMOTO, K. NISHIYAMA, H. YAMASHITA, M. IWAMURA, T. FURUTA, *Org. Lett.* **2003**, *5*, 4867–4870.

19 J. BRADLEY, D. REUTER, S. FRINGS, *Science* **2001**, *294*, 2176–2178.

20 U. B. KAUPP, J. SOLZIN, E. HILDEBRAND, J. E. BROWN, A. HELBIG, V. HAGEN, M. BEYERMANN, F. PAMPALONI, I. WEYAND, *Nat. Cell. Biol.* **2003**, *5*, 109–117.

21 M. MATSUMOTO, J. SOLZIN, A. HELBIG, V. HAGEN, S. UENO, O. KAWASE, Y. MARUYAMA, M. OGISO, M. GODDE, H. MINAKATA, U. B. KAUPP, M. HOSHI, I. WEYAND, *Dev. Biol.* **2003**, *260*, 314–324.

22 T. FURUTA, S. S.-H. WANG, J. L. DANTZKER, T. M. DORE, W. J. BYBEE, E. M. CALLAWAY, W. DENK, R. Y. TSIEN, *Proc. Natl. Acad. Sci. USA* **1999**, *96*, 1193–1200.

23 H. ANDO, T. FURUTA, R. Y. TSIEN, H. OKAMOTO, *Nat. Genet.* **2001**, *28*, 317–325.

24 W. Lin, D. S. Lawrence, *J. Org. Chem.* **2002**, *67*, 2723–2726.

25 H. J. Montgomery, B. Perdicakis, D. Fishlock, G. A. Lajoie, E. Jervis, J. G. Guillemette, *Bioorg. Med. Chem.* **2002**, *10*, 1919–1927.

26 M. Lu, O. D. Fedoryak, B. R. Moister, T. M. Dore, *Org. Lett.* **2003**, *5*, 2119–2122.

27 V. G. Robu, E. S. Pfeiffer, S. L. Robia, R. C. Balijepalli, Y. Pi, T. J. Kamp, J. W. Walker, *J. Biol. Chem.* **2003**, *278*, 48154–48161.

28 T. Furuta, H. Takeuchi, M. Isozaki, Y. Takahashi, M. Sugimoto, M. Kanehara, T. Watanabe, K. Noguchi, T. M. Dore, T. Kurahashi, M. Iwamura, R. Y. Tsien, *ChemBioChem.* **2004**, *5*, 1119–1128.

29 T. Nishigaki, C. D. Wood, Y. Tatsu, N. Yumoto, T. Furuta, D. Ellias, K. Shiba, S. A. Baba, A. Darszon, *Dev. Biol.* **2004**, *272*, 376–388.

30 R. O. Schoenleber, J. Bendig, V. Hagen, B. Giese, *Bioorg. Med. Chem.* **2002**, *10*, 97–101.

31 D. Geisler, W. Kresse, B. Wiesner, J. Bendig, H. Kettenmann, V. Hagen, *ChemBioChem*, **2003** *4*, 162–170.

32 V. Hagen, S. Frings, B. Wiesner, S. Helm, U. B. Kaupp, J. Bendig, *ChemBioChem*, **2003** *4*, 434–442.

33 F. M. Rossi, M. Margulis, C.-M. Tang, J. P. Y. Kao, *J. Biol. Chem.* **1997**, *272*, 32933-32939.

34 This seminal review still gives us useful information on the synthesis of substituted coumarins. S. M. Sethna, N. M. Shah, *Chem. Rev.* **1945**, *36*, 1–62.

35 W. Duenges, *Anal. Chem.* **1977**, *49*, 442–445.

36 H. Tsuchiya, T. Hayashi, H. Naruse, N. Takagi, *J. Chromatog.* **1982**, *234*, 121–130.

37 K. Ito, J. Maruyama, *Chem. Pharm. Bull.* **1983**, *31*, 3014–3023.

38 T. Furuta, H. Torigai, T. Osawa, M. Iwamura, *J. Chem. Soc., Perkin Trans. 1* **1993**, 3139–3142.

39 N. Ono, T. Yamada, T. Saito, K. Tanaka, A. Kaji, *Bull. Chem. Soc. Jpn.* **1978**, *51*, 2401–2404.

40 A. Takadate, T. Tahara, H. Fujino, S. Goya, *Chem. Pharm. Bull.* **1982**, *30*, 4120–4125.

## 1.3
p-Hydroxyphenacyl: a Photoremovable Protecting Group for Caging Bioactive Substrates

Richard S. Givens and Abraham L. Yousef

1.3.1
Introduction and History

One of the newer and more promising photoremovable protecting groups is the *p*-hydroxyphenacyl (p-$HOC_6H_4COCH_2$, p**HP**) chromophore. The introduction of pHP as a cage for bioactive substrates began less than a decade ago with the demonstrated release of ATP from p**HP**-ATP [Eq. (1)] [1, 2]. Although the p**HP** group was discovered only recently, several reviews have already noted its applications in biological studies [3–5]. This review will be limited, however, to the general photochemistry, the mechanism of this reaction, the synthetic methodology required to protect a substrate, and a few recent applications of the p**HP** series. Other sections of this monograph will more fully address the earlier applications.

$$(1)$$
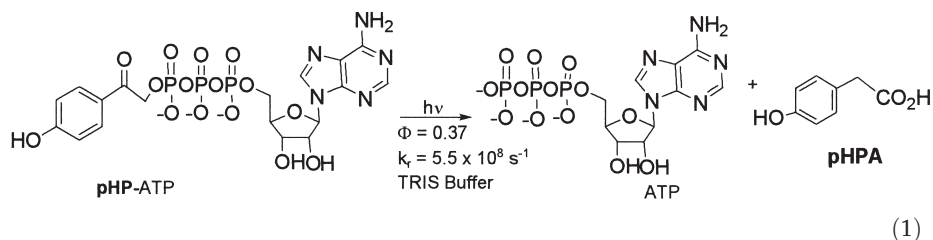
Historically, the parent phenacyl group ($C_6H_5COCH_2$) was first suggested as a photoremovable protecting group by Sheehan and Umezawa [6], who employed the *p*-methoxyphenacyl derivative for the release of derivatives of glycine. An earlier contribution from Anderson and Reese [7] reported the photoreactions of *p*-methoxy and *p*-hydroxy phenacyl chlorides, which rearranged, in part, to methyl phenylacetates when irradiated in methanol [Eq. (2)]. None of these earlier investigations, however, led to the development or exploited the potential of these chromophores as photoremovable protecting groups.

$$(2)$$
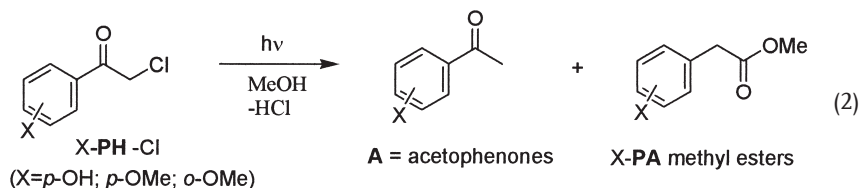
The *p*-hydroxyphenacyl group has several properties that make it appealing as a photoremovable protecting group. Ideally, such groups should have good aqueous solubility for biological studies. The photochemical release must be efficient, e.g., $\Phi \approx 0.10$–1.0, and the departure of the substrate from the protecting group should be a primary photochemical process occurring directly from the excited state of the cage chromophore. All photoproducts should be stable to the photolysis environment, and the excitation wavelengths should be greater than 300 nm with a reasonable absorptivity (*a*). The caged compounds as well as the photoproduct chromophore should be inert or at least benign with respect to the media and the other reagents and products. A general, high yielding synthetic procedure for attachment of the cage to the substrate including the separation of caged and uncaged derivatives must be available.

Of these properties, the *p*-hydroxyphenacyl photoremovable protecting group (ppg) satisfies most of them. It does have weak absorptivity above 300 nm. However, the chromophore can be enhanced by modifying the aromatic substituents through appending methoxy or carboxyl groups at the *meta* position or through extending the aryl ring (e.g., naphthyl, indole, etc.).

The "photo-Favorskii" rearrangement of the acetophenone chromophore to form a *p*-hydroxyphenylacetic acid derivative is shown in Eqs. (1) and (2) [8]. The realignment of the connectivity of the carbonyl and aryl groups results in a

significant hypsochromic shift of the chromophore; this has beneficial effects on the overall photochemistry, especially on the conversion to products [8]. Also, according to Reese and Anderson [7], rearrangement to methyl phenylacetates occurred for only the *o*- or *p*-methoxy- and *p*-hydroxy-substituted phenacyl chlorides, and the ratio of rearrangement to direct reduction to the acetophenone was approximately 1:1. All other substituents examined as well as the parent phenacyl chloride gave only the acetophenone reduction product that preserved the intact chromophore. As such, the acetophenone products would effectively compete for the incident light whenever such a reaction is carried to a modest or high conversion.

1.3.2
p-Hydroxyphenacyl

Following the leads provided by Sheehan [6] and by Reese and Anderson [7], we surveyed additional *p*-substituted phenacyl phosphate derivatives for their efficacy toward releasing phosphate [1, 2]. Among the substituents examined, the *p*-acetamido, methyl *p*-carbamoyl, and *n*-butyl *p*-carbamoyl groups proved untenable because they gave a plethora of products from the chromophore, most of which resulted from coupling or reduction of an intermediate phenacyl radical [9, 10]. Tab. 1.3.1 gives the disappearance quantum efficiencies for several *p*-substituted phenacyl phosphates, from which it is evident that photoreactions of the acetamido and carbamoyl derivatives are also very efficient. However, the large array of products of the phototrigger discouraged further development of these two electron-donating groups.

The methoxy substituent showed a much cleaner behavior, yielding only two products, the acetophenone and a rearrangement product, methyl or *t*-butyl ($R = CH_3$ or ^tBu) *p*-methoxyphenylacetate [Eq. (3)]. Most unexpectedly, the *p*-hydroxyphenacyl diethyl phosphate (p**HP**-OPO(OEt)$_2$) gave exclusively the rearranged *p*-hydroxyphenylacetic acid when photolyzed in aqueous buffers or in H_2O [Eq. (4)]. In fact, of all of the groups examined, only *p*-hydroxy and *p*-methoxy produced any rearranged phenylacetates.

Tab. 1.3.1 Disappearance and product efficiencies for ammonium salts of *p*-substituted phenacyl phosphates (pX-**P**–OPO(OEt)$_2$) in pH 7.2 Tris buffer at 300 nm

p-Substitutent (pX-)	Φ_{dis}	Φ_{pX-PA}	Φ_{pX-A}	Φ_{other}
NH_2	<0.05	0.0	<0.05	na
CH_3CONH	0.38	0.0	0.11	dimers
CH_3OCONH	0.34	0.0	nd	2 unknowns
CH_3O [a]	0.42	0.20	0.07	na
HO [b]	0.38	0.12	0.0	0.0

[a] Solvent was MeOH and diethyl phosphate was the leaving group.
[b] The diammonium salt of the mono ester. 10% CH_3CN was added to the solvent.

$$(3)$$

$$(4)$$
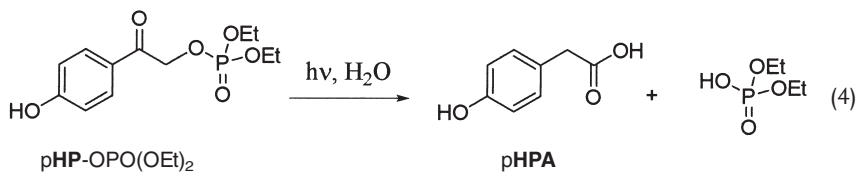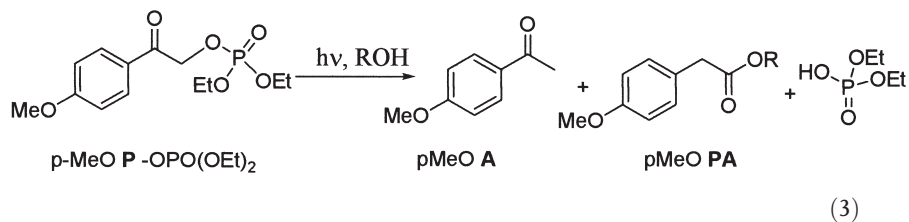
Extending the substrates to include *p*-hydroxyphenacyl ATP (p**HP**-ATP) demonstrated that ATP and *p*-hydroxyphenylacetic acid (p**HPA**) were the *only* photoproducts formed, and this occurred with a good quantum efficiency of 0.37 ± 0.01 and a rate constant of $5.5 \pm 1.0 \times 10^8 \, s^{-1}$ for appearance of ATP [Eq. (1)]. The photorelease of γ-aminobutyrate (GABA) and L-glutamate (L-Glu) was also observed by photolysis of the corresponding *p*-hydroxyphenacyl esters [Eq. (5)] [11].

$$(5)$$
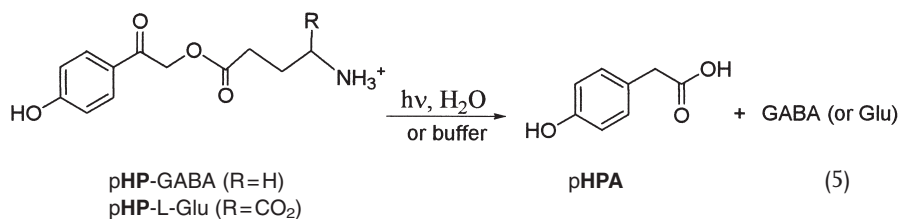
α-Amino acids have proven to be less amenable to the pHP methodology in aqueous environments, because these esters slowly hydrolyzed at pH 7.0 over a 24 h period, thus compromising the usefulness of the p**HP** group under these conditions. At pH 7, the protected *α*-ammonium ion must enhance the nucleophilic attack of H_2O at the ester carbonyl. This rationale is supported by the observation that p**HP**-protected dipeptide Ala-Ala and oligopeptides such as bradykinin, which lack the exposed *α*-amino group, are quite stable to hydrolysis [Eq. (6)] [11].
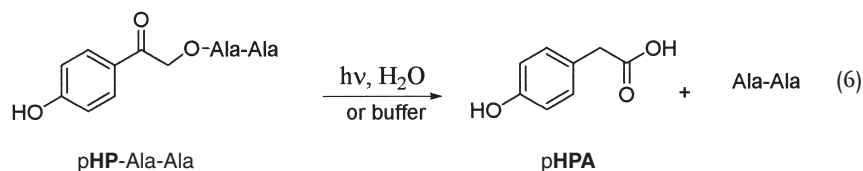
Release of Ala-Ala from **pHP**-Ala-Ala has served as a model for further studies on the release of oligopeptides. The most dramatic example of release of a small oligopeptide was the release of synthetic bradykinin [Eq. (7)] [8]. Applications using caged second messengers have aided our understanding of the biological functions of astrocytes [12].
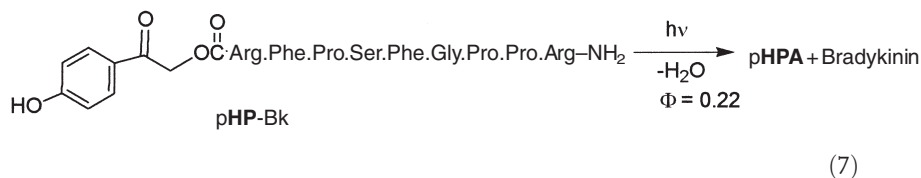
1.3.2.1 General Physical and Spectroscopic Properties

Substrate-caged **pHP** and its derivatives are generally isolated as water-soluble crystalline solids. They are stable for long periods of time when stored in the dark under cold, dry conditions, and in neutral aqueous buffered media they exhibit hydrolytic stability for 24 h or longer (for exceptions, see above) [2]. The *p*-hydroxy-acetophenone (**pHA**) chromophore is characterized by a moderately strong absorption band (λ_{max}) at 282 nm ($\varepsilon = 1.4 \times 10^4$ $M^{-1}cm^{-1}$) and significant absorptivity from 282 to 350 nm (shoulder at $\lambda_{max} \approx 330$ nm) at pH 7.0. In hydroxylic solvents, the conjugate base (**pHA⁻**) is in equilibrium with **pHA** and at higher pH shifts the λ_{max} to 330 nm [see Eq. (8) and Fig. 1.3.1]. Most reported studies of photochemical activation have used 300–340 nm light for excitation of **pHP**.
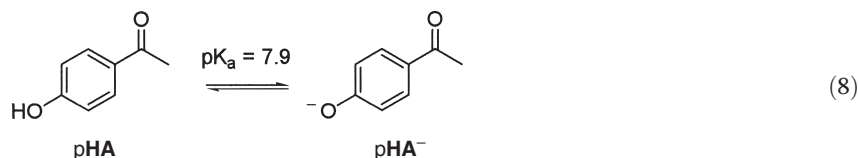
Placement of electron-donating methoxy groups at the meta positions of the aromatic ring effectively extend the absorption range of the **pHP** chromophore toward the visible region ($\lambda > 375$ nm) [13]. In contrast, electron-withdrawing carboxylic ester and carboxamide groups have little effect on the absorption properties of the **pHP** chromophore. However, the choice of substituents appears to have a significant effect on the quantum efficiency for release of the substrate
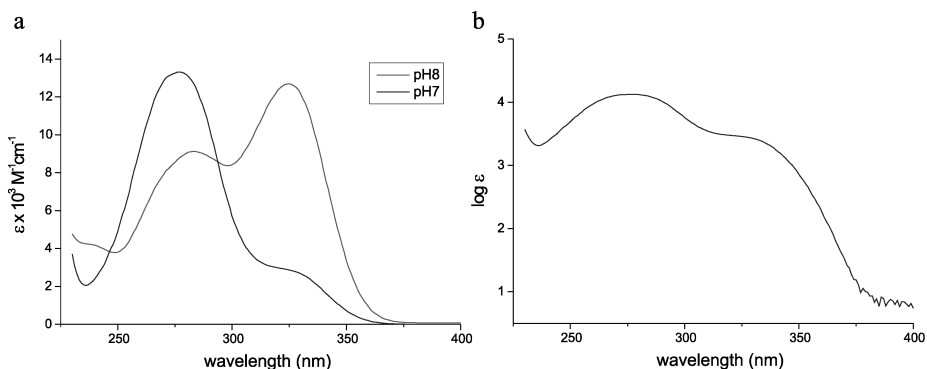
a

b

Fig. 1.3.1 UV spectral data for p**HA**. a Spectra (absorptivity as a function of λ) of a 0.13 mM solution of p**HA** in NaH_2PO_4 buffer (3% CH_3CN) at pH 7 and 8 showing the shift in absorption from the phenol to the conjugate base. b Absorbance (log ε vs wavelength (λ)) for p**HA** at pH 7.0.

Tab. 1.3.2 Spectral and photochemical properties of substituted p**HP** GABA derivatives

Substituted pHP	R	R'	λ_{max} (log ε) [a]	Φ_{rel} [b]	k_r (10^8 s^{-1})
	H	H	282 (4.16) 325sh	0.21	1.9
	OCH_3	H	279 (3.97) 307 (3.90) 341sh	0.04	26.1
	OCH_3	OCH_3	303 (3.90) 355 (3.55)	0.03	0.22
	$CONH_2$	H	324 (4.15)	0.38	0.7
	CO_2Me	H	272 (4.09) 310 (3.22) 330 (3.94)	0.31	13
	CO_2H	H	281 (4.23)	0.04	0.68

[a] In H_2O or aqueous buffered media.
[b] For the appearance of GABA at pH 7.0. sh=shoulder.

(Φ_{rel}), as seen in Tab. 1.3.2. In fact, electron-withdrawing groups gave the best quantum efficiencies, whereas the opposite was true for electron-donating groups. Overall, the release of the substrate is an efficient photochemical process and occurs within tens of nsec (i.e., $k_{release} \approx 10^8$ s^{-1}).

1.3.2.2 Synthesis of pHP-Caged Substrates
The p**HP** chromophore can be attached to many functional groups, including carboxylic acids, phosphates, and thiols, with relative ease using a stoichiometric equivalent of 2-bromo-4′-hydroxyacetophenone (p**HP**-Br) with the nucleophilic

function on the substrate. p**HP**-Br is most conveniently synthesized by bromination of commercially available p**HA** with copper(II) bromide in refluxing chloroform/ethyl acetate [14]. Substrates are normally used as their chemically protected derivatives with only the key nucleophilic group exposed. These are reacted with p**HP**-Br in an aprotic solvent in the presence of a mild base. The base-catalyzed S_N2 displacement of bromide from p**HP**-Br is a facile process, because of the enhanced reactivity of the *a*-haloketone. The increased reactivity is illustrated by a comparison of the rates for displacement of chloride from phenacyl chloride and *n*-C_4H_9Cl with potassium iodide. A rate enhancement of 10^5 s^{-1} is reported for this pair of halides [15]. Removal of the other protecting group(s) on the fully caged ester furnishes the corresponding photoprotected p**HP** substrate. Scheme 1.3.1 illustrates a specific example in which the Boc-protected dipeptide Ala-Ala was coupled with p**HP**-Br in 1,4-dioxane in the presence of 1,8-diazabicyclo-[5.4.0]undec-7-ene (DBU) to give Boc-protected p**HP**-Ala-Ala in 62% yield. Removal of the Boc group with TFA provided p**HP**-Ala-Ala in 78% yield [8].

A similar synthetic strategy was used to protect the C-terminal carboxylate group of the nonapeptide bradykinin (Bk). In this approach, the peptide sequence of bradykinin (Bk) was constructed first by a solid-phase Merrifield strategy, attaching of the C-terminus protected arginine of Bk to the 2-chlorotrityl resin. Fmoc, tBOC, and Pbf protection chemistry was employed [9, 10]. The resin-bound, fully protected bradykinin was then cleaved from the resin surface with dichloromethane/methanol/acetic acid (8:1:1), providing a protected Bk with only the C-terminal carboxylate exposed. Derivatization of the C-terminus with p**HP**-Br and DBU in DMF was followed by a two-step sequence to remove the *N*-Boc-, *tert*-butyl-, and *N*-Pbf-protecting groups employing a deprotection cocktail of 88% TFA, 7% thioanisole, and 5% water, as shown in Scheme 1.3.2. The p**HP**-Bk obtained in this sequence gave an overall yield of 60% after purification by RP-HPLC [8]. The strategy employed for p**HP** bradykinin should serve as a general one for C-terminus p**HP** protection of any oligopeptide.
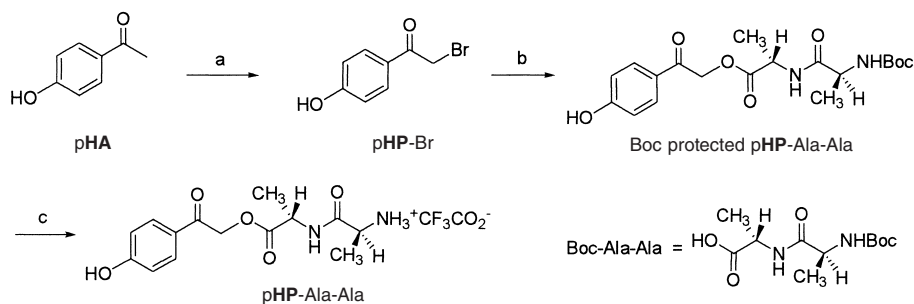
(a) CuBr$_2$, CHCl$_3$/EtOAc, 90 °C, 72%; (b) Boc-Ala-Ala, DBU, 1,4-dioxane, 15 °C, 62%; (c) TFA, 4 h, 0 °C, 78%

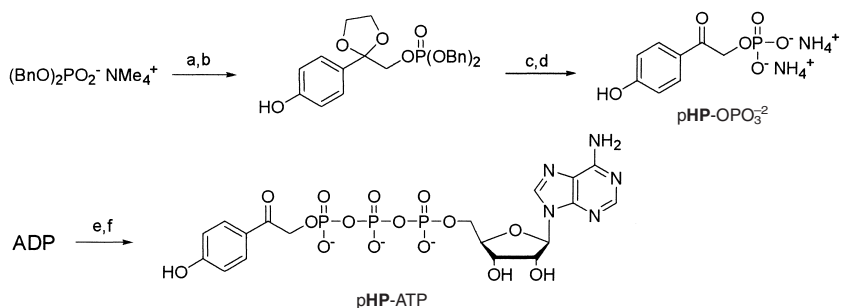**Scheme 1.3.1** Synthesis of p**HP**-Ala-Ala.
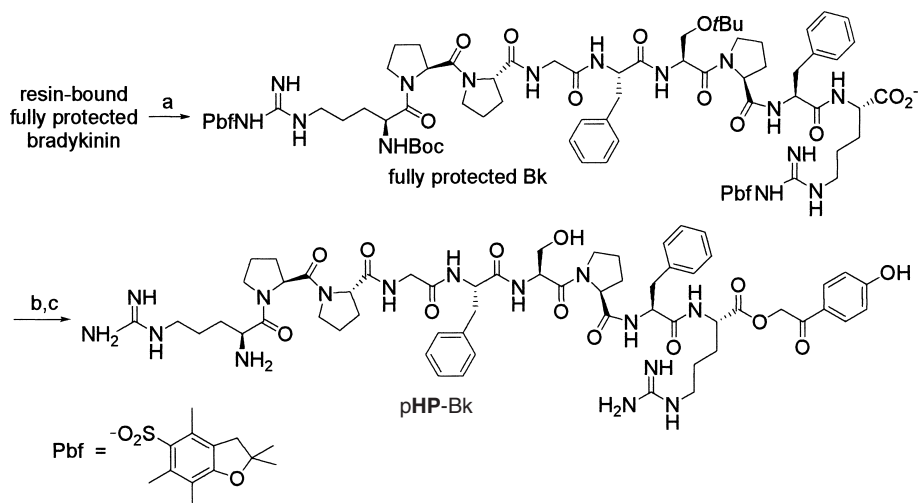
(a) CH_2Cl_2, CH_3OH, CH_3CO_2H (8:1:1), 2 h, quantitative; (b) p**HP**-Br, DBU, DMF, rt, 24 h, 72%; (c) 88% TFA, 7% thioanisole, 5% H_2O, 2.5 h, 84%

Scheme 1.3.2 Synthesis of *p*-hydroxyphenacyl bradykinin (p**HP**-Bk).

While the synthetic techniques outlined above are generally robust and applicable to a variety of oligopeptides, they are not appropriate for all substrates. For example, the synthesis of p**HP**-ATP required a modified approach in which p**HP**-OPO_3^{-2} was coupled to ADP using carbonyl diimidazole (CDI) as shown in Scheme 1.3.3 [2, 16]. The photoprotected phosphate p**HP**-OPO_3^{-2} was synthesized from alkylation of dibenzyl tetramethylammonium phosphate with p**HP**-Br, followed by removal of the benzyl groups by hydrogenolysis of the acetal-protected dibenzyl phosphate.

(a) p**HP**-Br, benzene, reflux, 85%; (b) ethylene glycol, *p*-TsOH, 82%; (c) Pd/C, H_2; (d) 1% HCl, then DEAE, Sephadex, NH_4OAc, 95%; (e) CDI; (f) p**HP**-OPO_3^{-2}, HMPA, then DEAE-Cellulose, $NH_4^+HCO_3^-$, 42%

Scheme 1.3.3 Synthesis of *p*-hydroxyphenacyl ATP (p**HP**-ATP).

In certain cases it may be necessary or desirable to avoid the use of organic solvents in the protection scheme. For example, if the substrate is an enzyme or large oligopeptide (>35 amino acids), its conformational structure may be irreversibly altered in non-aqueous media. In such cases, the caging reaction can be carried out in aqueous buffered solution, provided that there exists one predominant nucleophilic site in the protein. An elegant study by Bayley et al. [17] targeted the catalytic subunit of protein kinase A through a thiophosphorylated threonine residue using p**HP**-Br as the caging reagent. The caging reaction was accomplished by reacting the enzyme, $P_ST^{197}C_\alpha$, with an ethanolic solution of p**HP**-Br in an aqueous buffer containing 25 mM Tris · HCl, 200 mM NaCl, 2 mM EDTA, and 1% Prionex (pH 7.3) for 15 min at 25 °C in the dark, resulting in essentially quantitative derivatization [Eq. (9)].

$$(9)$$
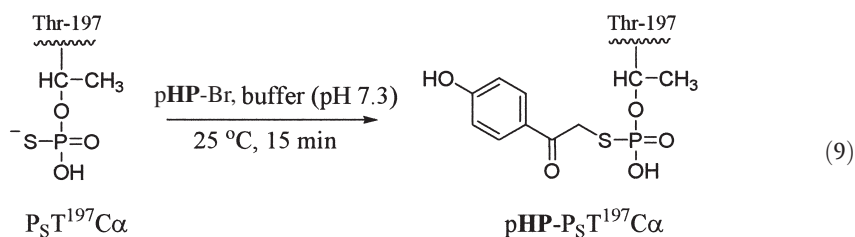
buffer = 25 mM Tris HCl, 200 mM NaCl, 2 mM EDTA, 1% Prionex

Pei et al. used a similar strategy to cage the active site of three protein tyrosine phosphatases (PTPs) with p**HP**-Br [18]. The caged phosphatase enzymes were PTP1B, SHP-1 (a phosphatase containing an Src homology 2 domain), and SHP-1(ΔSH2), the catalytic domain of SHP-1. Micromolar concentrations of each enzyme were incubated in HEPES buffer solution containing excess p**HP**-Br in DMF, yielding caged PTP [Eq. (10)]. Matrix-assisted laser desorption ionization mass spectroscopy of trypsin-digested fragments of inactivated p**HP**-SHP-1(ΔSH2) confirmed that derivatization occurred at the active site Cys-453 residue.

$$(10)$$
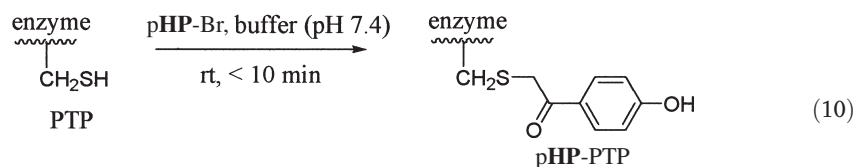
buffer: 50 mM HEPES (*N*-(2-hydroxyethyl)piperazine-*N*-(2-ethanesulfonic acid))

1.3.3
Mechanistic Studies

Recent experimental and theoretical studies provide mechanistic information on the photorelease of substrates from the *p*-hydroxyphenacyl group. However, there are questions remaining regarding the molecular changes involved in the photorelease processes and the identity of the intermediate(s). A brief general description of the mechanism based in part on laser flash photolysis (LFP) studies and density functional theory calculations is presented here. For a more detailed discussion, the reader is encouraged to consult Part II of this monograph.

1.3.3.1 **A Triplet "Photo-Favorskii" Rearrangement**
A proposed mechanism is outlined in Scheme 1.3.4. After initial excitation of the chromophore to its singlet excited state, rapid singlet-triplet (ST) intersystem crossing ($k_{ST}=2.7\times10^{11}$ s^{-1}) quantitatively generates the triplet state [19]. The triplet excited phenolic group rapidly undergoes an adiabatic proton transfer to solvent, generating triplet phenoxide anion ^{3}pHP-X$^-$. It is speculated that ^{3}pHP-X$^-$ is the precursor to the rate-limiting release of the substrate and the putative spirodienedione intermediate **DD**. **DD** may also be in equilibrium with the oxyallyl valence isomer **OA**. Hydrolysis of **DD** leads to *p*-hydroxyphenylacetic acid (pHPA), the only major photoproduct of the *p*-hydroxyphenacyl chromophore.

Previous mechanistic hypotheses involving the direct heterolytic cleavage of the p**HP**-substrate bond from the triplet phenol ^{3}pHP-X, or homolytic cleavage followed by rapid electron transfer also suggested intermediate **DD** [20, 21] but did not incorporate the seminal role of the phenolic hydroxy group. In a few instances, a minor amount of photohydrolysis of the substrate competes and results in the appearance of <10% of 2,4'-dihydroxyacetophenone among the photolysis products of pHP [8].
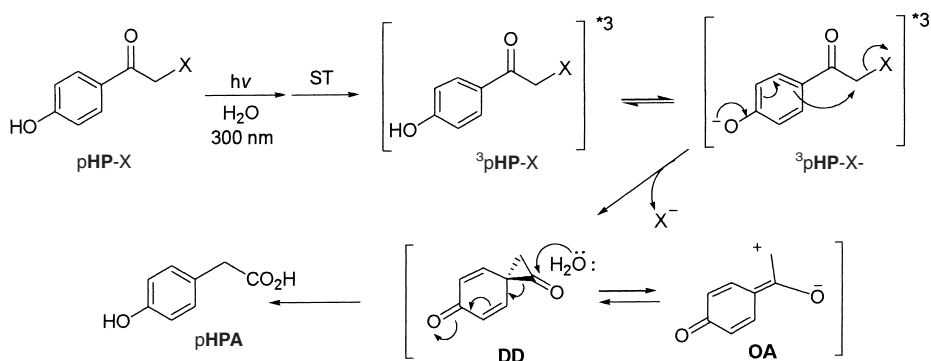
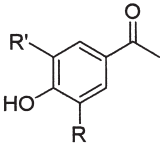**Scheme 1.3.4** Proposed mechanism for photorelease of substrates from p**HP**-X.

1.3.3.2 Role of the Triplet Phenol

The importance of the triplet phenoxide ion ^{3}pHP-X$^-$ in the photorelease mechanism is supported by LFP studies of pHA in aqueous acetonitrile [19]. The lower pK_a of ^{3}pHA (5.15) is a 60-fold increase in acidity compared with the ground state (7.93) [22]. This increased acidity was also determined for several meta-substituted pHA chromophores listed in Tab. 1.3.3. Thus the adiabatic ionization of the phenol on the triplet excited state energy surface drives the release of the conjugate base of the leaving group.

1.3.3.3 Correlation of the ^{3}pK$_a$ with the Quantum Efficiency

Further evidence of the important role of the conjugate base is found in the correlation between the ^{3}pK$_a$s and the efficiency of reaction shown in Fig. 1.3.2.

Tab. 1.3.3 Ground state and excited state pK_as for substituted **pHP** derivatives [22]

Substituted pHP	R	R'	pK_a [a]	^3pK_a [b]
	H	H	7.93	5.15
	OCH$_3$	H	7.85	6.14
	OCH$_3$	OCH$_3$	7.78	6.16
	CONH$_2$	H	6.15	3.75
	CO$_2$Me	H	7.66	4.28
	CO$_2$H	H	6.28	4.33

a) Measured in water containing 10% methanol at 22–23 °C with an ionic strength of 0.10 M (NaCl).
b) Determined from phosphorescence measurements in ethanol (5% methanol and isopropanol) in liquid nitrogen. (We thank Professor Wirz, University of Basel, for the ^{3}pK$_a$ measurements.)
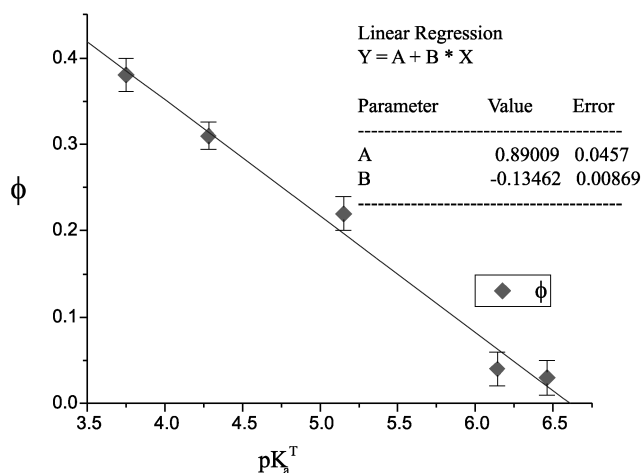

Fig. 1.3.2 Quantum efficiency for release of GABA as a function of the ^{3}pKa of the **pHP** derivative [22].

This trend suggests that the efficiency of release of the substrate hinges upon the chromophore's ability to form the corresponding phenoxide anion in the triplet excited state, suggesting a crucial role for the *p*-hydroxy function in the photorelease and photorearrangement mechanism.

1.3.4
Applications

1.3.4.1 Neurotransmitter Release

The rapid release rates of substrates from the **pHP** group ($k_r = 10^8$–10^9 s^{-1}) permit the study of the early, rapid events in neurotransmission and signal transduction processes. Caged derivatives of neurotransmitters, for example **pHP**-L-Glu [Eq. (11)], have been used successfully to probe the various aspects of chemical synaptic transmission in isolated brain cells. For example, Kandler et al. [23] employed **pHP**-L-Glu to study postsynaptic long-term depression (LTD) in CA1 hippocampal pyramidal cells. The changes in synaptic efficacy within such cells are thought to be an integral part of learning and memory. Caged glutamate was administered via bath application (50–200 µM) to hippocampal CA1 pyramidal cells in 300 µm rat brain slices. Tetrodotoxin (5 µM) blocked presynaptic transmission to isolate the responses to only the postsynaptic cell changes. Photolysis was conducted with time-resolved pulsed (20 ms) UV from a 100 W mercury arc lamp directed through two 10 µm diameter optical fibers to provide spatial control. Rapid glutamatergic currents, monitored by patch clamp electrodes, were elicited by the photorelease of glutamate (Fig. 1.3.3). The currents were suppressed by glutamate receptor antagonists, e.g., 6-cyano-7-nitroquinoxaline-2,3-dione (CNQX) and D-aminophosphonovalerate (D-APV), demonstrating that the observed responses were due to activation of ionotropic glutamate receptors. The rapid concentration jump in glutamate resulting from localized photolysis of **pHP**-L-Glu, combined with depolarization, led to LTD of the glutamate receptors.

pHP-L-Glu $\xrightarrow{h\nu}$ L-Glu   +   **pHPA**   (11)
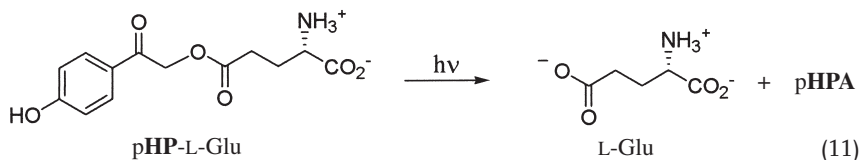
Caged bradykinin (**pHP**-Bk) was deployed by Haydon et al. to explore possible avenues for the connectivity among signaling astrocytes in hippocampal preparations [12]. Mice brain slices were bathed in calcium indicator solution (X-rhod-1 or fluo-$_4$AM) along with 1 nM Bk to identify the bradykinin-responsive cells in the stratum radiatum (Fig. 1.3.4A, B). The astrocytes responsive to Bk trigger the release of calcium within the cell upon binding free Bk. These cells were identified as targets for initiating the signal transduction of neighboring
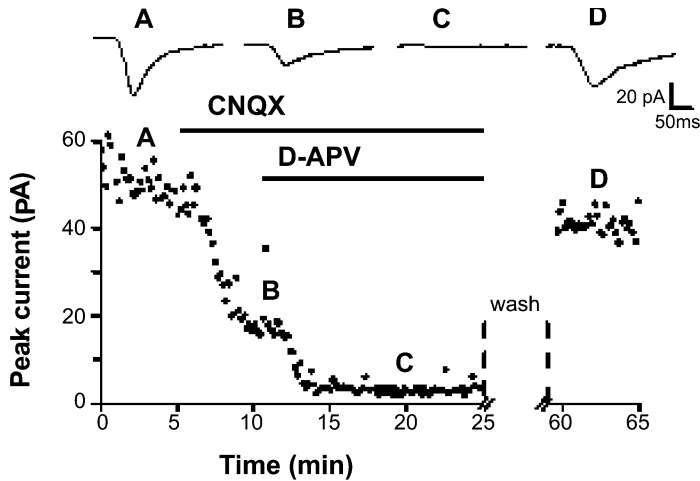
Fig. 1.3.3 Focal photolysis of p**HP**-L-Glu in CA1 hippocampal pyramidal cells. The elicited current (**A**) is attenuated upon bath application of CNQX, an AMPA-receptor antagonist (**B**); addition of the NMDA antagonist D-APV completely diminishes the current (**C**). Washing the tissue sample free of the antagonists restores the current (**D**). (With permission from Nature Neuroscience.)

cells. The preparation was then incubated in a 10 nM solution of caged p**HP**-Bk. Focal photolysis from a nitrogen-pulsed laser at 337 nm or a continuous-wave argon laser at 351 and 364 nm (1–20 ms pulses) photoreleased Bk from p**HP**-Bk, inducing the calcium signal in the Bk-responsive cell. Calcium signals were subsequently monitored by confocal imaging of the fluorescence of the calcium-bound indicator with an appropriate wavelength (e.g. 488 nm for X-rhod-1) from a second source. The initial fluorescent burst in the photostimulated cell was followed by delayed responses in neighboring cells six to twenty seconds after the initial response (Fig. 1.3.4 C, D). Since bath application of Bk only elicited a response from the cell that was directly photostimulated, it was concluded that the delayed calcium responses were not simply due to diffusion of photoreleased Bk. Furthermore, the pattern of the responses was asymmetric and did not include all astrocyte cells in the immediate vicinity of the focal cell. Simple diffusion of the signal transducer or any other diffusive activation mechanism is apparently ruled out by this observation. Thus, these results suggest that the astrocytes may be functionally connected. The cell did not respond in the presence of glutamate receptor antagonists CNQX, D-AP$_5$, and (s)-a-methyl-4-carboxyphenylglycine (MCPG), indicating that the glutamate that is naturally released in response to elevated calcium levels in astrocytes [24] is not responsible for the intercellular signaling mechanism.
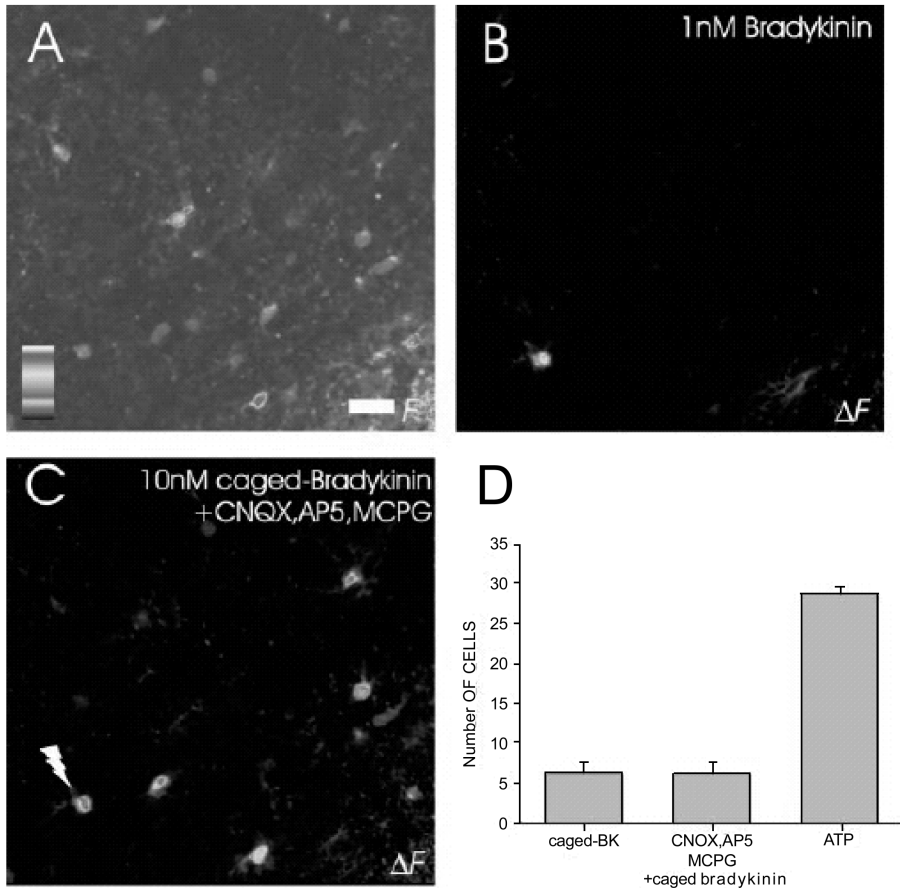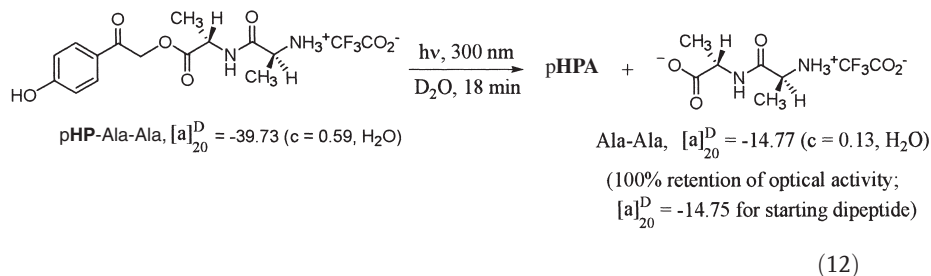
Fig. 1.3.4 Astrocyte intercellular calcium signaling upon focal photolysis of p**HP**-Bk. **A** A fluorescence image of the Bk-responsive astrocytes in the stratum radiatum, identified upon addition of 1 nM Bk. **B** A separate field of view showing only one bradykinin-responsive cell. **C** Delayed calcium responses observed upon photolysis of p**HP**-Bk near the Bk-responsive cell (lightning bolt) in the presence or absence of the glutamate receptor antagonists CNQX, D-AP$_5$, and MCPG. **D** Graph showing the number of cells for which delayed calcium responses were observed upon the photolytically induced calcium increase in the Bk-responsive cell. (With permission granted by the Journal of Neuron Glia Biology.)

1.3.4.2 **Peptide Release**

The p**HP** group can be used for the protection and photorelease of optically active peptides. Givens et al. [8] reported that the caged dipeptide p**HP**-Ala-Ala cleanly and efficiently releases Ala-Ala upon photolysis at 300 nm in D$_2$O [Eq. (12), Tab. 1.3.4]. The optical rotation of the released dipeptide was identical to that of free Ala-Ala. Similar conclusions were reported for the photolysis of p**HP**-Bk under analogous conditions, in which the released Bk CD spectrum

matched that of an authentic sample [Eq. (7), Fig. 1.3.5]. These results demonstrate that the chiral integrity of optically active peptide substrates is preserved throughout the synthetic protection/photolytic deprotection cycle.

pHP-Ala-Ala, $[a]_{20}^D$ = -39.73 (c = 0.59, H₂O)

Ala-Ala, $[a]_{20}^D$ = -14.77 (c = 0.13, H₂O)

(100% retention of optical activity;

$[a]_{20}^D$ = -14.75 for starting dipeptide)

(12)

Complete conversion of the starting **pHP** esters was observed. For example, **pHP**-Ala-Ala was photolyzed to 100% conversion as shown by ^{1}H NMR [8]. The exceptional conversions possible for **pHP** derivatives result from the transparent **pHPA**, the blue-shifted photoproduct formed by the rearrangement, a key feature of the **pHP** photochemistry.

Thiol-containing peptides have also been successfully used in the **pHP** protection strategy, as was demonstrated recently by Goeldner et al. [25], in which glutathione (GSH) was converted to **pHP**-SG in 92% yield [Eq. (13)]. As demonstrated from the study by Pei et al. discussed earlier, cysteines can be selectively modified in the presence of other functional groups in a protein upon direct reaction with **pHP**-Br.

buffer: 1N HEPES pH 7.0

(13)
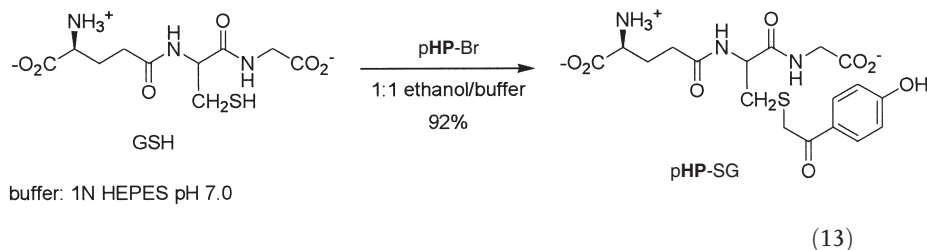
Tab. 1.3.4 Quantum efficiencies for pHP-Ala-Ala and pHP-Bk in D₂O [8]

Entry	Φ_{dis} [c]	Φ_{app} [d]	Φ_{rear} [e]
pHP-Ala-Ala [a]	0.27 (0.04)	0.25 (0.05)	0.24 (0.04)
pHP-Bk [b]	0.20 (0.02)	0.22 (0.02)	0.19 (0.01)

a) Determined by ^{1}H NMR and HPLC (averaged).
b) Determined by HPLC.
c) For the disappearance of the starting ester.
d) For the appearance of the released substrate.
e) For the appearance of pHPA. Standard deviations are given in parentheses.
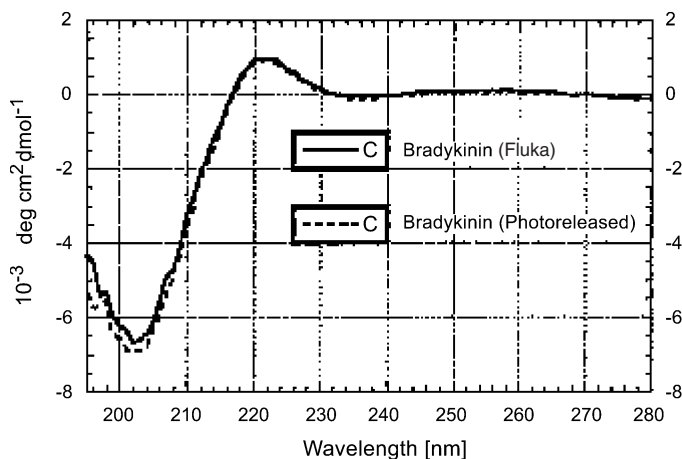
Fig. 1.3.5 CD Comparison of photoreleased Bk with authentic Bk. The broken line " **---**" represents Bk isolated by HPLC from the photolysis of p**HP**-Bk; the continuous line " ——" represents Bk (Fluka) [$\Theta_{max}=$ 954 deg cm^2 dmol^{-1} (222 nm), $\Theta_{min}=-6705$ deg cm^2 dmol^{-1} (202 nm). For Bk (photoreleased): $\Theta_{max}=918$ deg cm^2 dmol^{-1} (222 nm), $\Theta_{min}=$ -6965 deg cm^2 dmol^{-1} (202 nm), where $\Theta=$ mean residue ellipticity]. (With permission of the Journal of the American Chemical Society.)

Photolysis of p**HP**-SG in TRIS-buffer solution resulted in $\sim70\%$ release of free GSH, accompanied by 23% of the corresponding thioester, in addition to p**HPA** and p**HA**, as shown in Eq. (14). The thioester was likely the result of nucleophilic attack of the thiol on the spirodienedione intermediate **DD** (see above). The undesired side reaction with **DD** may not be as likely at a protein-binding site where the intermediate(s) may readily escape and not remain in close proximity to the released thiol.

(14)
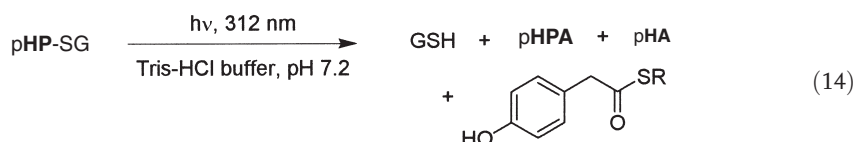
1.3.4.3 Nucleotide Release

Caged nucleotides have also been deployed as probes for physiological mechanism studies such as ion transport. Fendler et al. [26] used p**HP**-ATP to investigate the intracellular transport of sodium and potassium ions mediated by Na$^+$,K$^+$-ATPase. Lipid membranes to which were added membrane fragments containing Na$^+$,K$^+$-ATPase from pig kidney, along with p**HP**-ATP (10–300 μM) were exposed to light pulses (10 ns) from an XeCl excimer laser at 308 nm. The rapid jump in ATP concentration [see Eq. (1)] led to activation of the Na$^+$,K$^+$-

ATPase, which hydrolyzes ATP resulting in the generation of a transient current.

The release of ATP from p**HP**-ATP could be monitored using time-resolved Fourier transform infrared (TR-FTIR) spectroscopy. Among the most prominent changes observed were the disappearance of the $1270 \, \text{cm}^{-1}$ γ-PO_3^- diester band of p**HP**-ATP and the appearance of the free $1129 \, \text{cm}^{-1}$ γ-PO_3^{-2} band of the released ATP, shown in Fig. 1.3.6 A. To kinetically resolve the release of ATP, the absorbance changes at selected difference bands were tracked (Fig. 1.3.6 B). The positive signal observed at $1140 \, \text{cm}^{-1}$, corresponding to the released ATP, and a sharp negative signal at $1270 \, \text{cm}^{-1}$, representing p**HP**-ATP, were observed within the first few microseconds after the laser pulse. The signal at $1200 \, \text{cm}^{-1}$ was attributed to an artifact from the changes in transient absorption of water resulting from the energy absorbed by the sample. Fig. 1.3.6 C shows the corrected ATP release signal (solid line) obtained after subtraction of the artifact signal at $1200 \, \text{cm}^{-1}$. The integrated stray light signal of the laser pulse (dotted line) used to monitor the detector response time is also shown. Together these data show that the relaxation rate for ATP release occurs with a lower limit of $10^6 \, \text{s}^{-1}$. Additional details on these studies are available in Chapter 7.1 of this book.

In a similar study, p**HP**-GTP [Eq. (15)] was used as a probe in a study of the mechanism of hydrolysis of GTP by Ras, a protein that is involved in cell signaling [27]. Upon binding GTP, the resulting Ras-GTP complex acts as an "on" switch in the signaling pathway. Hydrolysis of the bound GTP to GDP extinguishes the signal. In this particular study, photolytic release of ^{18}O-labeled caged GTP was used in conjunction with time-resolved FTIR spectroscopy to probe the nature of the transition structure for the rate-determining step in the hydrolysis of Ras-bound GTP. Buffer solutions containing the Ras protein were
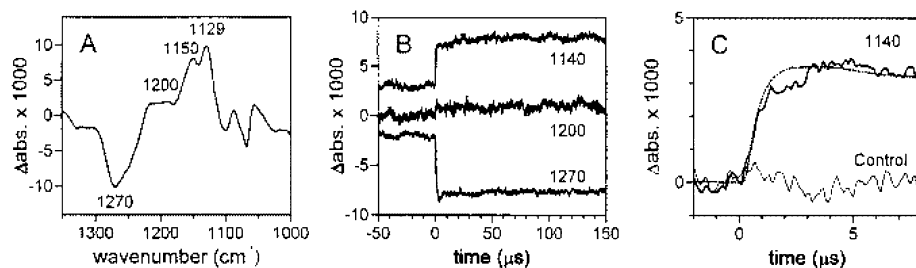

Fig. 1.3.6 TR-FTIR spectroscopic analysis of the release of ATP from p**HP**-ATP. **A** FTIR difference spectrum of the photolysis of p**HP**-ATP. The absorbance was measured 10 ms to 11 s after the photolysis flash and subtracted from the absorbance immediately prior to the flash. **B** The infrared absorbance changes at 1140, 1200, and $1270 \, \text{cm}^{-1}$ measured with a dispersive infrared spectrometer. **C** A closer look at the infrared absorbance change at $1140 \, \text{cm}^{-1}$ upon subtraction of the smoothed $1200 \, \text{cm}^{-1}$ signal. Bold line: ATP release signal (first flash), thin line: heat signal (second flash without measuring light), dotted line: integrated stray light signal of the laser pulse. (With permission of the Biophysical Journal.)

mixed with threefold equivalents of p**HP**-GTP, forming the caged GTP-Ras complex. A Tris·HCl:MgCl$_2$ buffer solution (pH 8.0) of the lyophilized protein was irradiated with a 308 nm pulsed laser for 30 s, and the subsequent changes in infrared absorption spectra of the phosphoryl groups were measured as a function of time. Monitoring of the hydrolysis of β-^{18}O$_3$ labeled GTP resulted in no detectable positional isotope exchange, suggesting a concerted hydrolysis mechanism. Further details on this application are available in Chapter 7.2 of this book.

$$(15)$$
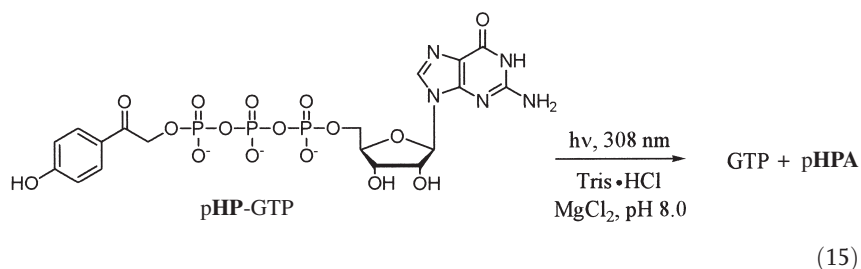
1.3.4.4 Enzyme Photoswitches

Normally, covalent attachment of inhibitors to key residues in an active site of an enzyme creates a non-reversible, inactive protein. However, photolabile groups attached at the active site become reversible inhibitors and thus act as switches that can alternately turn the enzyme off and reactivate it upon exposure to light. To date, two enzymes have been successfully caged and reactivated using the p**HP** group. The first enzyme, a protein tyrosine phosphatase (PTP), a class of enzymes that catalyze the hydrolysis of phosphotyrosine residues, was directly caged with p**HP**-Br. In this particular instance, the active site involves catalysis by a cysteine residue that participates in nucleophilic attack on a phosphate group of a bound phosphotyrosine substrate. This leads to a phosphorylated cysteinyl group at the active site, which is subsequently hydrolyzed by water [28]. Little is known about the specific role of these enzymes, other than as regulators of tyrosine phosphorylation. Pei et al. [18] explored a number of α-halophenacyl derivatives as potential PTP inhibitors by reacting a series of PTPs with p**HP**-Br and other phenacyl analogs. Derivatization of the key cysteine residue in the PTP active site with p**HP**-Br takes place in under 10 min in aqueous buffered media at room temperature, as shown previously in Eq. (10). Inactivation of the enzyme could be observed spectrophotometrically by using an assay with *p*-nitrophenyl phosphate and monitoring the change in absorbance at 405 nm as a function of time for varying concentrations of p**HP**-Br. Irradiation of the dormant PTPs at 350 nm resulted in reactivation of the enzymatic activity [Eq. (16)]. The extent of reactivation ranged from approximately 30% to as high as 80% of the original activity of the untreated enzyme, depending on the enzyme and the cage (Fig. 1.3.7).
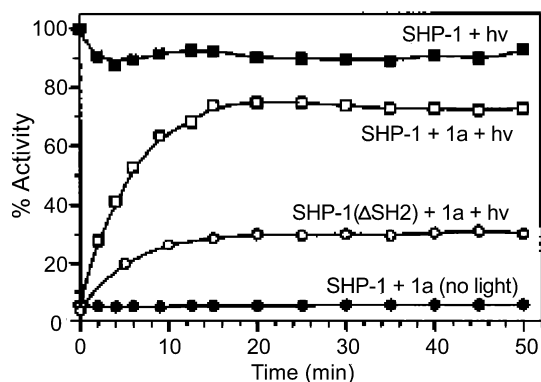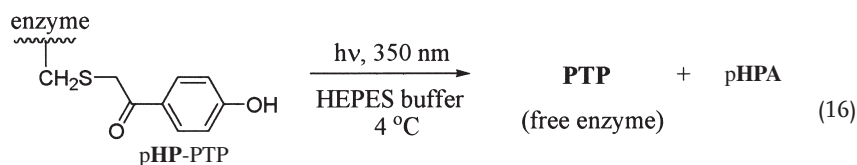
Fig. 1.3.7 Reactivation of p**HP**-caged SHP-1 and SHP-1(ΔSH2) enzymes [see Eq. (11) and accompanying text for details]. In the graph, **1a** represents p**HP**-Br [18]. (With permission from the Journal of the American Chemical Society.)

$$\text{p}\mathbf{HP}\text{-PTP} \xrightarrow[\substack{\text{HEPES buffer} \\ 4\ ^{\circ}\text{C}}]{\text{hv, 350 nm}} \quad \underset{\text{(free enzyme)}}{\mathbf{PTP}} \quad + \quad \text{p}\mathbf{HPA} \tag{16}$$

Protein kinase A (PKA) is a cell signaling protein that contains a pair of regulatory and catalytic (C) subunits. The regulatory subunits bind cAMP, which in turn induces a conformational change in the protein leading to release of an active monomeric C subunit. The C subunit of PKA contains two lobes as illustrated in Fig. 1.3.8. The small lobe is made up of the N-terminal sequences of the enzyme where ATP binding takes place, while the large lobe houses the C-terminal sequences with the residues necessary for substrate binding and catalysis. A key threonine residue (Thr-197) in the large lobe serves as a biological switch that, when phosphorylated, engages the enzyme in an active conformation [17].

An unphosphorylated C subunit of PKA was expressed from *Escherichia coli* and thiophosphorylated at Thr-197 with 3-phosphoinositide-dependent kinase 1. Bayley and coworkers [17] alkylated the resulting thiophosphate with p**HP**-Br to give the p**HP**(thio)-protected enzyme [Eq. (9)]. The modified enzyme p**HP**-$P_ST^{197}C_a$ exhibited a 17-fold reduction in activity toward the substrate kemptide, based on a ^{32}P assay. The covalently bound p**HP** group likely prevents the enzyme from achieving a fully active conformation. Photolysis of p**HP**-$P_ST^{197}C_a$ with near UV light in buffer solution released the free enzyme with a product quantum efficiency of 0.21 and an estimated deprotection yield of 85–90%, based on capture of photoreleased $P_ST^{197}C_a$ with 5-thio-2-nitrobenzoic acid (TNB)-thiol agarose [Eq. (17)].

Small lobe

ATP

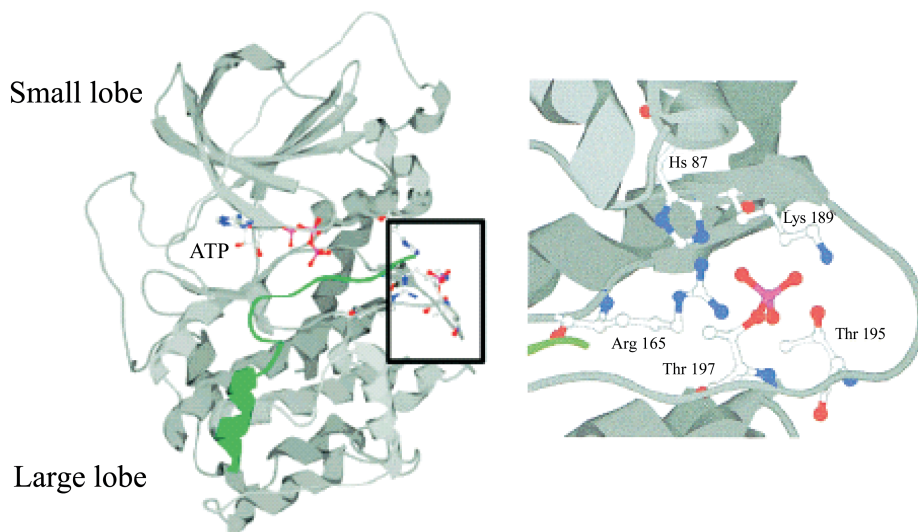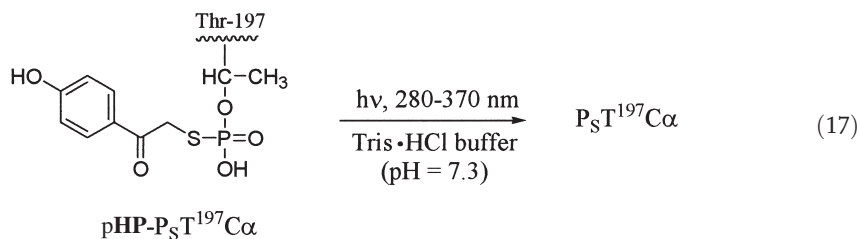Large lobe

Hs 87

Lys 189

Thr 195

Arg 165

Thr 197

Fig. 1.3.8 Structure of the C subunit of PKA. Both the large and small lobes of the C subunit are shown. ATP binding takes place at the small lobe; the large lobe houses the substrate, in this example a peptide inhibitor (green). The key residues involved in catalysis, including Thr-197, are highlighted in the expanded view [17]. (With permission from the Journal of the American Chemical Society.)

$$pHP\text{-}P_ST^{197}C\alpha \xrightarrow[\substack{\text{Tris·HCl buffer} \\ (pH = 7.3)}]{h\nu,\ 280\text{-}370\ nm} P_ST^{197}C\alpha \qquad (17)$$

1.3.5
Advantages and Limitations

The **pHP** group is a highly versatile photoremovable protecting group that is amenable to a wide range of applications in both synthetic and mechanistic bioorganic chemistry. The advantages are the ease of synthesis and the rate and efficiency of release of a variety of substrates. The current limitations are the excitation wavelengths required (<400 nm) and the requirement that the leaving group be the conjugate base of an acid (phosphate, carboxylate, and thiolate, for example). These limitations can be remedied by proper design of the chromophore and manipulation of the leaving group attachments. Research is in progress that addresses these issues.

Acknowledgements

References

1 GIVENS, R. S., PARK, C.-H. *Tetrahedron Lett.*, **1996**, *35*, 6259–6266.

2 PARK, C.-H., GIVENS, R. S. *J. Am. Chem. Soc.*, **1997**, *119*, 2453–2463.

3 PELLICCIOLI, A. P., WIRZ, J. *Photochem. Photobiol. Sci.*, **2002**, *1*, 441–458.

4 BOCHET, C. G. *J. Chem. Soc., Perkin Trans. 1*, **2002**, 125–142.

5 ADAMS, S. R., TSEIN, R.Y. *Annu. Rev. Physiol.*, **2000**, *18*, 755–784.

6 SHEEHAN, J. C., UMEZAWA, K. *J. Org. Chem.*, **1973**, *38*, 3771–3774.

7 ANDERSON, J. C., REESE, C. B. *Tetrahedron Lett.*, **1962**, *1*, 1–4.

8 GIVENS, R. S., WEBER, J. F.W., CONRAD II, P. G., OROSZ, G., DONAHUE, S. L., THAYER, S. A. *J. Am. Chem. Soc.*, **2000**, *122*, 2687–2697.

9 BARLOS, K., GATOS, D., STAUROS, K., PAPAPHOTIV, G., SCHAFER, W., WENQUING, Y. *Tetrahedron Lett.*, **1989**, *30*, 3947–3950.

10 BODI, J., SULI-VARGHA, H., LUDANYI, K., VEKEY, K., OROSZ, G. *Tetrahedron Lett.*, **1997**, *38*, 3293–3296.

11 GIVENS, R. S., JUNG, A., PARK, C.-H., WEBER, J., BARTLETT, W. *J. Am. Chem. Soc.*, **1997**, *119*, 8369–8370.

12 SUL, J.-Y., OROSZ, G., GIVENS, R. S., HAYDON, P.G. *Neuron Glia Biology*, **2004**, *1*, 3–11.

13 CONRAD II, P. G., GIVENS, R. S., WEBER, J. F.W., KANDLER, K. *Org. Lett.*, **2000**, *2*, 1545–1547.

14 CONRAD II, P. G. *Department of Chemistry*, PhD Dissertation, University of Kansas: Lawrence, **2001**.

15 HINE, J. *Physical Organic Chemistry*, McGraw-Hill Book Company, Inc.: New York **1962**.

16 GIVENS, R. S., WEBER, J. F.W., JUNG, A. H., PARK, C.-H. In *Methods Enzymol*, GERARD MARRIOTT, ed.; Academic Press, **1998**; Vol. *291*, pp. 1–29.

17 ZOU, K., CHELEY, S., GIVENS, R. S., BAYLEY, H. *J. Am. Chem. Soc.*, **2002**, *124*, 8220–8229.

18 ARABACI, G., GUO, X-C., BEEBE, K. D., COGGESHALL, K. M., PEI, D. *J. Am. Chem. Soc.*, **1999**, *121*, 5085–5086.

19 CONRAD II, P. G., GIVENS, R. S., HELLRUNG, B., RAJESH, C. S., RAMSEIER, M., WIRZ, J. *J. Am. Chem. Soc.*, **2000**, *122*, 9346–9347.

20 GIVENS, R. S., CONRAD, P. G. II, YOUSEF, A. L., LEE, J.-I. In *CRC Handbook of Organic Photochemistry and Photobiology*, W. HORSPOOL, LENCI, F., ed.; CRC Press: New York, **2004**.

21 GIVENS, R. S., LEE, J.-I. *J. Photosci.*, **2003**, *10*, 37–48.

22 WIRZ, J., GIVENS, R. S. *unpublished results*, **2002**.

23 KANDLER, K., KATZ, L. C., KAUER, J. A. *Nat. Neurosci.*, **1998**, *1*, 119–123.

24 PARPURA, V., HAYDON, P.G. *PNAS, USA*, **2000**, *97*, 8629–8634.

25 SPECHT, A., LOUDWIG, S., PENG, L., GOELDNER, M. *Tetrahedron Lett.*, **2002**, *43*, 8947–8950.

26 GEIBEL, S., BARTH, A., AMSLINGER, S., JUNG, A. H., BURZIK, C., CLARKE, R. J., GIVENS, R. S., FENDLER, K. *Biophys. J.*, **2000**, *79*, 1346–1357.

27 DU, X., FREI, H., KIM, S.-H. *J. Biol. Chem.*, **2000**, *275*, 8492–8500.

28 DIXON, J. E., ZHANG, Z.-Y. *Adv. Enzymol. Relat. Areas Mol. Biol.*, **1994**, *68*, 1–36.

1.4
Caging of ATP and Glutamate: a Comparative Analysis

Maurice Goeldner

1.4.1
Introduction

Light-sensitive biomolecules (caged compounds) enable the study of rapid biological processes by fast and efficient photochemical triggering of the release of the bioactive compound. The caging of many substances including second messengers, neurotransmitters, peptides, and functional proteins and their modulators will be described in detail in this book. However, a precise comparative analysis of different caging groups for a prototypical bioactive molecule has not been described thus far. Consequently, such analyses could shed new light on the opportunity to develop new caging groups for these reference molecules. ATP and glutamate each represent typical molecules for which numerous photoremovable protecting groups have been described, justifying such analyses. A second reason to select these two substances is that the incorporation of the photochemical group involves the chemical modification on phosphates or carboxylates, chemical functions which are found in many biological active molecules. As a consequence, the synthetic methods as well as the chemical and photochemical properties described here will most likely be directly applicable to these related substances.

This chapter will list exhaustively the different caging groups which have been described for these two molecules. It will delineate briefly the key steps for their syntheses and emphasize their respective physico-chemical and photochemical properties defining the overall quality of the caging process. These properties will be summarized in tables to facilitate a direct comparison and to help select the cage which would be best adapted for a potential use in a given biological experiment. This chapter will not describe the biological applications for which caged ATP and caged Glu derivatives have been used, not only because the list would be fairly long, but mainly because biologists usually use commercially available substances. I believe it is more important, in this chapter, to inform biologists about the existing substances by describing the properties of the different caging groups in an unbiased manner and possibly stimulate collaborations among chemists and biologists.

1.4.2
General Properties for Caging Groups

What are the chemical and photochemical properties required for a caging group?
- The chemical synthesis represents the first element that confronts an experimentalist, knowing that only a few caged biomolecules are commercially available. Clearly a simple and efficient synthetic pathway is preferred. For

the syntheses of more complex molecules, i.e. caged peptides, proteins, or oligonucleotides, a direct transformation of the biomolecule into a caged derivative will be necessary and raises the question of the selectivity of the chemical modification in a multifunctional molecule.

- Properties in the dark: the caged molecule should display hydrolytic stability and aqueous solubility. Most importantly, the caged biomolecule should be biologically inactive. Different enzymes and receptors are involved in individual biological events: therefore, each system will use its own criteria to define the biological inertness.

- Photochemical properties: these involve several parameters:
  - Irradiation wavelengths should be greater than 300 nm to avoid the absorption of light by proteins and nucleic acids; therefore, a high absorbance of the caging group above 300 nm is desirable.
  - The photolytic reaction should occur with high quantum efficiency, a value which defines the intrinsic quality of the photolytic reaction (i.e. ratio of molecule released to photons absorbed). Two types of quantum efficiencies will be considered: if possible the quantum efficiency of product formation (Φ_{ATP} or Φ_{Glu}) and/or the quantum efficiency of disappearance of the caged biomolecule (Φ_{Dis}).
  - Efficacy of photorelease in a photolytic reaction is determined by a combination of the absorption coefficient (ε) at the wavelength of irradiation and the product quantum efficiency (Φ). The uncaging action cross-section, which is defined by the product $\varepsilon_\lambda \times \Phi$ at the irradiation wavelength λ, therefore represents a quantification of the photolytic efficacy. The values shown in Tabs. 1.4.2 and 1.4.4 are usually not described; they have been deduced, when possible, from data described in the literature. These values allow a useful comparative analysis among the different caging groups, at different irradiation wavelength. When high concentrations (i.e. mM concentrations) of the released biomolecules are necessary, the higher ε values can become detrimental for the photolytic reaction (i.e. non-uniform release of the product within the sample); however this drawback, in most instances, can be easily counteracted by selecting a different irradiation wavelength.
  - The side product of the photolytic reaction should not interfere with the ongoing reaction by absorbing the light at the excitation wavelength, and in addition this compound should not interfere either chemically or biologically with the biological system.
  - Last, but not least, the release of the biomolecule should be very fast in comparison to the time course of the biological process to be studied. The rate constant for release of the biomolecule will be given, and in its absence the rate constant of disappearance of the caged substrate.

1.4.3
Caged-ATP

1.4.3.1 Introduction

ATP (adenosine triphosphate) represents an ubiquitous carrier of chemical energy in most energy-requiring processes in living cells. ATP hydrolysis has been involved in active transports, in muscle contraction, in endo- and exocytosis, in cytoplasmic streaming, in ciliary movements, in conformational changes of proteins, and in many other dynamic processes. It is not surprising that ATP was one of the first bioactive molecules to be targeted for caging studies, as will be discussed in the introduction by Jack Kaplan, one of the conceivers of the concept [1].

For many years, most biologists used for their studies the caged-ATP molecules that were commercially available, that is, the P^3-2-nitrobenzyl and the P^3-1-(2-nitrophenyl)ethyl caged derivatives (NB- and NPE-caged ATP, respectively) [2–4]. The need for more powerful caging groups for ATP prompted the syntheses of ATP substituted by different photoremovable protecting groups. In the nitrobenzyl series, several derivatives were developed such as the α-carboxy-2-nitrobenzyl (CNB-caged ATP) [5] and the 1-(4,5-dimethoxy-2-nitrophenyl)ethyl (DMNPE-caged ATP) [6]. Alternatively, different chemical series were investigated, such as the 3,5-dinitrophenyl derivative (DNP-caged ATP) [7], the desyl (desyl-caged ATP) [8–10] and the related 3′,5′-dimethoxy derivative (DMB-caged ATP) [11, 12], the *p*-hydroxyphenacyl (*p*HP-caged ATP) [10, 13], and more recently the [7-(dimethylamino)coumarin-4-yl]methyl (DMACM-caged ATP) [14] derivatives. These molecules, listed in Tab. 1.4.1, are all substituted at the P^3 phosphate group of ATP to ensure that, as caged derivatives, they lack biological activity. The same phosphate ester photo-protecting groups have also been used for the blocking of phosphate groups of other relevant nucleotides including AMP, ADP, cAMP, and cGMP, as will be illustrated by V. Hagen and colleagues in Part IV of this monograph [15].

1.4.3.2 Syntheses of the P^3-caged ATP Derivatives

Different strategies were developed to synthesize these derivatives. In most cases, these involve the synthesis of the caged monophosphates, which were subsequently coupled to ADP in the presence of an activating reagent such as a carbodiimide or carbonyl diimidazole (Scheme 1.4.1). Different methods were developed to synthesize the monophosphate derivatives, starting usually from the corresponding alcohol. The first derivatives (NB- and NPE-caged ATP) [2] used anhydrous phosphoric acid in CCl_3CN as the phosphorylating reagent and generated the expected derivatives in low yields. The hydroxyl group of *t*-butyl 2-nitromandelate was phosphorylated with phosphorus oxychloride followed by hydrolysis to give the phosphate precursor [5]. A series of improvements targeted the synthesis of phosphate esters as direct precursors of the phosphates, allowing an easier purification in organic medium. The NPE- and the DMB-caged ATP used a biscyanoethyl phosphoramidite reagent to couple with opti-

Tab. 1.4.1 Caged ATP molecules: chemical formulas and abbreviations

Chemical structure	Formulas – Cage acronyms	References
	R=H: NB R=CH$_3$: NPE R=CO$_2$H: CNB	[2] [2–4] [5]
	R=CH$_3$: DMNPE	[6]
	DNP	[7]
	R=H: Desyl R=OCH$_3$: DMB	[10] [7–9, 12]
	*p*HP	[10, 13]
	DMACM	[15]

cally active (R)- or (S)-1-(2-nitrophenyl)ethanol [4] or a protected benzoin derivative [11] before oxidation and deprotection to 1-(2-nitrophenyl)ethyl phosphate or 3′,5′-dimethoxybenzoin phosphate, respectively. The DMACM derivative used a bis-*t*-butyl phosphoramidite reagent [14] to couple with the 4-hydroxymethyl coumarin derivative before oxidation and deprotection to the DMACM phosphate derivative.

For the synthesis of the desyl-caged ATP, a symmetrical dioxaphosphole intermediate was used to generate a desyl monophosphate [16], while, for the synthesis of the *p*HP derivative, the 4-hydroxyphenacyl bromide was converted into the dibenzylphosphate derivative, a precursor of the 4-hydroxyphenacyl phosphate [13]. It appears that the use of a phosphoramidite coupling reagent and subsequent conversion to the phosphate group does offer a better control of the reaction in organic media and should be applicable to the synthesis of most caged ATP molecules.

Alternatively, an efficient and direct coupling of ATP with nitrophenyl diazoethane derivatives, under controlled pH in a biphasic medium, was described for the synthesis of the NPE and DMNPE probes (Scheme 1.4.2) [3, 6]. A detailed analysis of this coupling methodology can be found in Ref. [7]. However, this method gave disappointing results for the synthesis of the DMACM-caged derivative [14]. Although very short and appealing, it does not represent a general synthetic method for the caging of ATP or other nucleotide molecules.

### 1.4.3.3 General Properties of the Caged-ATP Molecules

To our knowledge, all the known P^3-caged ATP molecules that have been published are listed in Tab. 1.4.1. Their structures are shown and their commonly used acronyms are included. Tab. 1.4.2 summarizes the chemical and photochemical properties including UV absorption data, photochemical quantum yields of ATP formation or disappearance of the caged derivative, the uncaging action cross-section at a given wavelength, the rate constants of photolysis, and finally, when described, hydrolytic stability and aqueous solubility. As might be anticipated, not all these data for each caged ATP are available from the literature. However, most published data do provide two essential factors, the quantum efficiencies and the rates of photolysis. The fragmentation mechanisms of the different protecting groups will be discussed in detail in several chapters of this monograph and are summarized in Part II [17].

For many years, the *ortho*-nitro benzyl series, i.e. NPE-caged ATP, was frequently employed for biological experiments. It was the best probe available at that time, its excellent quantum efficiency for ATP release ($\Phi_{ATP} = 0.63$) compensated for its low absorptivity above 300 nm. Nevertheless this probe displayed several drawbacks such as a moderate rate of photolysis ($\sim 80\ s^{-1}$) and the formation of *ortho*-nitroso acetophenone, a highly absorbing product above 300 nm, which has been demonstrated to be chemically reactive toward proteins and cysteines in particular [18]. Unfortunately, the search for new derivatives in this series did not produce the expected improvements. For example, the probe substituted by
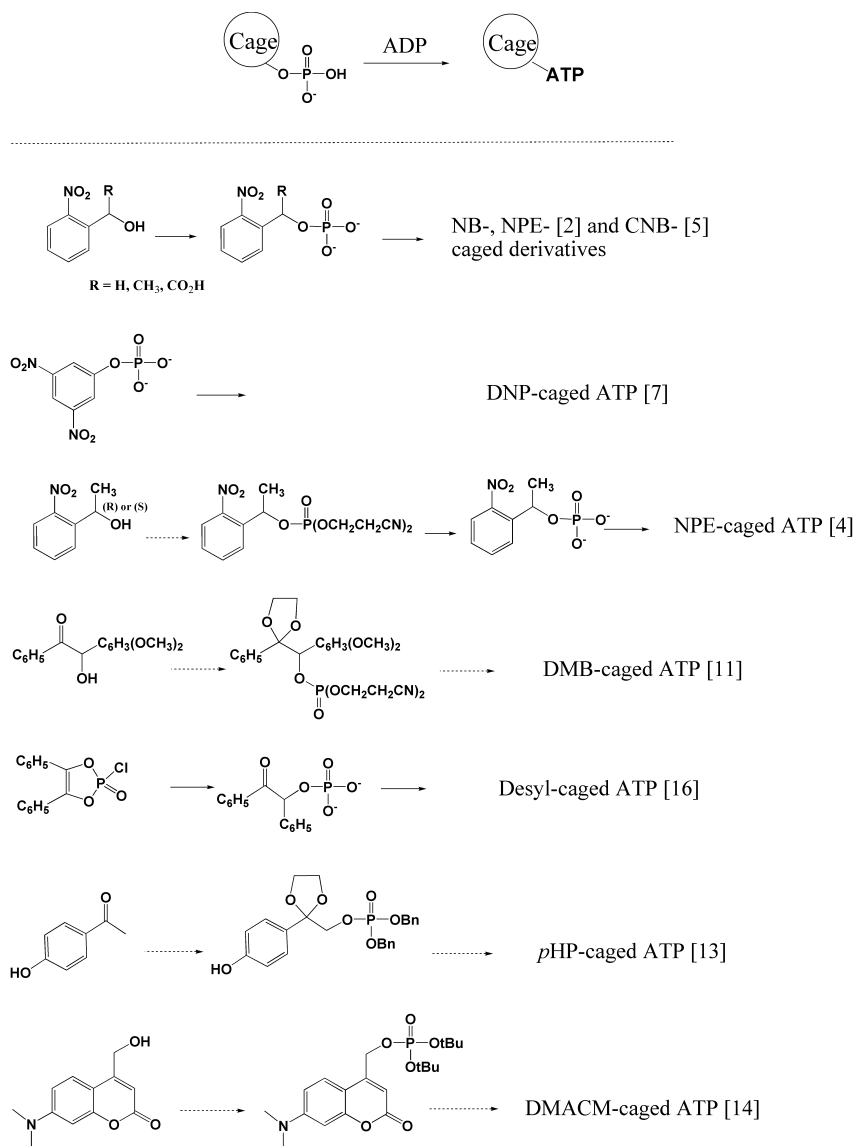
Scheme 1.4.1 Syntheses of caged-ATP derivatives: coupling of caged monophosphates to ADP

a carboxylic group at the benzylic position (CNB-caged ATP) showed increased water solubility. To our knowledge, the photochemical properties of this derivative are not available [5]. The 3,4-dimethoxy-2-nitrophenyl derivative (DMNPE-caged ATP), which displayed the expected UV-shift, showed a dramatic deficit in photo-chemical properties, i.e. a rather low quantum efficiency ($\Phi_{ATP} = 0.07$) together with a very slow rate of photolysis (18 s^{-1}).
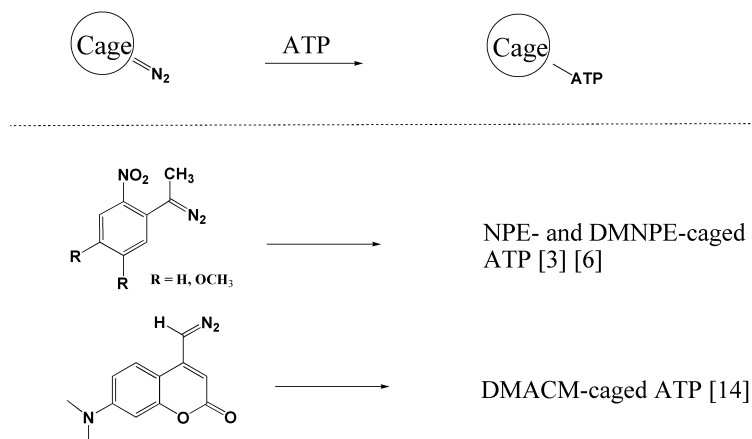
Scheme 1.4.2 Syntheses of caged-ATP derivatives: diazo-coupling approach

The quest for rapid photolytic reactions prompted the search for different photo-protecting groups for ATP, leading to the development of desyl-, DMB-, *p*HP- and DMACM-caged ATP derivatives (Tabs. 1.4.1 and 1.4.2). These molecules showed consistent improvement in chemical and photochemical properties. Clearly, the first two compounds to be developed, the desyl and the DMB-probe, despite fast rates of photolysis, displayed low photolytic efficiencies together with poor aqueous solubility, while the DMB-probe showed moderate hydrolytic stability. These probes have not been used further for biological experiments.

The *p*HP-probe displayed major improvements, high quantum yields ($\Phi_{ATP}=0.37$), fast fragmentation kinetics ($>10^7\,s^{-1}$) together with hydrolytic stability. The photolytic conversion of the *p*HP-caged ATP generates exclusively *p*-hydroxyphenylacetic acid as side-product [13], which does not interfere with the ongoing photolytic reaction. The only limitation of this probe was a moderate photolytic efficiency, around 350 nm. Finally, the very recent description of the DMACM-probe [14] allowed extremely fast fragmentation kinetics ($>10^9\,s^{-1}$) to be depicted together with a strong absorptivity above 350 nm of the coumarin chromophore to compensate for rather low quantum yields ($\Phi_{ATP}=0.086$) and ensure high photolytic efficiencies (Tab. 1.4.2). However, the formation of the strongly absorbing hydroxymethyl derivative during photolysis limits high conversions to wavelengths ≥ 360 nm. While showing hydrolytic stability, its water solubility, which represents a major drawback for the coumarin derivatives in general [20], has been improved by the presence of the dimethylamino substituent.

Tab. 1.4.2 Caged ATP derivatives: chemical and photochemical properties

Caged – ATP derivatives Abbreviations	λ_{max}; nm (ε: M^{-1} cm^{-1})	Quantum efficiencies Φ_{ATP} or Φ_{Dis} [a]	Uncaging action cross-section $\Phi \cdot \varepsilon$ (λ) [b]	Rate constants (s^{-1}) of release of ATP [c]	Stability and/or solubility in buffered media	References
NB-caged ATP	260 (26 600)	$\Phi_{ATP} \leq 0.19$ [c]	<130 (347 nm)			[2]
NPE-caged ATP	260 (26 600)	Φ_{ATP} 0.63	~410 (347 nm)	86 (pH 7.1)		[2, 3]
CNB-caged ATP						[5]
DMNPE-caged ATP	249 (17 200) 350 (51 00)	Φ_{ATP} 0.07	~350 (347 nm)	18 (pH 7.0)		[6]
DNP-caged ATP		$\Phi_{ATP} \leq 0.007$	Low			[7]
Desyl-caged ATP		Φ_{ATP} 0.3		fast [e]	Sol.: Poor	[10]
DMB-caged ATP	256 (25 600)	Φ_{ATP} 0.3	~50 (347 nm)	>10^5	Stab.: Medium 24 h pH 7.0	[7–9, 12]
pHP-caged ATP	286 (14 600)	Φ_{ATP} 0.3; Φ_{Dis} 0.38		~10^7	Stab.: Stable >24 h pH 6.5 and 7.2	[10, 13]
DMACM-caged ATP	385 (15 300)	Φ_{ATP} 0.086	~645 (347 nm)	>$1.6 \cdot 10^9$	Stab.: Stable <0.5% hydrol · 24 h pH 7.2	[14]

a) Product quantum efficiency (Φ_{ATP}) or quantum efficiency of the disappearance of the caged derivative (Φ_{Dis}).
b) Photolytic efficiency see text.
c) For discussion see text.
d) This value has been deduced from Fig. 4 in Ref. [2].
e) The kinetics are presumably very fast (~10^8 s^{-1}) according to data described on related compounds (see Ref. [17]).

1.4.3.4 **Conclusion**

Not all of the criteria for ideal caging of a biomolecule are ever completely satisfied for a given probe in a specific situation. Inevitably, a choice of the photo-protecting group will depend on the biological application. The DMACM-caged ATP represents at this time the most powerful caging probe for ATP at wavelengths ≥ 360 nm, especially if the release of the biological molecule has to be extremely fast ($\tau_{1/2} \ll 1$ µs). Using shorter wavelengths (300–340 nm) the *p*HP-caged ATP represents a useful alternative. The syntheses of these two probes are well described, reinforcing their potential for biological applications. It should be pointed out that the user-friendly (i.e., commercially available) NPE-caged ATP derivative, because of its well documented utilization, should be restricted to the study of slower ATP-dependent biological processes or situations where the rates of the biological processes are not germane to the study.
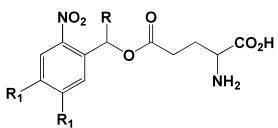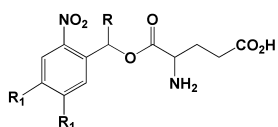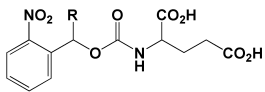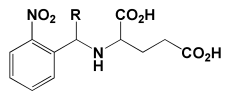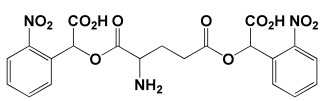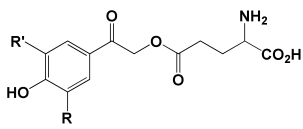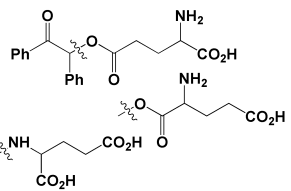
1.4.4
Caged Glutamate
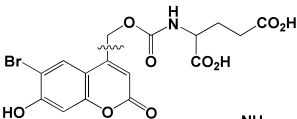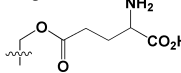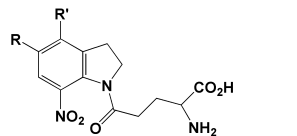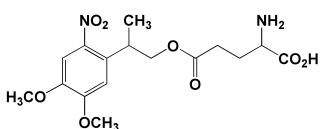
1.4.4.1 **Introduction**

Glutamate is the main excitatory neurotransmitter in the mammalian central nervous system, mediating neurotransmission across most excitatory synapses. The postsynaptic signal is transduced by three classes of glutamate-gated ion channel receptors, the AMPA, the kainate and the NMDA receptors, respectively. Glutamate has therefore become a primary target for caging studies, opening up new opportunities for a better understanding of the organization of neuronal networks. Besides its usage for rapid chemical kinetic investigations, uncaging of glutamate has been used to mimic synaptic input as well as to map the glutamate sensitivity of dendritic arbors of single cells. An efficient uncaging can be used to generate action potentials with precise spatial resolution, allowing mapping of the location of neurons connected to a single cell. Several of these aspects will be described in detail in Part IV of this monograph by G. Hess [20] and K. Kandler [21], respectively. Clearly, several of these investigations require high spatial resolution, for which two-photon optical methods are recommended, as are also discussed in Part VIII of this monograph by T. Dore [22].

Many caged glutamate derivatives have been described in the literature, illustrating the attractiveness of the target as well as the continuing quest for more powerful probes. Tab. 1.4.3 gives the structures and the common acronyms for 24 caged glutamate derivatives. Most of the caging groups are similar to those described for ATP, the modification being the replacement of the phosphate ester group with a carboxylate ester group. The glutamate molecule offers three different caging possibilities, two carboxylic acid functions, α and γ respectively, in addition to the photochemical masking of the amino group of the neurotransmitter. There is one example in which both α and γ carboxylic acid groups are protected [29]. As with ATP, the most frequently used probe has been the *ortho*-nitrobenzyl protecting groups [23–29]. The *p*-hydroxy phenacyl series [30, 31], the desyl group [32], and the coumarinyl series [33] are also described. The *ortho*-nitro indoline series

Tab. 1.4.3 Caged glutamate molecules: chemical formulas and abbreviations

Chemical structure	Formula	Cage acronyms	Refs.
	R=CH$_3$, R$_1$=H R=CO$_2$H, R$_1$=H R=CF$_3$, R$_1$=OCH$_3$ R=H, R$_1$=H,OCH$_2$CH=CH$_2$	γ-NPE γ-CNB γ-DMNPT γ-ANB	[23] [23] [24] [25]
	R=CO$_2$H, R$_1$=H R=H, R$_1$=OCH$_3$ R=CH$_3$, R$_1$=OCH$_3$	a-CNB a-DMNB a-DMNPE	[23] [26] [26]
	R=CH$_3$ R=CO$_2$H	*N*-NPEOC *N*-Nmoc	[27] [28]
	R=H R=CH$_3$ R=CO$_2$H	*N*-NB *N*-NPE *N*-CNB	[23] [23] [23]
		Bis-a,γ-CNB	[29]
	R, R'=H R=H, R'=OCH$_3$ R, R'=OCH$_3$	γ-pHP γ-pHPM γ-pHPDM	[30] [31] [31]
		γ-*O*-Desyl	[32]
		a-*O*-Desyl	[32]
		N-Desyl	[32]

Tab. 1.4.3 (cont.)

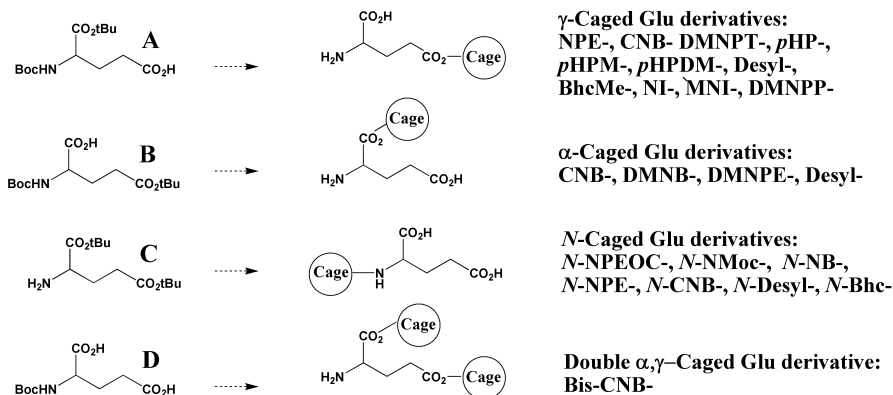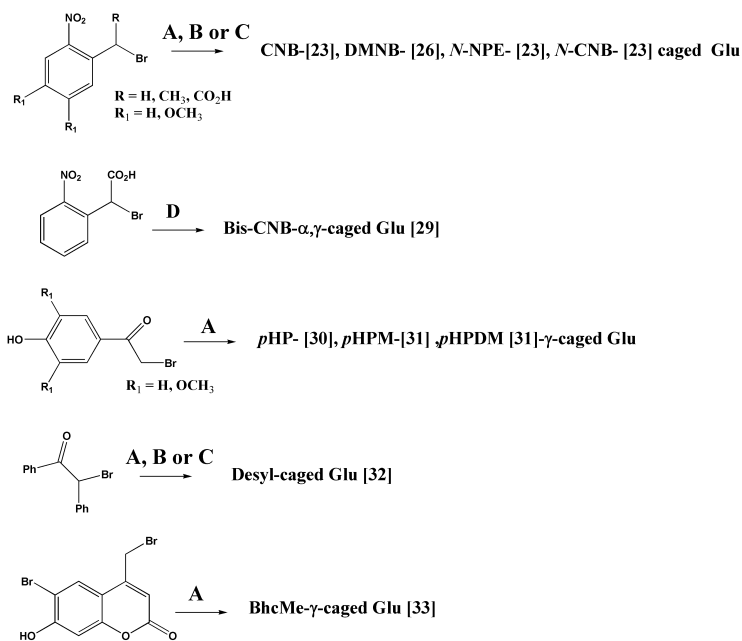| Chemical structure	Formula	Cage acronyms	Refs.
		N-Bhc	[33]
		γ-BhcMe	[33]
	R=CH₂CO₂Me, R′=H R=H, R′=OCH₃	*γ*-NI *γ*-MNI	[34, 35] [35]
		γ-DMNPP	[37]

has been introduced more recently by Corrie and colleagues [34–36] and is described by the author in this monograph [38]. Finally we have recently synthesized a glutamate derivative [37] in the *ortho*-nitrophenethyl series developed by Steiner and colleagues [39].

1.4.4.2 Syntheses of the Caged Glutamate Derivatives

All caged glutamate derivatives required either *N*-*t*-Boc (amino) or *t*-butyl (acid) group protection during the synthetic attachment of the chromophore. These protected intermediates, reagents **A**, **B**, **C**, and **D** respectively, were subsequently coupled to the appropriate caging group and the protecting groups removed under acidic conditions (Scheme 1.4.3). This general strategy does allow the purification of the protected precursors in organic medium before the acidic deprotection treatment (i.e. a solution of TFA in methylene chloride) and a final HPLC purification of the caged glutamates.

The different coupling methods which have been used for the syntheses of the caged glutamate precursors are listed in Scheme 1.4.3. Most of the probes used an S_N2 reaction by displacement of an activated halogen derivative by the protected glutamates **A**, **B**, **C**, or **D**, in different reaction conditions. The *α*- or *γ*-esters of caged-Glu (CNB- [23]; *p*HP- [30]; *p*M-HP-; *p*HPDM- [31]; desyl- [32]) and the coumarin-caged Glu [33] were synthesized, in the presence of DBU, in apolar solvent, e.g., benzene or a benzene/THF mixture for the bis-*α*,*γ*-CNB [29]. More polar solvents, e.g., CH_3CN, were used for the synthesis of the *N*-derived molecules in the presence of potassium carbonate (*N*-NPE-; *N*-CNB- [23]) or diisopropyl ethylamine

Used glutamate precursors:

γ-Caged Glu derivatives:
NPE-, CNB- DMNPT-, *p*HP-,
*p*HPM-, *p*HPDM-, Desyl-,
BhcMe-, NI-, MNI-, DMNPP-

α-Caged Glu derivatives:
CNB-, DMNB-, DMNPE-, Desyl-

N-Caged Glu derivatives:
N-NPEOC-, *N*-NMoc-, *N*-NB-,
N-NPE-, *N*-CNB-, *N*-Desyl-, *N*-Bhc-

Double α,γ–Caged Glu derivative:
Bis-CNB-

S$_N$2 coupling reactions:

CNB-[23], DMNB- [26], *N*-NPE- [23], *N*-CNB- [23] caged Glu

R = H, CH$_3$, CO$_2$H
R$_1$ = H, OCH$_3$

Bis-CNB-α,γ-caged Glu [29]

***p*HP- [30], *p*HPM-[31] ,*p*HPDM [31]-γ-caged Glu**

R$_1$ = H, OCH$_3$

Desyl-caged Glu [32]

BhcMe-γ-caged Glu [33]

Scheme 1.4.3 Syntheses of caged glutamate derivatives: protected glutamate derivatives (A, B, C, and D) and synthetic methods

Diazo coupling reactions:

NO$_2$ CH$_3$ N$_2$
R$_1$
R$_1$ = H, OCH$_3$

A or B → NPE- [23] , DMNPE- [26] caged Glu

Reductive amination:

NO$_2$ H O
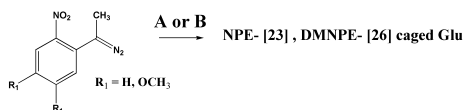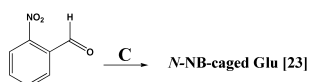
C → *N*-NB-caged Glu [23]

Carbamylation reactions:

NO$_2$ R O Cl O
R = CH$_3$, CO$_2$H

C → *N*-NPEOC- [27], *N*-Nmoc- [28] caged Glu

Br O Cl O HO O O

C → *N*-Bhc-caged Glu [33]
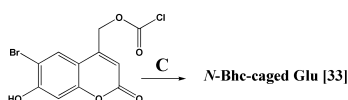
Carbodiimide coupling reactions

R$_1$ R N H NO$_2$

A → NI- [34], MNI- [35] γ-caged Glu

NO$_2$ CF$_3$ OH H$_3$CO OCH$_3$

A → DMNPT-γ–caged Glu [24]

NO$_2$ CH$_3$ OH H$_3$CO OCH$_3$

A → DMNPP-γ–caged Glu [37]
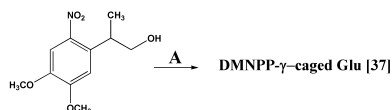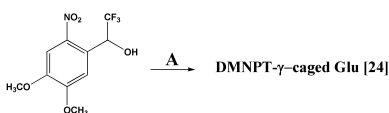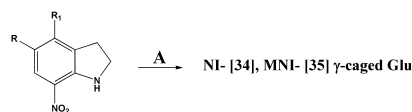
Scheme 1.4.3   (cont.)

(*N*-desyl-caged probes [32]). The synthesis of the precursor of the DMNB-caged *α*-Glu [26] used KF in refluxing acetone. The diazo precursors, developed for the caging of ATP, were used also for the syntheses of the *γ*- or *α*-NPE- and DMNPE-caged Glu respectively [23, 26]. One example of reductive amination was described on *ortho*-nitrobenzaldehyde for the synthesis of *N*-NB-caged Glu [23]. The syntheses of *N*-NPEOC- [27], *N*-Nmoc- [28] and Bhc- [33] caged Glu used an activated chloroformate, carbamate, or carbonate, respectively, to couple with the bis-*t*-butyl esters of glutamate **C** to generate the corresponding carbamates. The probes in the nitroindoline series (NI- and MNI-caged *γ*-Glu [34, 35]) provide an amide group in order to cage glutamate, using EDC-DMAP to couple the protected glutamic acid **A** onto the substituted indoline derivatives. Nitration and deprotection were achieved in a sub-

Tab. 1.4.4 Caged glutamate derivatives: chemical and photochemical properties

Caged Glu derivatives abbreviations	λ_{max}: nm (ε: M^{-1} cm^{-1})	Quantum efficiencies Φ_{Glu} or Φ_{Dis} [a]	Uncaging action cross section $\Phi \cdot \varepsilon$ (λ) [b]	Two-photon uncaging action cross section $\delta u(\lambda)$ (GM) [c]	Rate constant (s^{-1}) of release of Glu [d]	Stability and/or solubility in buffered medium	References
γ-NPE-caged Glu					~9 (pH 7.0)		[23]
γ-CNB-caged Glu	262 (5100)	Φ_{Glu} 0.14	~25 (365 nm) [33]		33×10^3 (pH 7.0)	Stab. Good <2% pH 7.0	[23]
γ-DMNPT-caged Glu						Unstable	[24]
γ-ANB-caged Glu							[25]
α-CNB-caged Glu		Φ_{Glu} 0.16			8.7×10^3 (pH 7.0)	Stab. Fair $\tau_{1/2}$ ~15 h pH 7.4	[23]
α-DMNB-caged Glu	345 (5900)	Φ_{Glu} 0.006 [33]	~30 (365 nm) [33]				[26]
α-DMNPE-caged Glu		Φ_{Glu} 0.65			⎰ ~93 (pH 5.5)		[26]
N-NPEOC-caged Glu					⎱ ~14 (pH 7.0)		[27]
N-Nmoc-caged Glu	265 (5700) 308 (2000)	Φ_{Dis} 0.11	~220 (308 nm)		~145 (pH 7.2)	Stable	[28]
N-NB-caged Glu		Φ_{Glu} 0.06			~210 (pH 7.0)		[23]
N-NPE-caged Glu		⎰ Φ_{Glu} 0.044 ⎱ Φ_{Glu} 0.036			~2.2×10^3 (pH 7.0)		[23]
N-CNB-caged Glu [e]					⎰ ~410 (pH 7.0) ⎱ ~365 (pH 7.0)		[23]
Bis-α,γ-CNB-caged Glu [f]		⎰ Φ_{Glu} 0.16 ⎱ Φ_{Glu} 0.14			⎰ 8.7×10^3 (pH 7.0) ⎱ 33×10^3 (pH 7.0)		[29]

Tab. 1.4.4 (continued)

Caged Glu derivatives abbreviations	λ_{max} nm (ε: M^{-1} cm^{-1})	Quantum efficiencies Φ_{Glu} or Φ_{Dis} [a]	Uncaging action cross section $\Phi \cdot \varepsilon$ (λ) [b]	Two-photon uncaging action cross section $\delta u(\lambda)$ (GM) [c]	Rate constant (s^{-1}) of release of Glu [d]	Stability and/or solubility in buffered medium	References
γ-pHP-caged Glu		$\begin{cases}\Phi_{Glu}\ 0.08\\ \Phi_{Dis}\ 0.12\end{cases}$			$\sim 7 \times 10^7$ (pH 7.0)	Stable	[30]
γ-pHPM-caged Glu	279 (9310) 307 (7930)	Φ_{Glu} 0.035	~ 280 (307 nm)				[31]
γ-pHPDM-caged Glu	304 (11730)	Φ_{Glu} 0.035	~ 410 (304 nm)		$\sim 2 \times 10^7$ (pH 7.0)		[31]
γ-O-Desyl-caged Glu		$\begin{cases}\Phi_{Glu}\ 0.14\\ \Phi_{Dis}\ 0.30\end{cases}$			$\sim 10^7$ (CH_3CN/H_2O) Poor solub.		[32]
α-O-Desyl-caged Glu		No Glu formed					[32]
N-Desyl-caged Glu		No Glu formed					[32]
N-Bhc-caged Glu	368 (17470)	Φ_{Glu} 0.019	~ 360 (365 nm)	~ 0.95 (740 nm) ~ 0.35 (800 nm)			[33]
γ-BhcMe-caged Glu	369 (19550)	Φ_{Glu} 0.019	~ 330 (365 nm)	~ 0.9 (740 nm) ~ 0.4 (800 nm)			[33]
γ-NI-caged Glu		Φ_{Dis} 0.043	~ 120 (347 nm)			Stable	[34, 35]
γ-MNI-caged Glu		Φ_{Dis} 0.085	~ 380 (347 nm)	~ 0.06 (730 nm)	$\sim 2.7 \times 10^3$ (pH 7.0)	Stable	[35, 36]

a) Product quantum efficiency (Φ_{Glu}) or quantum efficiency of the disappearance of the caged derivative (Φ_{Dis}).
b) Corresponds to the photolytic efficiency at a given wavelength: see text.
c) GM = Göppert-Mayer (10^{-50} $cm^4 \cdot$ s/photon).
d) For discussion of the "rate constant for release", see text.
e) Refer to the values of the two diastereoisomers.
f) The quantum yields and the rate constants values refer to the single α- and γ-CNB-caged derivatives respectively [23].

sequent step. The DMNPT ester [24] as well as the DMNPP ester [37] used the DCC, DMAP conditions which have been described for the synthesis of caged glycine [40] and which give excellent yields using 1-(*o*-nitrophenyl-[2,2,2]-trifluoro)ethanol [41] and 2-(4,5-dimethoxy-2-nitrophenyl)propanol [39] respectively.

1.4.4.3 General Properties of the Caged-Glutamate Molecules

In contrast to ATP, glutamate has been caged at three different positions generating distinct probes for the same photo-protecting group, leading to more complicated comparisons, *a* vs *γ* positions for the carboxylic acid functions and carboxylic acid vs amine functions. Another general observation relates to the impressive number of probes which have been synthesized at this point (twenty-four to our knowledge), emphasizing the interest in and need for powerful probes as well as the desire to find the ideal probe for glutamate. Tab. 1.4.4 summarizes the chemical and photochemical properties of the different probes. In the *ortho*-nitrobenzyl series (thirteen derivatives), overall slow kinetics are observed, the fastest derivative being the *γ*-CNB-caged Glu ($k = 33 \times 10^3$ s^{-1}). The slow rates may still be satisfactory for studies of phenomena involving slower glutamate receptors such as the NMDA receptor. For the *N*-caged carbamate derivatives (*N*-NPEOC, *N*-Nmoc, *N*-Bhc), the fragmentation kinetics are governed by the rates (ms time range) of decarboxylation of the intermediate carbamic acids. For the *N*-substituted nitrobenzyl derivatives (*N*-NB, *N*-NPE and *N*-CNB), caution should be taken that the published rate constant values, which refer to the decomposition of the *aci*-nitro intermediates are related to the actual glutamate release. Recent studies on the photochemical decomposition of related *o*-nitrobenzyl ether derivatives [42, 43] demonstrated that the rate-limiting step for the release of the alcohol was the decomposition of an *o*-nitroso hemiacetal intermediate which display much slower kinetics. Similar intermediates (i.e. *o*-nitroso hemiaminals) are likely to occur during the fragmentations of *N*-substituted nitrobenzyl derivatives.

Noticeably, all the caged glutamate derivatives which show fast fragmentation kinetics ($\tau_{1/2} \ll 1$ μs), i.e., the *p*HP, the desyl and the coumarin derivatives, have lower product quantum efficiencies, which in some cases (coumarin series) are compensated by a strong absorptivity around 350 nm. In the *p*-hydroxyphenacyl series, the photolytic efficiency above 350 nm could not be substantially improved by the addition of *meta*-methoxy substituents, mainly because of a decrease in the product quantum efficiencies [31]. The desyl series was disappointing; only the *γ*-substituted derivative showed the expected photo-fragmentation reaction [32] but with a low photolytic efficiency at higher wavelength and a recurrent poor water solubility. The derivatives in the nitro-indoline series, the NI- and MNI-caged *γ*-Glu probes [34–36], are very stable caged probes. These derivatives require photolytic cleavage of an amide bond. They exhibit an excellent photolytic efficiency due mainly to a strong absorptivity around 350 nm and are not hindered by the formation of the nitroso indole product during the photolysis. Nevertheless, the observed fragmentation kinetics restrict their use to biological events occurring in the sub-ms to ms time range.

1.4.4.4 **Conclusion**

This survey on ATP and glutamate, very likely the mostly targeted biomolecules for caging studies, underlines the fact that none of the described molecules can be quoted as the perfect caging group even though several of them had very satisfactory overall properties. Not all of the necessary data are available from the literature, and therefore a complete and precise comparison cannot be made. Tabs. 1.4.2 and 1.4.4 are intended to gather together the maximum available information for the reader to make an unbiased comparison among the probes. As already pointed out, the selection of a caged derivative will depend mainly on the biological experiment for which it is intended. Selection of a probe will have to take into account all the important properties: aqueous stability and solubility, photochemical kinetics, and efficiencies. In addition, for the caged glutamate derivatives or other caged neurotransmitters, neurobiological applications may be able to address the study of cellular events where two photon-uncaging techniques provide the improved spatial resolution during photoactivation [33, 44]. These techniques require high photochemical efficiencies around 350 nm [45] and do represent one of the key issues in the search for new caged neurotransmitters as will be discussed in detail in Part VIII of this monograph [22].

Abbreviations

ATP Derivatives

CNB-caged ATP: Adenosine triphosphate P^3-(a-carboxy-2-nitrobenzyl) ester.
DMACM-caged ATP: Adenosine triphosphate P^3-[(7-dimethylaminocoumarin-4-yl)methyl] ester.
DMB-caged ATP: Adenosine triphosphate P^3-[1-(3,5-dimethoxyphenyl)-2-phenyl-2-oxo]ethyl ester.
O-Desyl-caged ATP: Adenosine triphosphate P^3-(1,2-diphenyl-2-oxo)ethyl ester.
DMNPE-caged ATP: Adenosine triphosphate P^3-1-(4,5-dimethoxy-2-nitrophenyl)-ethyl ester.
DNP-caged ATP: Adenosine triphosphate P^3-(3,5-dinitrophenyl) ester.
*p*HP-caged ATP: Adenosine triphosphate P^3-(*p*-hydroxyphenacyl) ester.
NB-caged ATP: Adenosine triphosphate P^3-(2-nitrobenzyl) ester.
NPE-caged ATP: Adenosine triphosphate P^3-1-(2-nitrophenyl)ethyl ester.

Glutamate Derivatives

γ-ANB-caged Glu: L-Glutamic acid, γ-(5-allyloxy-2-nitrobenzyl) ester.
N-Bhc-caged Glu: *N*-(6-bromo-7-hydroxycoumarin-4-ylmethoxycarbonyl)-L-glutamic acid.
γ-BhcM-caged Glu: L-Glutamic γ-[(6-bromo-7-hydroxycoumarin-4-yl)methyl] ester.
Bis-a, γ-CNB-caged Glu: L-Glutamic acid, bis-a, γ-(a-carboxy-2-nitrobenzyl) diester.
a-CNB-caged Glu: L-Glutamic acid, a-(a-carboxy-2-nitrobenzyl) ester.

γ-CNB-caged Glu: ʟ-Glutamic acid, γ-(α-carboxy-2-nitrobenzyl) ester.
N-CNB-caged Glu: *N*-(α-carboxy-2-nitrobenzyl)-ʟ-glutamic acid.
α-*O*-Desyl-caged Glu: ʟ-Glutamic α-[(1,2-diphenyl-2-oxo)ethyl] ester.
γ-*O*-Desyl-caged Glu: ʟ-Glutamic γ-[(1,2-diphenyl-2-oxo)ethyl] ester.
N-Desyl-caged Glu: *N*-(1,2-Diphenyl-2-oxo)ethyl-ʟ-glutamic acid.
γ-DM*p*HP-caged Glu: ʟ-Glutamic γ-(*m*-dimethoxy-*p*-hydroxyphenacyl) ester.
α-DMNB-caged Glu: ʟ-Glutamic acid, α-(4,5-dimethoxy-2-nitrobenzyl) ester.
α-DMNPE-caged Glu: ʟ-Glutamic acid, α-[1-(4,5-dimethoxy-2-nitrophenyl)ethyl] ester.
γ-DMNPP-caged Glu: ʟ-Glutamic acid, γ-[2-(4,5-dimethoxy-2-nitrophenyl)propyl] ester.
γ-DMNPT-caged Glu: ʟ-Glutamic acid, γ-[1-(4,5-dimethoxy-2-nitrophenyl)-2,2,2-trifluoroethyl] ester.
γ-*p*HP-caged Glu: ʟ-Glutamic γ-(*p*-hydroxyphenacyl) ester.
γ-*p*HMP-caged Glu: ʟ-Glutamic γ-(*p*-hydroxy-*m*-methoxy-phenacyl) ester.
γ-MNI-caged Glu: 1-[*S*-(4-amino-4-carboxybutanoyl)]-4-methoxy-7-nitroindoline: (4-Methoxy-1-acyl-7-nitroindoline) derivative.
N-NB-caged Glu: *N*-(2-Nitrobenzyl)-ʟ-glutamic acid.
γ-NI-caged Glu: Methyl 1-[*S*-(4-amino-4-carboxybutanoyl)]-7-nitroindoline-5-acetate: (1-acyl-7-nitroindoline) derivative.
N-Nmoc-caged Glu: *N*-(*o*-Nitromandelyl)oxycarbonyl-ʟ-glutamic acid.
γ-NPE-caged Glu: ʟ-Glutamic acid, γ-[1-(2-nitrophenyl)ethyl] ester.
N-NPE-caged Glu: *N*-(2-nitrophenyl ethyl)-ʟ-glutamic acid.
N-NPEOC-caged Glu: *N*-1-(2-Nitrophenyl)ethoxycarbonyl-ʟ-glutamic acid.

References

1 J. H. Kaplan, "Introduction" of this monograph.

2 J. H. Kaplan, B. Forbush III, J. F. Hoffman, *Biochemistry* **1978**, *17*, 1929–1935.

3 J. W. Walker, G. P. Reid, J. A. McCray, D. R. Trentham, *J. Am. Chem. Soc.* **1988**, *110*, 7170–7177.

4 J. E. T. Corrie, G. P. Reid, D. R. Trentham, M. B. Hursthouse, M. A. Mazid, *J. Chem. Soc. Perkin Trans. I* **1992**, 1015–1019.

5 R. P. Haugland, K. R. Gee, US Patents 5 635 608 and 5 888 829.

6 J. W. Wootton, D. R. Trentham, *NATO ASI Ser., Ser. C* **1989**, *272*, 277–296.

7 J. E. T. Corrie, D. R. Trentham, "Caged Nucleotides and Neurotransmitters" in *Biological Applications of Photochemical Switches*, H. Morrison Ed., John Wiley & Sons, New York, **1994**, pp 243–305.

8 H. Thirlwell, J. E. Corrie, G. P. Reid, D. R. Trentham, M. A. Ferenzi, *Biophys. J.* **1994**, *67*, 2436–2447.

9 V. S. Sokolov, H.-J. Apell, J. E. T. Corrie, D. R. Trentham, *Biophys. J.* **1998**, *74*, 2285–2298.

10 R. S. Givens, C.-H. Park, *Tetrahedron Lett.* **1996**, *37*, 6259–6262.

11 J. E. T. Corrie, D. R. Trentham, *J. Chem. Soc. Perkin Trans. I* **1992**, 2409–2417.

12 J. E. T. Corrie, Y. Katayama, G. P. Reid, M. Anson, D. R. Trentham, *Philos. Trans. R. Soc. Ser. A* **1992**, *340*, 233–244.

13 C.-H. Park, R. S. Givens, *J. Am. Chem. Soc.* **1997**, *119*, 2453–2463.

14 D. Geissler, W. Kresse, B. Wiesner, J. Bendig, H. Kettenmann, V. Hagen, *ChemBioChem* **2003**, *4*, 162–170.

15 V. Hagen, B. Kaupp, "Caged Cyclic Nucleotides", Chapter 5.1, this monograph.

16 R. S. Givens, P. S. Athey, B. Matuszewski, L. W. Kueper, J.-Y. Xue, T. Fister, *J. Am. Chem. Soc.* **1993**, *115*, 6001–6012.

17 "Mechanistic Overview of Phototriggers and Cage Release" Part II, this monograph.

18 A. Barth, J. E. T. Corrie, M. J. Gradwell, Y. Maeda, W. Mäntele, T. Meier, D. Trentham, *J. Am. Chem. Soc.* **1997**, *119*, 4149–4159.

19 V. Hagen, J. Bendig, S. Frings, T. Eckard, S. Helm, D. Reuter, U. Benjamin Kaupp, *Angew. Chem. Int. Ed.* **2001**, *40*, 1046–1048.

20 G. Hess, "Photochemical Release of Neurotransmitters" Chapter 6.1, this monograph.

21 G. Hess, "Caged Neurotransmitters for Probing Neuronal Circuits, Neuronal Integration and Synaptic Plasticity" Chapter 6.2, this monograph.

22 T. Dore, "Two-photon and multiphoton phototriggers" Part VIII, this monograph.

23 R. Wieboldt, K. R. Gee, L. Niu, D. Ramesh, B. K. Carpenter, G. P. Hess, *Proc. Natl. Acad. Sci. USA* **1994**, *91*, 8752–8756.

24 S. Guillou, M. Goeldner, Unpublished.

25 *Soc. Neurosci.* **1995**, Abstract 21, 579, abstract #238.11.

26 M. Wilcox, R. W. Viola, K. W. Johnson, A. P. Billington, B. K. Carpenter, J. A. McCray, A. P. Guzikowski, G. P. Hess, *J. Org. Chem.* **1990**, *55*, 1585–1589.

27 J. E. T. Corrie, A. Desantis, Y. Katayama, K. Khodakhah, J. B. Messenger, D. C. Ogden, D. R. Trentham, *J. Physiol.* **1993**, *465*, 1–8.

28 F. M. Rossi, M. Margulis, C.-M. Tang, J. P. Y. Kao, *J. Biol. Chem.* **1997**, *252*, 32933–32939.

29 D. L. Pettit, S. S-H. Wang, K. R. Gee, G. J. Augustine, *Neuron* **1997**, *19*, 465–471.

30 R. S. Givens, A. Jung, C.-H. Park, J. Weber, W. Bartlett, *J. Am. Chem. Soc.* **1997**, *119*, 8369–8370.

31 P. G. Conrad II, R. S. Givens, J. F. W. Weber, K. Kandler, *Org. Lett.* **2000**, *2*, 1545–1547.

32 K. R. Gee, L. W. Kueper, J. Barnes, G. Dudley, R. S. Givens, *J. Org. Chem.* **1996**, *61*, 1228–1233.

33 T. Furuta, S. S.-H. Wang, J. L. Dantzker, T. M. Dore, W. J. Bybee, E. M. Callaway, W. Denk, R. Y. Tsien, *Proc. Natl. Acad. Sci. USA* **1999**, *96*, 1193–2000.

34 G. Papageorgiou, D. C. Ogden, A. Barth, J. E. T. Corrie, *J. Am. Chem. Soc.* **1999**, *121*, 6503–6504.

35 M. Canepari, L. Nelson, G. Papageorgiou, J. E. T. Corrie, D. Ogden, *J. Neurosci. Methods* **2001**, *112*, 29–42.

36 G. Papageorgiou, J. E. T. Corrie, *Tetrahedron* **2001**, *56*, 8197–8205.

37 W. Wittayanan, M. Goeldner, Unpublished

38 "Photoremovable Protecting Groups Used for the Caging of Biomolecules" Part I, this monograph.

39 S. Walbert, W. Pfeiderer, U. E. Steiner, *Helv. Chim. Acta* **2001**, *84*, 1601–1611.

40 C. Grewer, J. Jäger, B. K. Carpenter, G. P. Hess, *Biochemistry* **2000**, *39*, 2063–2070.

41 A. Specht, M. Goeldner, *Angew. Chem. Int. Ed. Engl.* **2004**, *43*, 2008–2012.

42 J. E. T. Corrie, A. Barth, V. R. N. Munasinghe, D. R. Trentham, M. C. Hutter, *J. Am. Chem. Soc.* **2003**, *125*, 8546–8554.

43 Y. Il'ichev, M. A. Schwörer, J. Wirz, *J. Am. Chem. Soc.* **2004**, *126*, 4581–4595.

44 O. D. Fedoryak, T. M. Dore, *Org. Lett.* **2002**, *4*, 3419–3422.

45 M. Matsuzaki, G. C. R. Ellis-Davies, T. Nemoto, Y. Miyashita, M. Iino, H. Kasai, *Nature Neurosci.* **2001**, *4*, 1086–1092.